Alma Mater Studiorum – Università di Bologna

DOTTORATO DI RICERCA IN

SCIENZE E TECNOLOGIE AGRARIE, AMBIENTALI E ALIMENTARI

Ciclo XXXIII

Settore Concorsuale: 07/B1

Settore Scientifico Disciplinare: AGR02

EVAPOTRANSPIRATION: PRESENT AND FUTURE CHALLENGES

Presentata da: Ghaieth Ben Hamouda

Coordinatore Dottorato — Prof. Massimiliano Petracci

Supervisore — Prof.ssa Francesca Ventura

Esame finale anno 2021

Abstract

Evapotranspiration, particularly reference evapotranspiration (ET_o), is an essential component of both climate and hydrological cycles and a fundamental prerequisite for determining the water requirement in irrigated areas and analyzing the impacts of climate change on water resources. However, the standard equation for calculating ET_o adopted by the Food and Agriculture Organization (FAO) necessitates several meteorological parameters that are not always available. It also neglects the effect of rising atmospheric carbon dioxide (CO_2) on crop water use. This creates additional challenges for farmers as agricultural water resources planning should consider explicitly the short-term effect and longer-term implications of hydrological alterations brought about by evapotranspiration changes in response to water stress and climate change. Accurate reference evapotranspiration estimations are then crucial as farmers have to decide not only the amount of irrigation water to be used, but also the pattern of its use over the production period. The thesis first explored and evaluated some of the most used models that were developed to account for the effect of CO_2 on evapotranspiration. This review gives an idea about the complexity of the modeling procedure and underlines the advantages and shortcomings of each model. Then, the projected climate change in the near future (2021-2050) in different locations in Emilia-Romagna (Italy) was studied, with an emphasis on the opposite effect of an increase in both air temperature and CO_2 levels on ET_o. The case study used reanalysis data as a surrogate to historical weather stations measurements and an ensemble of regional climate models (RCMs) for the future projections. Results show that higher CO_2 levels moderated the increase in ET_o that accompanies an increase in air temperature, taking in consideration the change in other weather variables i.e. solar radiation, wind speed and dew point temperature. The outcomes of this study show that considering the CO_2 fertilization effect when calculating reference evapotranspiration might give a more realistic estimation of water use efficiency and irrigation requirements in Emilia-Romagna and a better analysis of the future availability and distribution of water resources in the region. Finally, data from a model forecasting reference evapotranspiration (FRET) and the different variables involved in its calculation for the state of California (USA) were compared with similar data from the regional weather station network (CIMIS) to evaluate their accuracy and reliability. The evaluation was done in locations with different microclimates and included also sample irrigation schedules developed using FRET ET_o that were provided to illustrate the use of forecast

ET_o alongside with soil hydraulic properties and irrigation system's performance parameters to optimize water applications for specialty crops and urban landscape. The obtained results demonstrate that FRET ET_o forecasts are a viable alternative to traditional ET_o measurements with some differences depending on the climatic condition of the location considered in this study. This implies that FRET could be replicated in other areas with similar climate settings.

Acknowledgements

Undertaking this PhD has been a truly life-changing experience for me, and it would not have been possible to do without the support and guidance that I received from many people.

First and foremost, I would like to thank my supervisor, Professor Francesca Ventura, for her patience, comments, encouragement and continuous support of my PhD research. Many thanks also to Dr. Daniele Zaccaria and Dr. Richard L. Snyder for their guidance and collaboration throughout this journey and particularly during my research period at The University of California Davis.

I would like to express my gratitude to The Institute of the Advanced Studies (ISA) and its director Prof. Dario Braga. Their hospitality and their support made my study and life in Bologna a wonderful experience.

Finally, I cannot forget to thank my parents and sisters. Without their unconditional support and encouragement in the past few years, it would have been impossible for me to complete this thesis.

Table of Contents

Chapter 1

General Introduction

1. General introduction

Civilization began with agriculture, and although its contribution to the global gross domestic product (GDP) has decreased, the agricultural sector still remains the backbone of the economic system of a given country and its growth has always been the precursor to a wider economic development. Agricultural lands occupy a third of the global ice-free land area, and a fifth of the world population depend on agriculture for their livelihoods either as actively engaged workers or as dependents (FAO 2020). Agriculture's most basic task and main objective is providing adequate food supplies for mankind. Improving food availability and achieving food security has been possible for a long time with the emergence of the "industrial revolution" and associated rapid growth and development of human societies as croplands and pasturelands each expanded fivefold in the last three centuries (Ramankutty et al. 2018), allowing global agricultural production to reach an average growth between 2% and 4% per year over the last 50 years (FAO 2013). This steady growth increased global per capita food supply from about 2200 kcal/person/day in the early 1960s to more than 2800 kcal/person/day by 2013 (Figure 1-1), which is superior to the recommended average daily caloric intake.

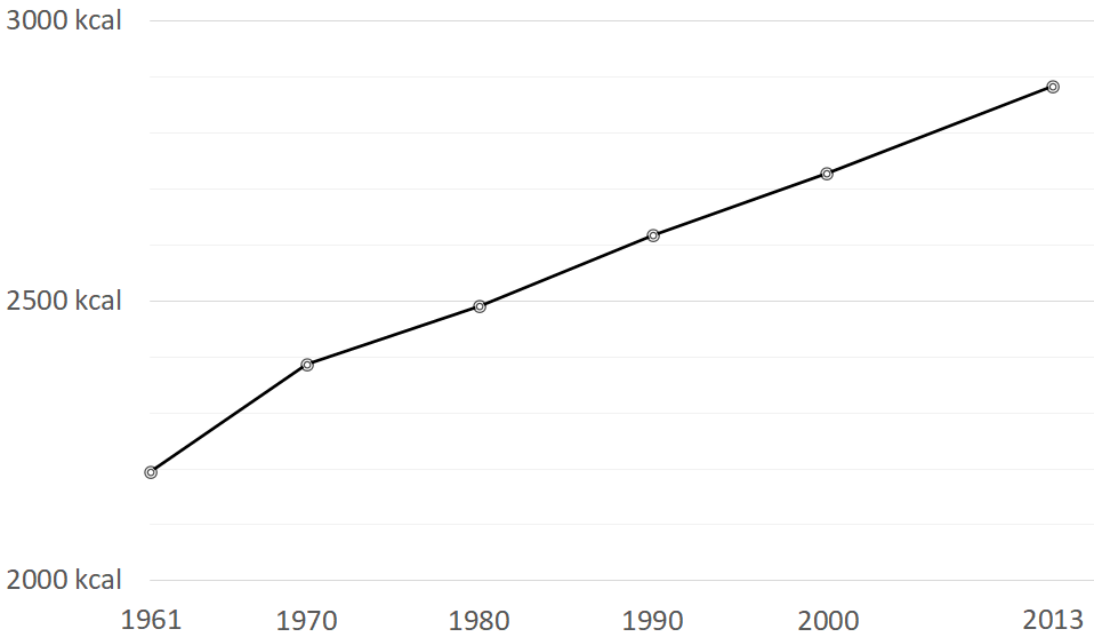

Fig.1-1. Global daily supply of calories from 1961 to 2013. Caloric supply is measured in kilocalories per person per day (FAOSTAT 2020).

However, keeping this performance is likely to become more difficult in the future, as global population exceeded 7.6 billion people in 2018, and is predicted to reach 9.7 billion by 2050 (UN 2019). To meet the projected 50% rise in food demand, it will be necessary to increase agricultural production by the same percentage to provide food for the global population in 2050 (FAO 2017). Besides, the role of agriculture goes above and beyond food production. It also includes production of non-food products e.g. Biofuels, natural biopolymers, building and construction materials, natural fibers, cosmetics, pharmaceuticals and chemicals. Knowing that urbanization and rising incomes in much of the developing world have pushed demand for food and other agricultural products to unprecedented levels (FAO 2013), agriculture is hence facing an increasing pressure to meet the needs of current and future human populations. This is further complicated by the fact that the cultivated area (permanent cropland and arable land) has grown by only 1% annually over the last 50 years as agricultural land expansion has become increasingly difficult due to its associated high costs, the competition from urban development, the large carbon losses caused by deforestation (Burney et al. 2010) and for other environmental reasons (FAO 2013). So far, this relatively slowly growing land base has been compensated mainly by increasing the output per unit of land to meet the rapidly rising demands placed on agriculture. The increase in land productivity has been the result of a combination between an input intensification, that is, using more labor, capital, and material inputs per unit of agricultural land, and increases in the efficiency with which both land and non-land inputs are used, known as total factor productivity (TFP) (Villoria 2019). Productivity growth in agriculture has enabled farmers to produce a greater abundance of food causing its prices to fall by an average of 1% per year between 1900 and 2010 even as population growth accelerated (Figure 1-2). This was facilitated by a plethora of technological advances e.g. progress in plant biology and animal breeding techniques, which improved crops and livestock genetic material and introduced new and optimized crop varieties and livestock breeds (Evenson and Gollin 2003; Thornton 2010; Glenn et al. 2017); improvements in the mechanization of agriculture (Pingali 2007); use of fertilizers and pesticides (Carvalho 2006). These developments, combined with subsidized energy costs, boosted the use of surface and groundwater resources by farmers for irrigation purposes. In fact, all the net increase in cultivated area over the last 50 years is attributable to a net increase in irrigated cropping, with land under rainfed systems showing a very slight decline. Irrigation has been then crucial for gains in food production with more than

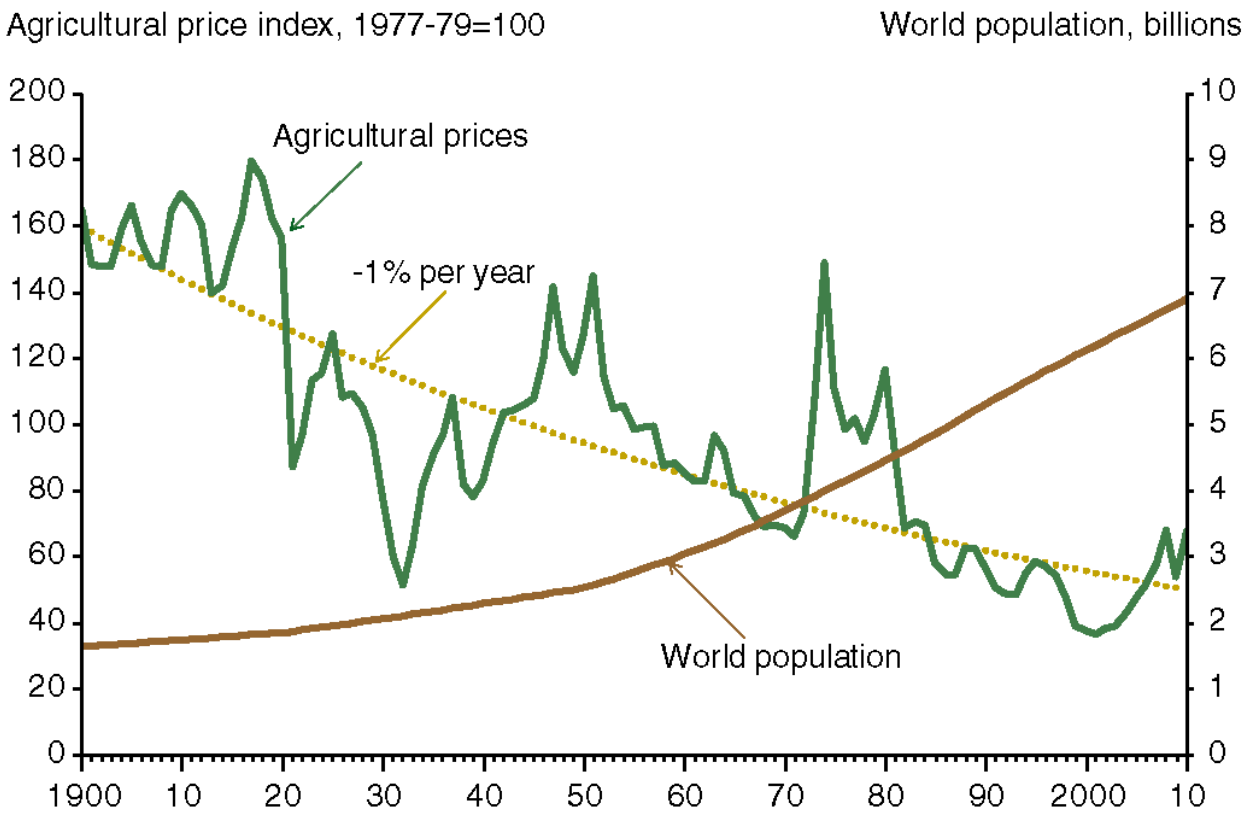

Fig 1-2. USDA Economic Research Service using Fuglie et al. (2012). Depicted in the chart is the Grilli-Yang agricultural price index adjusted for inflation by the U.S GDP implicit price index. The Grilli-Yang price index is a composite of 18 crop and livestock prices, each weighted by its share of global agriculture trade (Pfaffenzeller et al. 2007). World population estimates are from the United Nations.

40% of these gains coming from irrigated areas, which have more than doubled in size since the 1960s (Figure 1-3). Moreover, irrigation reduced dramatically the number of hectares needed to feed one person from 0.44 to 0.21 ha per person. However, the constant expansion of the irrigated area has put an increasing pressure on global water resources with irrigation currently accounting for 70% of the total global renewable water resources (FAO 2011), making it the primary driver of groundwater depletion worldwide and pushing global water withdrawals to their near maximum sustainable level at about 4600 km^3 per year (Gleick and Palaniappan 2010). Projections of the global irrigated area suggest that it will continue increasing linearly, reaching between 250 and 450 million hectares by 2050 (Rosegrant et al. 2002; Shiklomanov and Rodda 2003; Alcamo et al. 2005, 2007; Fischer et al. 2007; Molden 2007; Alexandratos and Bruinsma 2012), while agricultural withdrawals are projected to increase to almost 3000 km^3 yr^{-1} by 2050 (FAO 2011).

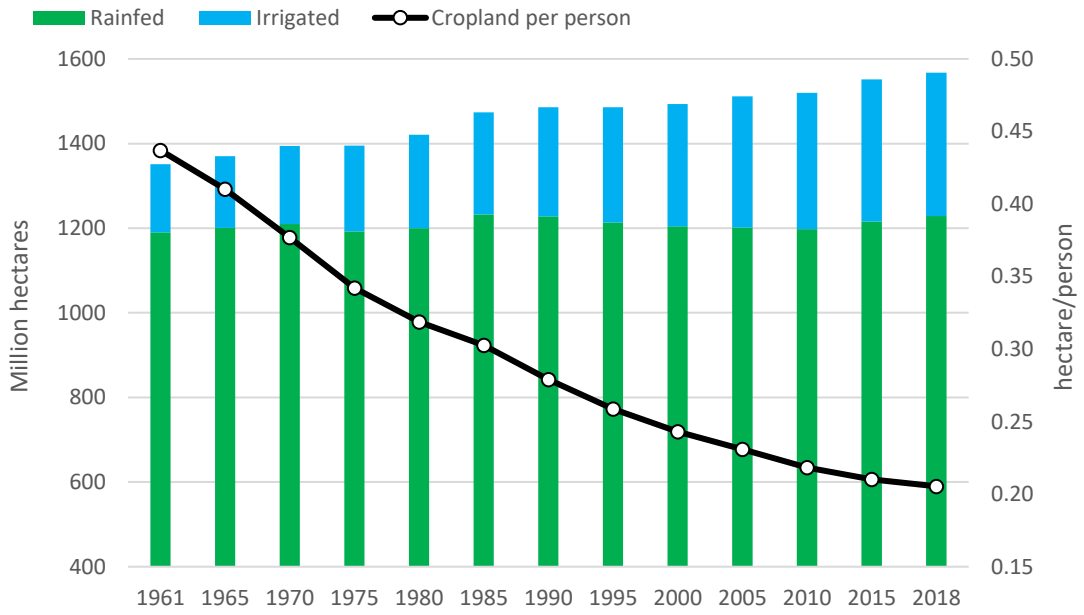

Fig. 1-3. Evolution of land under irrigated and rainfed cropping (1961-2018) (FAOSTAT 2020)

This indicates a net increase of 10% between 2011 and 2050, which could be even higher according to Puy et al. (2020). They projected that the amount of irrigated land could increase to as high as 1.8 billion hectares by 2050 because the aforementioned projections underestimate the potential extension of irrigation by ignoring basic parametric and model uncertainties. Much larger irrigated areas might force agricultural land to extend toward new ecosystems or non-cultivated areas with the consequent loss of biodiversity, which might also be larger than expected. At the same time, needing more water for irrigation will affect intersectoral water allocation causing more stress on water resources than expected. Besides, current irrigation efficiencies are often below 50%, as much of the diverted water is lost in the conveyance system or through inefficient application to the plants (Jägermeyr et al. 2015). Therefore, the irrigation potential created in the world is not being fully used and creates even further irrigation demands in the existing system for agricultural production. In this context, improving agricultural water resources management becomes crucial in order to meet the increased food demands of a growing population and to avoid environmental damages such as water systems pollution, soil infertility and erosion and the natural ecosystems destruction. The key to understanding water requirements, and getting the most efficiency with irrigation systems, is understanding evapotranspiration (ET). Accurate quantification of ET is of a paramount importance to water allocation, irrigation management, evaluating the effects of changing land use on water yield, environmental assessment, and development of best management

practices to protect surface and groundwater quantity and quality (Irmak 2008). Evapotranspiration is composed of two-subprocesses: evaporation from soil and vegetation surfaces and transpiration that consists of the exchange of moisture between the plant and atmosphere through plant stomata. It is an important component of the water cycle (Figure 1-4) as global land ET returns approximately 60% of annual land precipitation to the atmosphere (Oki and Kanae 2006) and consumes more than half of the solar radiation in the form of latent heat (Trenberth et al. 2009).

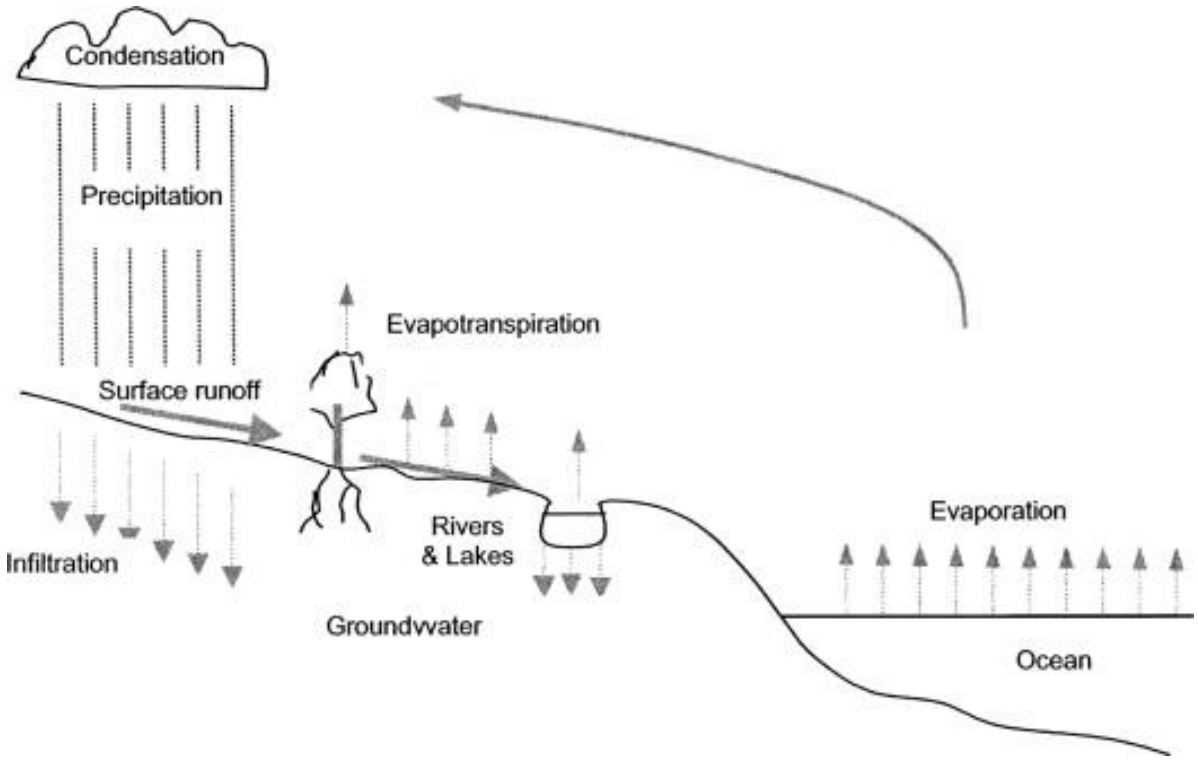

Fig. 1-4. The hydrological cycle (Schroeder 2003)

Evapotranspiration is governed by several factors: weather parameters, essentially solar radiation, air temperature, humidity and wind speed; crop factors such as crop type, variety, development stage, height, roughness and rooting characteristics, resistance to transpiration, reflection and ground cover; management and environmental conditions e.g. soil salinity, water content, penetration resistance and management, land fertility, application of fertilizers and pest and disease control (Allen et al. 1998). Since its first definition by Thornthwaite (1948), ET has been measured using several methods such as lysimeters (Fenner et al. 2019), Eddy correlation systems (Parent and Anctil 2012; Maestre-Valero et al. 2017), Bowen ratio energy balance systems (Irmak et al. 2014), atmometers, including evaporation pans (Lamine et al. 2015), scintillation techniques

(Rambikur and Chávez 2012; Vendrame et al. 2019), remote sensing (Zhang et al. 2016) and soil water balance (Bargaoui 2012). However, these methods are often costly, time consuming, demanding in terms of accuracy of field measurements and require an in-depth experience and expertise with the different instruments and data acquisition and processing. Besides, they are strongly influenced by crop type, crop development and management practices, which prompted the scientific community to estimate evapotranspiration independently from vegetation and soil characteristics, using solely meteorological data. This was made possible by relating ET to a reference surface having an inexhaustible water supply, thus leaving only meteorological factors to be considered. Linking evapotranspiration to a specific surface would also provide a reference for comparison with ET from other surfaces and eliminate the need to define a separate ET level for each crop and stage of growth. Hence, the concept of reference evapotranspiration (ET_o) was introduced. To calculate ET of other surfaces, ET_o is multiplied by a crop coefficient K_c, which is as an aggregation of the physical and physiological differences between crops and the reference definition (Guerra et al. 2016). In its Irrigation and Drainage Paper No.56, the Food and Agriculture Organization of the United Nations (FAO) defines ET_o as "the rate of evapotranspiration from a hypothetic crop with an assumed crop height (12 cm) and a fixed surface resistance (70 s m^{-1}) and albedo (0.23) which would closely resemble evapotranspiration from an extensive surface of green grass cover of uniform height, actively growing, completely shading the ground and not short of water" (Allen et al. 1998). For its calculation, FAO adopted an adjusted version of the Penman-Monteith method (FAO-PM), which is a combination between Penman (1948; 1963) equations and the Monteith (1965) equation:

$$ET_o = \frac{0.408\,\Delta\,(R_n - G) + \gamma\,\frac{900}{T+273}\,u_2\,(e_s - e_a)}{\Delta + \gamma\,(1 + 0.34\,u_2)} \quad (1\text{-}1)$$

where ET_o is the reference evapotranspiration (mm d^{-1}); R_n is the net radiation at the crop surface (MJ m^{-2} d^{-1}); G is soil heat flux density (MJ m^{-2} d^{-1}); T is the mean daily air temperature at 2 m height (°C); u_2 is the wind speed at 2 m height (m s^{-1}); e_s is the saturation vapour pressure (kPa); e_a actual vapour pressure (kPa); e_s-e_a is the saturation vapour pressure deficit (kPa); Δ is the slope vapour pressure curve (kPa $°C^{-1}$); γ is the psychrometric constant (kPa $°C^{-1}$).

The FAO-PM equation uses standard climatological records of solar radiation (sunshine), air temperature, humidity and wind speed that should be measured at 2 m (or converted to that height)

above an extensive surface of green grass, shading the ground and not short of water, to ensure the integrity of the computations (Allen et al. 1998). The FAO-PM equation proved its superiority over several previously used empirical and semi-empirical equations (Suleiman and Hoogenboom 2007; Trajkovic and Gocic 2010; Ngongondo et al. 2013), and was widely applied in different locations mainly for estimating crop water requirements and irrigation scheduling (Beutler and Keller 2005; Adeniran et al. 2010; Bouraima et al. 2015; Hossain et al. 2017; Islam et al. 2017; Memon and Jamsa 2018; Ewaid and Al-Ansari 2019; Abrishambaf et al. 2020). Nevertheless, a large number of empirical and semi-empirical equations are still being used by irrigation engineers and researchers for the calculation of reference evapotranspiration, as the FAO-PM equation requires input of several measurements of often unavailable climatic variables due mainly to the high costs of weather stations installation and maintenance (Exner-Kittridge and Rains 2010). This is especially true in developing countries (Tabari 2010; Hou et al 2013). Yet, this large number of simpler equations often yielded inconsistent results as their assumptions and meteorological data requirements differ (Grismer et al. 2002; Lu et al. 2005), urging researchers to compare a multitude of different approaches to choose the best one according to the situation investigated (Trajkovic and Kolakovic 2009; Xystrakis and Matzarakis 2011; Rahimikhoob et al. 2012; Sheikh and Mohammadi 2013; Djaman et al. 2015; Celestin et al. 2020). Moreover, since the accuracy of each of these methods is largely affected by the climatic conditions of the study area, it is highly recommended to locally calibrate them before they can be used to estimate ET_o (Poyen et al. 2016).

An alternative approach to obtain the missing data for the ET_o calculation is to use weather forecast data. Time series forecasting has gained remarkable interest from researchers in the last few decades, and ET_o forecasts are becoming fundamental to real-time irrigation scheduling and agricultural water management, especially in semi-arid and arid climates where supplemental or full irrigation is often needed to produce a crop. This is mainly due to important advances in weather forecasting based on statistical and numerical weather prediction (NWP) models (Bauer et al. 2015), that gave a solid proof of the suitability of ET_o forecasts as a substitute to weather stations measurements (Perera et al. 2014; Luo et al. 2015; Traore et al. 2016; Manikumari et al. 2017; Liu et al. 2020). Furthermore, the potential for ET_o forecasting is projected to improve and the forecasts uncertainties will decline as the performance of the statistical and NWP models increases or systematic errors are removed from the forecast weather variables. Using forecast ET_o has many advantages: It helps farmers making optimal irrigation scheduling decisions because it

permits the irrigation scheduling based on expected weather conditions rather than on intuition or past weather data (Vanella et al. 2020), which would increase farmers profits from higher yields and/or greater irrigation water efficiency. Moreover, reliable ET_o forecasts reduce costs and provide ET_o data in a more timely fashion by eliminating or decreasing the number of automated weather networks that are currently needed to provide near-real time ET_o data for irrigation scheduling purposes (Duce et al. 2000). Another important advantage of ET_o forecasts from models is their ability to produce spatially distributed data, which are very relevant for regional scale studies, unlike in-situ observations obtained by weather stations that are unable to provide reliable spatial ET_o at large scales, mostly because of the sparsity and heterogeneity of weather stations networks and the complexity of the land surface (Tomas-Burguera et al. 2018). The same issue is also experienced with remote sensing techniques because daily spatial ET_o is not often available due to temporal resolution of satellites and/or gaps in image acquisition due to cloud cover (Ju and Roy 2008). However, forecast models' outputs are usually open for researchers, but not for the public, and these outputs are also difficult for non-professionals to analyze (Yang et al. 2019). Considering this fact, it becomes necessary to develop more free and user-friendly models with a simple and intuitive design which will make daily real-time ET_o data accessible to the public.

Reanalysis may also represent a good alternative dataset for the calculation of reference evapotranspiration in regions where weather stations are sparsely distributed or nonexistent. They combine past short-range weather forecasts with observations through data assimilation from past to present-day (Parker 2016). Reanalysis contain estimates of a myriad of atmospheric and surface parameters (Wang et al. 2011; Balsamo et al. 2015) produced at a global scale, and spanning a long time period that can extend back several decades or more. Since their first appearance in the early 1990s, reanalysis products have been improving in accuracy and temporal and spatial resolution and they have become among the most used datasets in the study of weather and climate, especially as substitutes for traditional observations (Shiu et al. 2012; Kravtsov et al. 2014; Essou et al. 2017; Tarek et al. 2020).

Detailed weather information, which includes past records, present weather and future forecasts allow farmers to make valuable and effective short-term decisions regarding crop planning, pest management and water allocations strategies. To further increase their profitability and competitiveness, farmers need to develop long-term strategies using future climate projections to assess the effect of climate change especially in developing countries (Hewitson et al. 2014). Climate change is the long-term alteration in Earth's climate and weather patterns mainly caused by greenhouse gas emissions (GHGs) from natural systems and human activities. Anthropogenic emissions, primarily from burning fossil fuels and deforestation, account for approximately 55% of the total global GHGs emissions (Yue and Gao 2018), with carbon dioxide (CO_2) accounting for 76% of the total anthropogenic greenhouse gas effect (Blanco et al. 2014). Man-made CO_2 in the atmosphere has increased from pre-industrial levels of about 278 ppm (parts per million) to about 408 ppm in 2018 (Feely et al. 2019), creating an artificial forcing of global temperatures which, by the that same year, had already warmed the planet by 0.92°C (Figure 1-5).

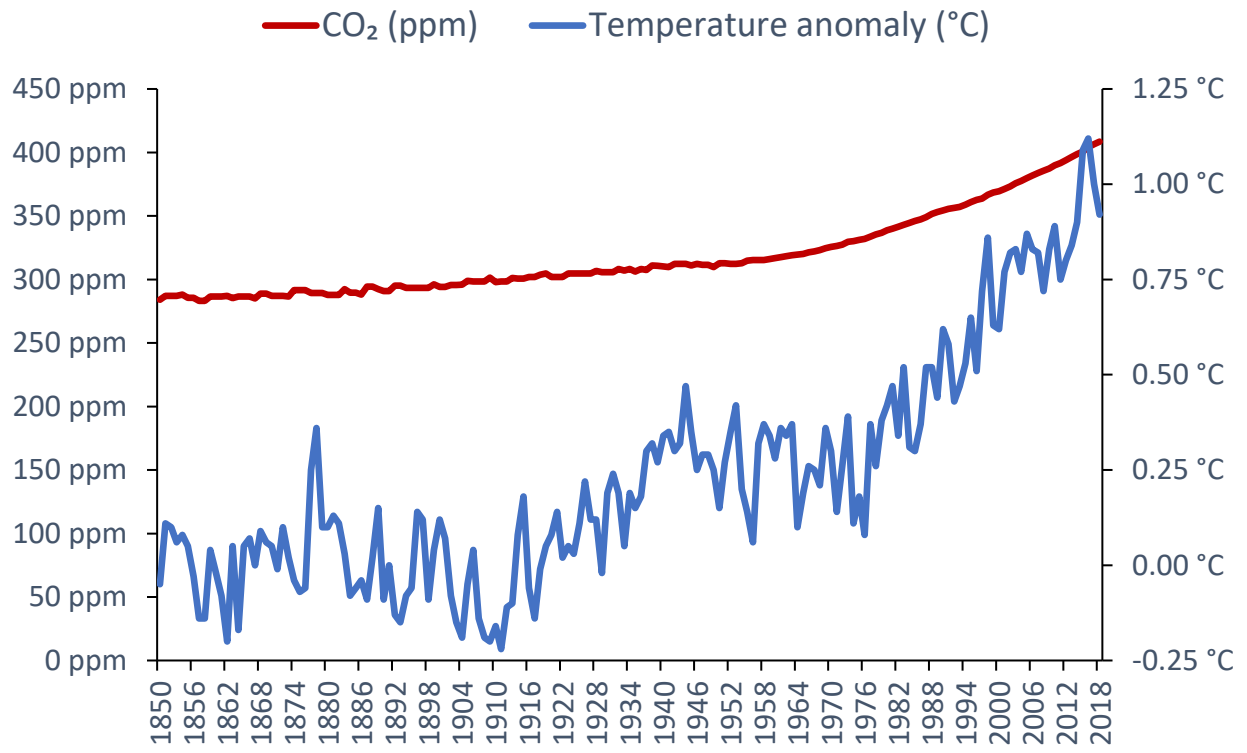

Fig. 1-5. Global average long-term atmospheric concentration of carbon dioxide (CO_2) (NOAA 2018) and global average temperature anomalies (relative to a pre-industrial period between 1850 and 1899) based on the HadCRUT4 dataset (Met Office Hadley Centre 2020).

If no mitigation measures are taken, the CO_2 levels are projected to reach or exceed 550 ppm by 2050 (Smith and Myers 2018) causing global warming to reach 1.5°C between 2030 and 2052 with regards to pre-industrial levels (Allen et al. 2018). Increases in temperature enhance the moisture holding capacity of the atmosphere and thus, lead to an intensification and an acceleration of the global hydrological cycle (Stagl et al. 2014), which will exacerbate precipitation variability and change seasonal patterns increasing the periodicity and intensity of some climate extremes such as storms, hurricanes, floods, heatwaves, cold spells, landslides, droughts and associated large-scale wildfires (França et al. 2020). This will also cause changes in disease distribution, desertification, arable land and freshwater salinization, sea levels rise and coastal degradation, accentuating the vulnerability of multiple sectors in many countries (UNCCS 2019), especially agriculture. By altering the water cycle, temperature rise will generally impact the agricultural sector by increasing evapotranspiration, limiting crop productivity and by reducing water availability in areas where irrigation is most needed or has comparative advantage (Turral et al. 2011), thus adding to the many economic and social challenges already being faced by water management in agricultural areas and further affecting global food production (Iglesias et al. 2011). Nevertheless, in mid- to high-latitude regions, an altered climate is projected to rather slightly increase crop productivity and water-use efficiency depending on the crop type, the temperature, and the availability of water and nutrient (van Vuuren et al. 2009). This is known as the "CO_2 fertilization effect". Carbon dioxide is a basic building block for plant growth. Increased atmospheric concentrations of CO_2 enhance photosynthetic activity at the leaf level and reduce rates of respiration, offsetting the loss of production potential due to temperature rise and water stress (Ueyama et al. 2020). Higher CO_2 levels influence the hydrological cycle by reducing stomatal conductance (Cheng et al. 2017) resulting in a decrease in continental evapotranspiration and an increase in water runoff (Betts et al. 2007). Since evapotranspiration is the highest outgoing water flux in the hydrological cycle and directly influenced by these opposing forces, a clear understanding of historical trends and future changes in evapotranspiration, particularly reference evapotranspiration, are essential for a better apprehension of the interaction between CO_2 and temperature and an efficient use of water resources in agricultural management under conditions of global climate change. The effect of elevated CO_2 levels on evapotranspiration can be accounted for by modifying the canopy resistance (r_c) term in the FAO-PM equation. However, this term was first fixed by Smith et al. (1992) and Allen et al. (1994a; 1994b), then adopted by FAO in order to obtain a standard equation that can

be applied worldwide, which resulted in an underestimation of the measured ET_o in semiarid and windy areas with high atmospheric evaporative demand, and an overestimation with low demand (Rana et al. 1994; Steduto et al. 1996; Ventura et al. 1999). Yang et al. (2019) pointed out that the FAO-PM equation with the fixed canopy resistance is appropriate for an idealized reference crop in the current climate. However, neglecting the increase of r_c under an elevated CO_2 would overestimate the future aridity changes, and thus fail to properly assess the response of terrestrial water availability under future climate change (Roderick et al. 2015; Milly and Dunne 2016; Yang et al. 2018; Greve et al. 2019; Dong et al. 2020).

Thesis objectives and outline

This thesis investigates a number of challenges related to the estimation of evapotranspiration in both the short and long term and applies some of the concepts described in the literature review to assess if they can be viable solutions for a better monitoring and planning of agricultural water use on local, regional and global scales in a context of water scarcity and climate change.

Overall, the key objectives of this research can be summarized as following:

- Identify the importance of accounting for the ongoing and projected increase in CO_2 levels on evapotranspiration estimation, review some of the most used models to account for this increase and analyze their strengths and weaknesses.
- Quantify the effect of an increase in CO_2 concentrations on evapotranspiration and evaluate its conflicting effect with other meteorological factors, particularly air temperature.
- Assess the suitability and performance of alternative sources to weather stations records for the estimation of evapotranspiration using the FAO-PM equation.

The following chapters represent a series of manuscripts that are published or submitted to international peer reviewed journals. While the chapters might have different scopes and research questions, they form an integral part of the whole thesis. Thus, some common background and literature review in the chapters can be expected, which is due to the interdependence of the application and uncertainty issues in ET estimation. In Chapter 2, a review of the different canopy resistance models that attempted to explain the relationship between evapotranspiration and carbon dioxide, is given. In Chapter 3, an application of one of these models is done in different locations in Emilia-Romagna region in Italy to assess the effect of climate change on reference

evapotranspiration in the near future (2021-2050). In Chapter 4, the accuracy and reliability of NWP-based daily reference evapotranspiration forecasts (FRET) are evaluated by comparing them with measured data from California weather stations network (CIMIS) in locations with different climate characteristics. Some sample irrigation schedules developed using FRET ET_o were provided to illustrate the use of forecast ET_o alongside with soil hydraulic properties and irrigation system's performance parameters to optimize water applications for specialty crops and urban landscape. Results of this chapter should help to decide whether FRET data could be a viable alternative to weather stations measurements and whether they could be reproduced and used in other locations with similar climatic conditions.

Chapter 2

Evaluation of some evapotranspiration estimation models under CO_2 increasing concentrations

The original research described in this Chapter has been published as:

Ben Hamouda G, Ventura F (2020) Evaluation of Some Evapotranspiration Estimation Models under CO_2 Increasing Concentrations: A Review. Ital. J. Agrometeorol. 2020 (1): 85–98. https://doi.org/10.13128/ijam-831

Reprinted with minor modifications

2. Evaluation of some evapotranspiration estimation models under CO_2 increasing concentrations

Abstract

The total volume of CO_2 emissions is building up dramatically, and because of the effect of this gas on the growth, physiology, and biochemistry of plants, it is becoming increasingly necessary to look into the impact of the relentless rise of carbon dioxide. Although there are several developed approaches that tried to model the canopy resistance, many of these methodologies ignored the effect of CO_2 or were not incorporated with the existing evapotranspiration calculation methodologies, mainly due to the complexity of the modeling procedure and the short time framework of the conducted studies. This review explores the few models estimating crop water requirements that account for this effect and examines their assumptions and theories. The inclusion of canopy resistance models in evapotranspiration calculation may be of questionable utility without improvements in some modeling aspects, such as the relationship between the stomatal conductance and CO_2 and the climatic variables taken in consideration in the modeling process.

Keywords: Penman Monteith, ET_o, carbon dioxide, canopy resistance, surface resistance, climate change.

2.1. Introduction

According to (UNDESA 2017), the world population is foreseen to grow between 20-30% by 2050, going from 7.7 billion people in 2017 to between 9.2 and 10,2 billion. Naturally, the global demand for food production is also expected to increase by almost 60% by 2025 (Alexandratos and Bruinsma 2012; OECD 2012). On the other side, global water consumption has already known a leap of 600% over the last century (Wada et al. 2016), and it keeps increasing by 1% yearly (AQUASTAT n.d.). Water demand is currently evaluated at 4.600 km^3 and could reach almost 6000 km^3 by 2050 (Burek et al. 2016). All this will put more pressure on the agricultural sector, which is the actual largest world consumer of freshwater, mostly for irrigation, accounting for 70% of freshwater withdrawals, up to 90% by 2050 (WWAP 2012). Agriculture is also expected to face a fierce competition for water resources from other sectors, resulting in a decrease in its share of total water use in developing countries from 86% in 1995 to 76% in 2025 (Rosegrant et al. 2002).

In addition, global warming is meanwhile affecting the water cycle and shifting weather patterns (IPCC 2014b). Therefore, the agricultural sector is in great need of creating strategies to improve water management and, consequently, attain greater levels of water savings in order to face these aforementioned challenges (de Fraiture and Wichelns 2010).

One of the key components to improving the management of water resources is accurately determining the water requirements of irrigated crops. These needs depend on the management strategy chosen, and are based on the demand for atmospheric water, known as evapotranspiration. Evapotranspiration (ET) is a major component of the hydrological cycle and has an important effect on the quality of water, since in the evaporation process the water is purified. This clean H_2O restores about 60% of global land surface water. For vegetated ecosystems, it is also the main component of energy balance, employing more than 50% of absorbed solar radiation (Trenberth et al. 2009). In fact, evapotranspiration is a component of the energy budget involving incoming energy and outgoing water, occurring at the crop surface. The other components of the budget are net radiation, sensible heat flux, soil heat flux, and solar radiation stored as photochemical energy. This exchange process creates an atmospheric demand that is satisfied by transferring water out of the plant system through evapotranspiration. Such phenomenon is regulated by the principle of energy conservation or energy balance: energy arriving at the vegetation surface equal energy leaving the same surface for the same time period. The energy balance equation for an evaporating surface can be written as:

$$R_n - G - \lambda ET - H = 0 \tag{2-1}$$

where R_n is net radiation, H sensible heat, G soil heat flux and λET is the latent heat flux. Terms can be either positive or negative: positive R_n supplies energy to the vegetation surface and positive G, λET and H remove energy from the vegetation surface. The latent heat flux (λET) is the evapotranspiration fraction and can be derived from the energy balance equation, if all other components are known. ET is an important hydrological variable for irrigation water management, hydrological modeling and water balance calculations. Penman (1963) defines ET as the combination of two separate processes occurring simultaneously, evaporation from the soil surface and transpiration from the crop. Since the evapotranspiration is strongly affected by crop type, crop development and management practices, there was a need to find a concept to express the evaporative demand of the atmosphere independently of those factors. Hence, reference

evapotranspiration (ET_o) was introduced for this purpose. ET_o is defined as the evapotranspiration rate from a well irrigated hypothetical grass reference crop with specific characteristics. It expresses the evaporating power of the atmosphere at a specific location and time of the year and does not consider crop characteristics and soil factors. Instead, it is driven by weather parameters, which are solar radiation, air temperature humidity and wind speed. A thorough understanding of ET_o is the first step to achieving efficient and effective water management and irrigation scheduling. The United Nations Food and Agriculture Organization (FAO) has adopted an updated Penman–Monteith equation (FAO-PM) as a global standard for estimating grass reference evapotranspiration (Allen et al. 1998). This equation was chosen as it provides a better prediction compared to other methods in a wide variety of geographic locations and climatic conditions (Kashyap and Panda 2001; Yoder et al. 2005; López-Urrea et al. 2006; Suleiman and Hoogenboom 2007; Adeboye et al. 2009; Rasul and Mahmood 2009; Rácz et al. 2013). It includes all the different atmospheric variables that influence ET, which makes it suitable for climate change impact studies (Kingston et al. 2009; Islam et al. 2012; Priya et al. 2014). However, despite the completeness of this equation, it simulates poorly the effect of CO_2, that is represented by the "canopy resistance" or "surface resistance" term, r_c. In fact, daily r_c is fixed at 70 s m^{-1} and is considered constant regardless of climate type and change in climate patterns, thus contradicting published reports (Long et al 2004; Damour et al. 2010). Although Allen et al. (2006) considered that fluctuation in its value would have a negligible effect on the ET_o calculation, many experimental studies disagree with their statement on hourly, daily and seasonal scales (Steduto et al. 2003; Katerji and Rana 2006, 2011, 2014; Yan et al. 2018). This is particularly true when the crop is under well-watered conditions, i.e. when the physiological component of r_c is at its minimum. The alarming increase of CO_2 concentrations due to climate change, the physiological effects that it would have on crop plants (Tubiello et al. 2000; Long et al. 2004; Mall et al. 2017) and the uncertainties affecting the calculation of ET_o using the FAO-PM equation, have prompted many researchers to develop other approaches and models to estimate reference evapotranspiration, taking into account the variability of the canopy resistance r_c. Following a short discussion on the effect of rising CO_2 on crops evapotranspiration, this paper provides an overview of these different methods, delineating their main theories and assumptions, and exploring their strengths and weaknesses.

2.2. Effect of CO_2 on crops evapotranspiration

Our planet's atmosphere witnessed a gradual change throughout history, experiencing a wide range of CO_2 concentration. Studies suggest that this concentration may have been about 4000 to 5000 ppm some 500 million years ago (Ehleringer et al. 2005). Then, this concentration decreased to around 1000 ppm between 35 and 55 million years ago, falling abruptly to about 390 ppm during Oligocene by approximately 32-25 million years ago (Tipple and Pagani 2007). This decline in CO_2 limited the efficiency of photosynthesis, triggering the evolution of C_4 plants from ancestral C_3 species as a clever solution to the problem of low atmospheric CO_2. Since the pre-industrial era, anthropogenic greenhouse gas (GHG) emissions have been causing new increases in the atmospheric concentrations of carbon dioxide, going from 270 ppm before 1700 to about 410 ppm in 2020, reaching unprecedented levels in at least 800,000 years. The concentration will keep increasing if no additional efforts are made to reduce emissions (IPCC 2014a; 2014b). These increasing concentrations have important physiological effects on plants, e.g. faster rate of photosynthesis, greater leaf area, increase in biomass and yield and decrease in stomatal conductance and transpiration rate (Allen 1990; Ainsworth and Long 2004; van der Kooi et al. 2016). The latter effect has been confirmed by several experimental studies conducted in open-top and closed-top chambers or using the Free-Air Carbon dioxide Enrichment (FACE) method (Shams et al. 2012; Wullschleger et al. 2002). On the other hand, more biomass means more evapotranspiration because of a higher leaf area index (LAI) (Wand et al. 1999; Piao et al. 2010), potentially offsetting the effect of the reduction in stomatal conductance (Bernacchi et al. 2007). However, even under experimental conditions, there is a large uncertainty in the CO_2 induced change in stomatal conductance, especially when scaling from the single leaf to a full canopy where other factors affect the whole process (Polley 2002). For example, CO_2 effect is significantly different between C_3 and C_4 plants and between trees and smaller plants (Taiz and Zeiger 1991), but also seems to depend on the scale of the experiment (Jarvis and McNaughton 1986; Bunce 2004). In fact, most of the existing knowledge on plants response to higher CO_2 concentrations is based on small scale research experiments conducted in open field with controlled environment. Even if there are techniques such as FACE that allow the exposure of plants to elevated CO_2 concentrations under natural and fully open-air conditions, they can be difficult and expensive to construct and operate, which limits the inference space of these experiments with regards to the range of global ecosystems (Norby et al. 2016). Moreover, there could be an overestimation of the

CO_2 effect due to artificial ventilation and advection from outside the FACE area (Kruijt et al. 2008). Given the complexity of the effect of CO_2-sensitivity of evapotranspiration on future climate simulations and the large uncertainty in the CO_2 induced change in stomatal conductance under experimental conditions (Kruijt et al. 2008), understanding plant responses to CO_2 is becoming increasingly important. The following sections summarize some of the most documented r_c models, precisely those directly used or modified to account for the effect of CO_2 on the evapotranspiration. The models presented have their limitations that the authors tried to underline. However, because the literature is limited regarding this particular topic, the primary purpose of this review was to provide a brief reference document for researchers and the scientific community in general on the different models developed so far and their main findings and challenges.

2.3. Description and discussion of evapotranspiration approaches accounting for CO_2 effect

2.3.1. Penman-Monteith method adapted to an increase in CO_2 concentrations

The standardized Penman–Monteith equation (FAO-PM) (Allen et al. 1998) is based on the Penman–Monteith equation (Monteith 1965). It is the most widely used method and has been proven to be a good ET_o estimator when compared with other methods, especially for daily computations (Chiew et al. 1995; Liu et al. 1997; Ventura et al. 1999; Jacobs and Satti 2001; Garcia et al. 2004; Temesgen et al. 2005). For a grass reference surface and for a daily time step, this equation is expressed as:

$$ET_o = \frac{0.408\Delta(R_n - G) + \gamma \frac{900}{T_{2m}+273} u_2 (e_s - e_a)}{\Delta + \gamma(1 + 0.34u_2)} \quad (2\text{-}2)$$

where ET_o is the reference evapotranspiration (mm day^{-1}); R_n is the net radiation at the crop surface (MJ m^{-2} day^{-1}); G is the soil heat flux density (MJ m^2 day^{-1}); T_{2m} is the mean daily air temperature at 2 m height (ºC); u_2 is the wind speed at 2 m height (m s^{-1}); e_s is the saturation vapour pressure (kPa); e_a is the actual vapour pressure (kPa); $(e_s - e_a)$ is the saturation vapour pressure deficit (kPa); Δ is the slope of the vapour–pressure curve (kPa ºC^{-1}) and γ is the psychometric constant (kPa ºC^{-1}). The canopy resistance r_c describes the resistance of vapour flow through the transpiring crop and evaporating soil surface. It is represented in the equation above by the value 0.34 in the denominator:

$$0.34u_2 = \frac{70}{208/u_2} = r_c/r_a \quad (2\text{-}3)$$

where r_a is the aerodynamic resistance (s m^{-1}), which describes the transfer of heat and water vapour from the evaporating surface into the air above the canopy. For a grass reference surface, assuming a constant crop height of 0.12 m and a standardized height for wind speed, temperature and humidity at 2 m, r_a becomes:

$$r_a = 208/u_2 \quad (2\text{-}4)$$

Under the same reference conditions, and knowing that the stomatal resistance r_s of an actively transpiring C_3 grass leaf surface has a value of about 100 s m^{-1}, r_c is represented as the following:

$$r_c = \frac{r_s}{0.5\ LAI} = \frac{100}{0.5\times 2.88} = 69 \approx 70\ s\ m^{-1} \quad (2\text{-}5)$$

where *LAI* is the leaf area index of the upper half of dense clipped grass, which is generally the only part actively contributing to the surface heat and vapour transfer (LAI = 24 × crop height (h) = 24 × 0.12 = 2.88). Assuming that the $r_c \approx 70$ s·m^{-1} applies to a specific CO_2 concentration of 372 ppm, estimating a new r_c value for higher CO_2 concentration provides a method to estimate possible impacts of higher CO_2 on ET_o. Thus, the following form of FAO-PM equation should be adopted:

$$ETo = \frac{0.408\Delta(R_n - G) + \gamma \frac{900}{T_{2m}+273} u_2 (e_s - e_a)}{\Delta + \gamma(1 + r_c/r_a)} \quad (2\text{-}6)$$

Lovelli et al. (2010) and Snyder et al. (2011) used this method in a Mediterranean climate, introducing in the equation published values regarding atmospheric CO_2 on stomatal conductance (Ainsworth and Long 2004; Long et al. 2004a), and considering the temperature increment effect on the reference evapotranspiration (ET_o) variation. They concluded that the effect of increasing CO_2 concentration may be annulled by an increase in air temperature and subsequent increase in evapotranspiration rate. On the other hand, Moratiel et al. (2011) found out that the CO_2 increase from 372 ppm to 550 ppm would create a reduction of the ET_o increment by half, from 11% to 5% in the next 50 years, as compared to the current situation in northern Spain. By recalibrating the canopy conductance for the widely acclaimed and recommended FAO-PM equation, this approach

may be particularly effective in evaluating the effects of climate change on crop water use. However, The FAO-PM model is based on the "big leaf" approximation with constant canopy resistance, which is a simplistic assumption that could limit the accuracy of the predictions of the model. Considering the driving meteorological variables at a particular site, estimates made with the FAO-PM equation rely on the correct modeling of the effective values of both aerodynamic resistance r_a and canopy resistance r_c. Hence, the fixed value for r_c may be the cause of the tendency for the FAO-PM method to underestimate the higher values of measured ET_o, and to overestimate the lower ET_o values in semi-arid and windy areas with a high evaporative demand (Hussein 1999; Ventura et al. 1999; Berengena and Gavilán 2005). As r_a can be calculated from meteorological conditions, in order to provide more accurate estimations of evapotranspiration using the FAO-PM equation, it may be necessary to parameterize r_c as a primary factor in the evapotranspiration process (Monteith 1965). Canopy resistance r_c is a physiological parameter with an aerodynamic component (Alves et al. 1998). It is difficult to estimate it for different climatic and crop water conditions, as it is influenced by solar radiation, temperature, vapor pressure deficit and soil water content (Pereira et al. 1999; Lecina et al. 2003). Nevertheless, a simple attempt to model this resistance may yield a better estimation when the FAO-PM equation is applied over both short and tall crops (Pereira et al. 1999; Alves and Pereira 2000) and over other types of vegetation (Margonis et al. 2017; Chávez and López-Urrea 2019). It could also be useful to incorporate the effects of the resistance due to vegetation into climatic and hydrological models (Bie et al. 2015; Yang et al. 2019).

In this context, some studies incorporated a "CO_2-factor" into the FAO-PM equation (Easterling et al. 1992; Ficklin et al. 2009; Parajuli 2010; Islam et al. 2012; Wu et al. 2012; Priya et al. 2014; Fares et al. 2015). Then, equation (1) can be rewritten as:

$$ET_o = \frac{0.408\Delta(R_n - G) + \gamma \frac{900}{T_{2m}+273} u_2 (e_s - e_a)}{\Delta + \gamma\left(1 + \frac{0.34 u_2}{CO_2 - factor}\right)} \quad (2\text{-}7)$$

where, in the denominator, a linear relationship for stomatal conductance as a function of CO_2 level is introduced. It was developed by Stockle et al. (1992), and based on 80 data sets comparing leaf conductance at 330 ppm and at 660 ppm of CO_2 concentration for a wide range of species including C_3 and C_4 crops:

$$g_{CO_2} = g\left[1.4 - 0.4\ {}^{CO_2}/_{330}\right] \quad (2\text{-}8)$$

where g_{CO2} is the leaf conductance modified to reflect CO_2 effects (m s^{-1}); g is the conductance without the effect of CO_2 (m s^{-1}); CO_2 is the actual atmospheric CO_2 concentration (ppm) and 330 represents the baseline atmospheric CO_2 concentration (ppm). The new r_c is as follows:

$$r_c = \frac{1}{g_{CO_2} \times 0.5\ LAI} \quad (2\text{-}9)$$

The "CO_2-factor" is based on experimental observations of a 40% linear decrease in stomatal conductance between 330 and 660 ppm CO_2 concentrations (Morison and Gifford 1983). Islam et al. (2012) incorporated this model in the FAO-PM equation to evaluate the effects of possible future anthropogenic climate change on ET_o. Results of the different simulation studies showed an increase in ET_o with changing climate, but the impact of increasing temperatures was almost offset by increasing CO_2 levels. In fact, sensitivity analysis showed that the effect of a 1°C rise in temperature was offset by an increase in CO_2 levels up to 450 ppm, whereas the effect of a 2°C temperature rise was offset by CO_2 concentrations of 660 ppm, thus in close agreement with results found by Priya et al. (2014) using the same model. Authors pointed out that, due to its linearity, this "CO_2- factor" is only valid in the range of 330 to 660 ppm. For CO_2 concentrations beyond 660 ppm, factors for specific crops reported by Allen (1990) were used. The same remark was made by Ficklin et al. (2009) when increasing CO_2 concentration to 970 ppm and temperature by 6.4 °C caused watershed-wide average evapotranspiration, averaged over 50 simulated years, to decrease by 37.5%, resulting in an increase of water yield by 36.5%. They explained that the linear assumption of eq. (2-8) means that it is suitable for all plant species, which may lead to an overestimation of the aforementioned reduction in ET_o in the presence of multiple types of land cover. They concluded that because of this broad simplification of the effects of CO_2 on plant growth, their analysis was still too uncertain for water management purposes. The presumed overestimation of ET_o is because this "CO_2-factor" is based on the assumption that a doubling of CO_2 concentration would lead to a general decrease of 40% in stomatal conductance (Morison 1987) irrespective of the land cover type. This reduction of conductance is assumed to be linear over the entire range of CO_2 concentrations between 330 ppm and 660 ppm (Morison and Gifford 1983). To overcome this issue, Wu et al. (2012) proposed an optimized equation:

$$g_{CO_2} = g\left[(1 + p) - p\ {}^{CO_2}/_{330}\right] \quad (2\text{-}10)$$

where *p* is the percentage decrease in leaf conductance specific to vegetation types (Authors provided different values in their study). The modified equation inherently gave a better representation of this increasing CO_2 effects than the original equation by incorporating the CO_2 effects dynamically in more process-based details.

Olioso et al. (2010) suggested multiplying the FAO-PM ET_o by another factor F to correct the daily values of reference evapotranspiration taking into account the effect of higher CO_2 concentrations. This factor was derived from evapotranspiration simulations of the ISBA-A-gs model (Calvet et al. 1998) at different CO_2 levels, and used in different studies (Martin et al. 2011; Lardy et al. 2012; 2014; Salmon-Monviola et al. 2013; Katerji et al. 2017):

$$F = 1.1403 - 3.8979 \times 10^{-4} \times [CO_2] \quad (2\text{-}11)$$

The value of *F* is approximately 1 when the mean annual value of the air CO_2 concentration is equal to 370 ppm. *F* decreases or increases when the CO_2 concentration is higher or lower than this threshold. For example, the decrease in ET_o is approximately 8 and 20 % when the CO_2 concentration reaches 550 and 900 ppm, respectively (Olioso et al. 2010). The factor is also based on a linear relationship between the decrease of ET_o and the increase of the CO_2 concentration, which raises the same concerns previously discussed.

According to Katerji et al. (2017), the issue of the approaches mentioned above is that they are insufficient to adapt the FAO-PM equation to the increasing concentrations of CO_2. These solutions always consider the resistance r_c to be constant by neglecting its reliance on climatic variables, which means that r_c parameterization is required to reduce the difference between the directly measured ET_o values, and those estimated using the FAO-PM model.

2.3.2. Penman-Monteith method with variable canopy resistance models

2.3.2.1. Jarvis Model

Jarvis model is a phenomenological and multiplicative empirical model that interprets field measurements of stomatal conductance g_{CO2} in relation to environmental variables. It calculates g_{CO2} by multiplying the maximum conductance g_{max}, which is a value which represents the highest *g* recorded under optimal conditions (Korner et al. 1979), with a number of empirical response functions, including one for CO_2-sensitivity, and it is assumed that each variable acts independently (Jarvis 1976; Whitehead 1998):

$$g_{CO_2} = \frac{1}{r_s} = g_{max}\, f(I) f(T_a) f(C_a) f(VPD) f(\Psi) \quad (2\text{-}12)$$

where I is the absorbed photosynthetic photon flux density (μmol m^{-2} s^{-1}), T_a is the air temperature (°C), C_a is the CO_2 concentration (ppm), VPD is the Vapour Pressure Deficit (kPa) and Ψ is the soil water potential (Pa).

Same as the aforementioned models, Jarvis model is also based on a linear function between the stomatal conductance g_{CO2} and atmospheric CO_2. In fact, Jarvis (1976) concluded that g_{CO2} decreased linearly when the increase in CO_2 concentration is within the range of 100-1000 ppm, and that it stays constant when the CO_2 concentration is <100 ppm or >1000 ppm. Also, equation (12) may underestimate g_{CO2} when relative humidity (RH) is high because it correlates g_{CO2} linearly to RH (Wang et al. 2009). In this case, a nonlinear function of RH or VPD may reduce the bias (Leuning 1995; Wang et al. 2009). Nevertheless, Jarvis model has been used in different forms in many studies (Hanan and Prince 1997; Gharsallah et al. 2013; Zhang et al. 2016; Zhou et al. 2019). In the east coast region of North America, elevated atmospheric CO_2 was found to reduce ET at a rate of 0.84 mm y^{-1} between 1901 and 2008 when calculating stomatal conductance with a Jarvis-type equation in the Dynamic Land Ecosystem Model (DLEM) 2.0 (Yang et al. 2015). Using the same model in a global scale, Pan et al. (2015) concluded that increasing atmospheric CO_2 will lessen the positive effect of warming temperature and increasing precipitation on ET by the end of the 21st century. Medlyn et al. (2001) analyzed data from 13 long-term (>1 year) field-based studies of the effects of elevated CO_2 concentration (350 ppm and 700 ppm) on European forest tree species by fitting data to two models namely Jarvis and Ball (Ball et al. 1987). Their meta-analysis indicated a significant decrease (21%) in stomatal conductance in response to growth in elevated CO_2 concentrations across all studies, resulting in a decrease of ET. Some authors think that another limit of the Jarvis model is that each response function has to be adjusted to the data to be able to provide good predictions for any type of vegetation, since they are specific for only certain crops and climate conditions and they cannot be used for general purposes (Yu and Wang 2010). Consequently, a site-specific calibration of the empirical response functions becomes necessary. Another criticism formulated against this approach is that the knowledge of stomatal resistance r_s alone may not be sufficient to calculate ET because the FAO-PM equation requires r_c. Hence, the upscaling of r_s to the canopy level is required to calculate r_c, which could be quiet challenging (Irmak et al. 2008). Besides, Alves and Pereira (2000) questioned the validity of the multiplicative

model because it only includes the physiological component of r_c but not the aerodynamic component r_a and because of the assumption of environmental variables acting independently.

2.3.2.2. Katerji and Perrier (KP) model

Based on the fact that r_c, for well-watered crops, varies during the day with different climatological variables, Katerji et al. (1983) suggested a new semi-empirical procedure to determine both resistances r_c and r_a by applying the Buckingham π-theorem (Kreith and Bohn 2001). They established a linear relationship between the canopy resistance r_c and the climatic resistance r^* (Monteith 1965):

$$r_c/r_a = a\, r^*/r_a + b \tag{2-13}$$

where a and b are empirical calibration coefficients which vary with crop type but not with site (Rana et al. 1998). Parameter values for a few crops were provided by Katerji and Rana (2014). r^* (s m^{-1}) is represented by the following equation:

$$r^* = \frac{\Delta+\gamma}{\Delta\gamma}\frac{\rho C_p D}{R_n - G} \tag{2-14}$$

where ρ is the air density (kg m^{-3}), C_p the specific heat of moist air (J kg^{-1} °C^{-1}) and D is the vapor pressure deficit (VPD) (kPa).

However, this model still does not take into account the impact of the air CO_2 concentration value on the resistance r_c. After incorporating their model into the FAO-PM equation (PM-KP), Katerji et al. (2017) used a CO_2 correction factor (Olioso et al. 2010) with the PM-KP equation to compare it to the standard Penman- Monteith method (FAO-PM) with a fixed r_c value. PM-KP yielded better performances in forecasting the ET_o directly measured by weighing lysimeters during the summer season for the measured period (1986–2006) in Apulia region in southern Italy (Katerji et al. 2017). The results demonstrated that the FAO-PM formula underestimated the measured ET_o values by 20 %, whereas the underestimation is only 3 % for the PM-KP formula.

This semi-empirical KP approach has been widely used in the subsequent literature (Peterschmitt and Perrier 1991; Alves and Pereira 2000; Lecina et al. 2003; Steduto et al. 2003; Pauwels and Samson 2006; Liu et al. 2012; Margonis et al. 2017). However, one of its main limitations is the need for a specific calibration, even if it can be unnecessary under certain circumstances (Rana et al. 1998; 2001; Katerji and Rana 2008). Furthermore, Gharsallah et al. (2013) insisted that the

model's performance would probably be improved calibrating the *a* and *b* parameters for the main phenological phases of crops, making the use of this model even more complicated. A second limitation is the fact that it depends on the temporary value of the Bowen ratio *β,* which is not readily available (Perez et al. 2006). Besides, the KP model seems to fail under irrigated conditions in semiarid to arid regions (Allen et al. 2006).

2.3.2.3. Modified Makkink equation

Makkink model (Makkink 1957) is a simple empirical method for ET_o estimation that uses only temperature and radiation parameters:

$$ET_o = \alpha \frac{S}{\lambda (S+\gamma)} K\downarrow \quad (2\text{-}15)$$

where $K\downarrow$ is the incoming short-wave (global) radiation (W m^{-2}), λ is the latent heat of vaporization of water (J kg^{-1}), S is the temperature-dependent gradient of the saturated vapour pressure curve (Pa K^{-1}) and α is an empirical coefficient (= 0.65).

This formula does not take into consideration the effects of CO_2. To fix that, Kruijt et al. (2008) multiplied eq. (2-15) with a correction factor *c*:

$$c = S_g \times S_T \times F_T \times \Delta_{CO2} \quad (2\text{-}16)$$

$$S_g = (dg/g)/dCO_2 \quad (2\text{-}17)$$

$$S_T = (dT/T)/(dg/g) \quad (2\text{-}18)$$

where g is the stomatal conductance (mol m^{-2} s^{-1}), S_g is the sensitivity of g to CO_2 (ppm^{-1}), S_T is the relative sensitivity of transpiration T to g (kg m^{-2} s^{-1}), F_T is the transpiration share of evapotranspiration and Δ_{CO2} is the change in atmospheric CO_2 concentration (ppm).

After parametrizing S_g, S_T and F_T based on the literature, Kruijt et al. (2008) provided correction factors applied to a projected additional increase of atmospheric CO_2 concentrations in 2050 and 2100 by 150 and 385 ppm respectively for various vegetation categories. Results of their study suggest that direct effects of CO_2 reducing evapotranspiration can be expected to be moderate, up

to 5% in the coming 50 years and up to 15% by 2100. Applying their methodology in Central and Eastern Europe resulted in a decrease in reference evapotranspiration rates compared with runs that did not consider increases in CO_2 levels (Eitzinger et al. 2013). Similarly, Huntington et al. (2016) concluded that crop evapotranspiration is projected to increase in all basins of Western United States, especially areas where perennial crops are grown, and with smaller increases in areas where annual crops are grown.

Based on the extensive number of manuscripts on the topic reviewed by the authors, there is an abundance of models with a modified canopy resistance r_c (e.g. Shuttleworth and Wallace 1985; Massman 1992; Stannard 1993; Todorovic 1999; Irmak and Mutiibwa 2010). However, very few of them took in consideration the change in atmospheric CO_2, hence the small number of models discussed in this study. This is essentially because when the time span of the research is short, the change in atmospheric CO_2 concentration is very small and is generally ignored (Zhang et al. 2008; Li et al. 2014). Furthermore, some of these models were not even incorporated into the FAO-PM equation to estimate ET responses to increased CO_2 concentration (e.g. (Ball et al. 1987; Wang and Wen 2010). The main issue with the previously reviewed models is that the relationship between stomatal conductance and CO_2 concentration is assumed to be a simple linear one, which is an assumption only valid within the limited range of 330–660 ppm (Li et al. 2019). In fact, those models rarely went beyond that range where data are better fitted with a nonlinear curve. This observation is consistent with the findings of Heath and Russel (1954), Morison and Gifford (1983) and Wang and Wen (2010). Thus, it is crucial and indispensable to validate the accuracy and reliability of these models when applying them into the FAO-PM equation especially when the CO_2 concentration is higher than 660 ppm, and to choose the appropriate one to improve the estimation of ET under elevated CO_2 concentration. Although some studies applied modified simple empirical equations, such as Makkink (Kruijt et al. 2008) and Priestley-Taylor (Rosenzweig and Iglesias 1998; Hatch et al. 1999; Strzepek et al. 1999) to account for the vegetation responses to an elevated atmospheric CO_2, the FAO-PM method has been always considered to be the most reliable one for various climatic conditions due to its physically based characteristic with incorporating both physiological and aerodynamic parameters (Xu et al. 2006). However, its use of a fixed canopy resistance of 70 s m^{-1} is perceived as weakness, as surface resistance may change with climate and weather parameters, variation in day length, or differences between daytime and nighttime wind (Pereira et al. 1999). In fact, this fixed r_c hypothesis has not been verified in

experimental trials carried out on irrigated grass surfaces which underlined significant variations in the canopy resistance r_c on daily and seasonal scales (Rana et al. 1994; Lecina et al. 2003; Steduto et al. 2003; Katerji and Rana 2006; Perez et al. 2006). The same criticism applies to the models discussed above since they are replacing the constant daily values of the grass r_c with different but always constant values or using a simple correction factor with the FAO-PM formula, which could be because of the complexity of the canopy resistance modelling (Katerji and Rana 2006).

2.4. Conclusion

This paper provides an overview of surface resistance models found in literature that included the effect of CO_2 on crop evapotranspiration. The paper reports a brief explanation of the main theories and assumptions involved in the models' development and underlines their main characteristics. Using these models would help improving the accuracy of ET estimations. Yet, modeling canopy resistance is a difficult task as its value depends on vegetation type, climate, plant architecture and, in water scarcity conditions, on plant and/or soil water status (Shuttleworth and Gurney 1990). This complexity caused the dissimilarity in results when using some of the aforementioned models in this review, which is also due to the conflicting effect that increase in CO_2 concentration has with increase in temperature. Hence, there is still a need to enhance the robustness of the resistance modeling procedure in order to be applied to different crops under different climatic conditions and under diverse future climate change scenarios. Actually, the great bulk of studies carried out on canopy resistance modelling compared the performance of these models with that of the FAO-PM approach or with different models for estimating ET_o, and very few researchers have actually attempted to estimate future changes in ET_o based on projected climate change scenarios and estimates of increased CO_2 concentrations. Furthermore, many models were not even tested with the FAO-PM equation, justifying Yang et al. (2019) statement that many present climate models do not account for vegetation responses to an elevated atmospheric CO_2, thus seriously questioning the claim of 'warming leads to drying' in earlier studies.

We note in conclusion that there is a growing need for improved surface resistance models, that may simulate better the changes in stomata physiological responses, thus enhancing the accuracy, reliability and applicability of ET estimates.

Chapter 3

Impacts of Climate Change and Rising Atmospheric CO_2 On Future Projected Reference Evapotranspiration in Emilia-Romagna (Italy)

The original research described in this Chapter has been submitted for publication as:

Ben Hamouda G, Tomozeiu R, Pavan V, Antolini G, Snyder RL, Ventura F. Impacts of Climate Change and Rising Atmospheric CO_2 On Future Projected Reference Evapotranspiration in Emilia-Romagna (Italy). Theor. Appl. Climatol. In Review

3. Impacts of Climate Change and Rising Atmospheric CO_2 On Future Projected Reference Evapotranspiration in Emilia-Romagna (Italy)

Abstract

The continuous increase of atmospheric CO_2 content mainly due to anthropogenic CO_2 emissions is causing a rise in temperature on earth, altering the hydrological and meteorological processes and affecting crop physiology. Evapotranspiration is an important component of the hydrological cycle. Thus, understanding the change in evapotranspiration due to global warming is essential for better water resources planning and management, and agricultural production. In this study, the effect of climate change with a focus on the combined effect of temperature and elevated CO_2 concentrations on reference evapotranspiration (ET_o) was evaluated using the Penman-Monteith equation. A EURO-CORDEX regional climate model (RCM) ensemble was used to estimate ET_o in five locations in Emilia-Romagna region (Northern Italy) during the period 2021–2050. Then, its projected changes in response to different CO_2 concentrations (i.e. 372 ppm and 550 ppm) under two Representative Concentration Pathways (RCP) scenarios (i.e. RCP4.5 and RCP8.5) were analyzed. Simulation results with both scenarios, without increasing CO_2 levels (372 ppm), showed that the annual and summertime ET_o for all locations increased by an average of 4% to 5.4% with regard to the reference period 1981-2005, for an increase of air temperature by 1 °C to 1.5 °C. When the effect of elevated CO_2 levels (550 ppm) was also considered in combination with projected changes in temperature, changes in both annual and summer ET_o demand for all locations varied from -1.1% to 2.2% during the 2021-2050 period with regard to the reference period 1981-2005. This shows that higher CO_2 levels moderated the increase in ET_o that accompanies an increase in air temperature.

Keywords: Penman Monteith equation; Evapotranspiration; CO_2 effect; Stomatal resistance; CORDEX RCM; Climate change.

3.1. Introduction

The increase of anthropogenic emissions of carbon dioxide (CO_2) and other radiatively active gases, due to activities such as fossil fuel combustion and deforestation, are one of the most prominent causes of climate change (Hamza et al. 2020). The relentless rise of CO_2 concentrations will most probably influence water fluxes and resources at both local and global scales (Haddeland

et al. 2014). This effect will be intensified by the projected increases in global surface air temperature (IPCC 2013) leading to an uneven distribution of water resources and causing several problems in water availability (Estrela et al. 2012; Boehlert et al. 2016; Akbarpour and Niksokhan 2018). This is especially true in the Mediterranean region as it has shown large climate shifts in the past and it has been identified as one of the most prominent "Hot-Spots" in future climate change projections, with an expected greater than average warming, mostly in summer, and an increase of heat waves and dry spells (Olesen and Bindi 2002; Giorgi and Lionello 2008). Similar conclusions were drawn on a smaller scale in Northern Italy and Emilia Romagna region. The future projections constructed at local scale through statistical downscaling techniques in the framework of different emission scenarios indicate that significant changes in temperature are very likely to occur during all seasons. A shift of the probability distribution functions to warmer values is projected for both minimum and maximum air temperature. The shift will be more noticeable in summer, when the changes of mean values are expected to be about 2.5 °C in the 2021-2050 period (with respect to 1961-1990) (Tomozeiu et al. 2007, 2014). These changes are projected to became more pronounced toward the end of the century. To better understand the effect of climate change on the hydrological cycle, evapotranspiration is widely used as it is the only link between the energy balance and water balance (Wang et al. 2020). Evapotranspiration represents the simultaneous processes of transfer of water to the atmosphere by transpiration and evaporation in a soil-plant system (Allen et al. 1998). In particular, reference evapotranspiration (ET_o) is an important hydrological variable for irrigation water management and hydrological modeling (Immerzeel and Droogers 2008; Pereira et al. 2020). Since the agricultural sector accounts for 70% of freshwater withdrawals (Kummu et al. 2012) and around 90% of global freshwater consumption (Wada et al. 2012), improved understanding of changes in evapotranspiration is essential for dependable projections of global freshwater availability under conditions of climate change. An increase in air temperature is known to cause an increase in crop water requirements because it tends to stimulate plant transpiration (Allen et al. 2003), hence decreasing water use efficiency (WUE). This is mainly due to a decrease in leaf photosynthesis and an increase in stomatal conductance to water vapor (Kirschbaum 2004). Additionally, higher temperatures, especially when combined with lower precipitation, would raise the irrigation requirements of crops (Döll 2002; Moreno et al. 2005), alter the length of the growing season (Menzel and Fabian 1999; Linderholm 2006) and negatively affect crop yield (Lobell and Field 2007). On the other hand, the increase in CO_2 concentration has opposite physiological effects

on plants, e.g. faster photosynthesis rate, greater leaf area, increase in biomass and yield, and decrease in stomatal conductance and evapotranspiration rate (Allen 1990; Ainsworth and Long 2004; van der Kooi et al. 2016), which could offset the consequences of air temperature increase. However, the magnitude of this effect is uncertain and still controversial within the scientific community (Allen 2000; Long et al. 2005; Tubiello et al. 2007) because evapotranspiration is a complex and nonlinear phenomenon depending on several other interacting factors such as humidity, wind speed, radiation, and type and growth stage of crops (Polley 2002). The impact of the interaction of these different factors on evapotranspiration was assessed using a modification of the standardized (FAO-PM) Penman–Monteith equation (Allen et al. 1998) by Snyder et al. (2011) and Moratiel et al. (2011). They adjusted the stomatal resistance factor (the reciprocal of stomatal conductance) to account for an increase in CO_2 concentration (Lovelli et al. 2010). Other approaches could also be used in association with the FAO-PM equation (Ben Hamouda and Ventura 2020). However, they are either more complex or insufficiently tested. The main issue with the Penman Monteith equation is data availability and the difficulty to access to these data, especially in Italy were weather monitoring networks are managed by regional and national services, without a common data sharing policy and data distribution platform (Pavan et al. 2013; Pelosi et al. 2020). This prompted researchers to look for alternative ways for obtaining the input data: estimation (de Carvalho et al. 2013; Córdova et al. 2015), weather forecast (Cai et al. 2007; Silva et al. 2010; Lorite et al. 2015), satellite imagery (Montero et al. 2018), remote sensing (Teixeira 2010), a combination of remote sensing and machine learning (Zhang et al. 2018), artificial neural networks (ANNs) (Kumar et al. 2002), fuzzy and neuro-fuzzy systems and genetic algorithms (Kisi and Cengiz 2013; Shiri et al. 2012). Another alternative choice is using reanalysis data. Climate reanalysis combine past observations with models to generate consistent time series of multiple climate variables, providing comprehensive snapshots of conditions at regular intervals over long time periods often years or decades (Parker 2016). The main advantages of reanalysis products is their spatial and temporal resolution consistency over three or more decades, the large quantity of variables available and the continuous improvements of their model resolution and biases (Schubert et al. 2008; Dee et al. 2016). This is why reanalysis products are among the most-used datasets in the study of weather and climate (Fuka et al. 2014; Essou et al. 2017; Bhattacharya et al. 2019; Uniyal et al. 2019; Luo et al. 2020). However, few studies compared ET_o computed using reanalysis data with observed ET_o data (Yao et al. 2014; Martins et al. 2017; Tian et al. 2018).

The aim of this study is to assess the effect of future climate, with focus on evapotranspiration (ET_o), in Emilia-Romagna (Northern Italy) over the 2021-2050 period and under different emission scenarios. We use two Representative Concentration Pathway scenarios (RCPs) and three Regional Climate Models (RCMs). ET_o is first evaluated using reanalysis data as an alternative to observations. Then, the bias-correction of the different RCMs is performed. Finally, changes in ET_o under different RCPs with or without the effects of elevated CO_2 levels are evaluated.

3.2. Methodology

3.2.1. Study area

Emilia-Romagna is an administrative region located in Northern Italy, between 43° 80′ and 45° 10′ N, and 9° 20′ and 12° 75′ E. Agriculture is an important sector in the region: within the total area of 22 452 km^2, 10 642 km^2 are devoted to agriculture (Regione Emilia-Romagna 2010). Climate in the region is mainly influenced by a variable geomorphology, represented by the Po River in the North, the Adriatic Sea in the East and the Apennines Mountains to the South. The Köppen- Geiger climate classification indicates a temperate fully humid climate with hot summers (Cfa) in the North, central, and northeastern plain areas, and fully humid climate with warm summers (Cfb) in the mountain and highlands areas, especially in the South and South-West (Kottek et al. 2006). The locations of the five agrometeorological stations selected for this study and their details are shown in Figure 3-1 and Table 3-1. The choice of these stations is based mainly on their data availability and their representativeness of the regional territory.

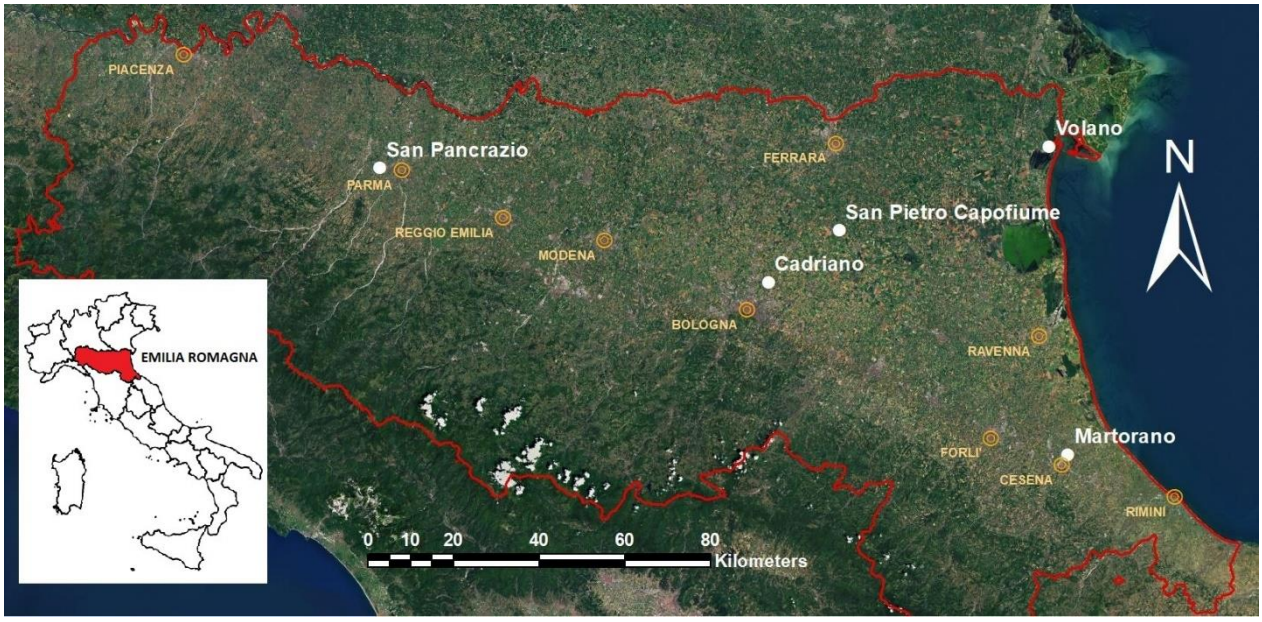

Fig. 3-1. Location of the agrometeorological stations considered in this study

Table 3-1. Description of the agrometeorological stations

Station	Latitude	Longitude	Elevation (m)	Location
Cadriano	44° 32' 59.99' N	11° 23' 59.98" E	31	Central Emilia-Romagna plain (University of Bologna)
Martorano	44° 9' 58.10" N	12° 16' 4.71" E	19	Southeastern Emilia-Romagna plain
San Pancrazio	44° 48' 29.02" N	10° 16' 20.82" E	55	Western Emilia-Romagna plain
San Pietro Capofiume	44° 39' 13.59" N	11° 37' 21.50" E	6	Central Emilia-Romagna plain (The Reno basin)
Volano	44° 48' 46.32" N	12° 15' 1.32" E	0	Coastal area

3.2.2. Climate data

3.2.2.1. Reanalysis data

Since it is difficult to find continuous observed dataset long enough to make climatological estimates of ET_o, it was decided to evaluate it starting from hourly ERA5-Land reanalysis data downloaded from the Copernicus Climate Data Store (Copernicus CDS)

(https://cds.climate.copernicus.eu). ERA5-Land is a reanalysis dataset developed by the Copernicus Climate Change Service (C3S) at the European Centre for Medium-Range Weather Forecasts (ECMWF), providing a consistent view of the evolution of land variables over several decades at 9 km resolution, which is an enhanced resolution compared to ERA5 (31 km). ERA5-Land has been produced by replaying the land component of the ECMWF ERA5 climate reanalysis. The core of ERA5-Land is the Tiled ECMWF Scheme for Surface Exchanges over Land incorporating land surface hydrology (H-TESSEL). Reanalysis data and specifically ERA5 and ERA5-Land give satisfactory results when compared with observations (Ben Hamouda et al. 2019; Mahto and Mishra 2019; Tarek et al. 2020; Pelosi et al. 2020).

ERA5-Land data are produced with an hourly time-step from 1981 to present. The 25 years between 1981-2005 will be used as reference period. Extracted data for that period include mean 2m air temperature (K), mean 2m dew point temperature (K), mean downward surface solar radiation (J m^{-2}), and mean 10m u and v components of wind (m s^{-1}). The retrieved 10 m wind speed components were adjusted for a 2 m height using a logarithmic wind speed profile (Allen et al. 1998), then wind speed was calculated as: $WS = \sqrt{u^2 + v^2}$. Maximum and minimum air temperature were transformed to °C. All data were aggregated to a daily timescale.

3.2.2.2. Observed data

Observed data for the different meteorological variables needed for the calculation of ET_o for the reference period 1981-2005 were not available or incomplete. Since data were only available for the period 2008-2018 for the five agrometeorological stations, they were hence used only for validation purpose. Data for the stations of Martorano, San Pancrazio, San Pietro Capofiume and Volano were made available by the "Regional Agency for Prevention, Environment and Energy of Emilia-Romagna" (Arpae) via their Dext3r application (https://simc.arpae.it/dext3r). Data include daily mean 2 m air temperature (°C), daily mean relative humidity (%), hourly mean global solar irradiance (W m^{-2}) and daily mean 10 m wind speed (m s^{-1}). The August-Roche-Magnus (Lawrence 2005) approximation was used in order to compute the dew point temperature from the mean relative humidity and air temperature. The retrieved 10 m wind speed was adjusted for 2 m height. The same meteorological variables were also available at an hourly basis from the agrometeorological station of the Department of Agricultural and Food Sciences of the University of Bologna (Distal), installed at the experimental farm of Cadriano (Bologna). The only difference

is that mean wind speed data were measured at 2 m height. Finally, all hourly data were aggregated to a daily timescale.

3.2.2.3. Euro-Cordex climate projections

To study the future changes in ET_o, we used data made available by EURO-CORDEX Regional Climate Models (RCMs) with a daily time step. In particular, data from three regional models were used, RCA4 (Christensen et al. 2007), RACMO22E (Van Meijgaard et al. 2008) and HIRHAM5 (Samuelsson et al. 2015), with a horizontal resolution of 0.11° (12 × 12 km). EURO-CORDEX is the European branch of the international CORDEX initiative, which is a program sponsored by the World Climate Research Program (WRCP). It is the largest ensemble of RCM simulations covering all of Europe (Jacob et al. 2014). The choice of the RCMs was mainly based on the availability of the data necessary for the calculation of ET_o. Data were extracted from Copernicus CDS for the reference period 1981-2005 and the future period 2021-2050, and for two Representative Concentration Pathways RCP4.5 and RCP8.5. Representative Concentration Pathways (RCPs) were defined by the Intergovernmental Panel on Climate Change (IPCC) for its 5th Assessment Report (AR5) to provide time-dependent projections of atmospheric greenhouse gas (GHG) concentrations based on socio-economic scenarios of how global society grows and develops (van Vuuren et al. 2011). RCP4.5 was developed using the MiniCAM model (Thomson et al. 2011) and represents a future where climate policies limit and achieve stabilization of greenhouse gas radiative forcing to 4.5 W m^{-2} by 2100, while RCP8.5 was developed using the MESSAGE model (Riahi et al. 2011) and is called a business-as-usual scenario, where high emissions of greenhouse gases continue as no policy changes are taken to reduce emissions. Daily data were downloaded from the Copernicus-CDS portal for the entire available period of 25 years from 1981 to 2005. Data include 2 m mean air temperature (K), 2 m mean relative humidity (%), surface solar downward irradiance (W m^{-2}) and 10 m wind speed (m s^{-1}). Dew point temperature was calculated using the August-Roche-Magnus approximation and the 10 m wind speed was adjusted for 2 m height.

3.2.3. The Penman-Monteith model

Reference evapotranspiration (ET_o) is the ET estimate from a standardized hypothetical crop having fixed height, albedo and canopy resistance (Allen et al. 1998). In this study, daily ET_o (mm day^{-1}) was computed using the FAO-Penman Monteith equation (FAO-PM):

$$ET_o = \frac{0.408\Delta(R_n - G) + \gamma \frac{900}{T_{2m}+273} u_2 (e_s - e_a)}{\Delta + \gamma(1 + 0.34u_2)} \quad (3\text{-}1)$$

where:

R_n net radiation at the surface (MJ m^{-2} day^{-1});

G soil heat flux density (MJ $m^2 day^{-1}$);

T_{2m} mean daily air temperature at 2 m height (°C);

u_2 wind speed at 2 m height (m s^{-1});

e_s saturation vapour pressure (kPa);

e_a actual vapour pressure (kPa);

$(e_s - e_a)$ saturation vapour pressure deficit (kPa);

Δ slope of the vapour–pressure curve (kPa $°C^{-1}$);

γ psychometric constant (kPa $°C^{-1}$).

To modify the CO_2 concentration in the FAO-PM equation, it is possible to estimate a new canopy resistance r_c value (Snyder et al. 2011; Ben Hamouda and Ventura 2020), which is represented in the equation above by the 0.34 in the denominator:

$$0.34u_2 = \frac{70}{208/u_2} = r_c/r_a \quad (3\text{-}2)$$

where r_a is the aerodynamic resistance to sensible and latent heat transfer (s m^{-1}). The stomatal resistance r_s of an actively transpiring C_3 grass leaf surface has a value of about r_s = 100 s m^{-1}. Using a leaf area index (LAI = 24 × crop height (h) = 24 × 0.12 = 2.88) and, assuming only half of the LAI contributes to transpiration, the canopy resistance for 0.12 m tall C_3 species grass r_c is calculated as:

$$r_c = \frac{r_s}{0.5\ LAI} = \frac{100}{0.5 \times 2.88} = 69 \approx 70\ s\ m^{-1} \quad (3\text{-}3)$$

The canopy resistance value of 70 sm^{-1} in the FAO-PM equation is assumed to apply to a CO_2 concentration of 372 ppm. Thus, to estimate possible impacts of higher CO_2 concentrations on ET_o, r_c is modified using the following form of the FAO-PM equation:

$$ET_o = \frac{0.408\Delta(R_n - G) + \gamma \frac{900}{T_{2m}+273} u_2 (e_s - e_a)}{\Delta + \gamma(1 + r_c/r_a)} \quad (3\text{-}4)$$

According to Long et al. (2004), stomatal conductance of many C_3 plants grown in Free-Air CO_2 Enrichment (FACE) experiments decreased about 20% when the CO_2 concentration was increased from 372 to about 550 ppm for about 200 independent measurements. Assuming this is true for the stomatal conductance of 0.12 m tall C_3 species grass with a stomatal resistance of 100 s m^{-1}, the stomatal conductance for C_3 grass should decrease from about 10 mm s^{-1} to 8 mm s^{-1}, which corresponds to r_s = 125 s m^{-1}. Using the same approach used to calculate r_c in eq. (3-3), the r_c for 550 ppm is calculated as:

$$r_c = \frac{r_s}{0.5\ LAI} = \frac{125}{0.5 \times 2.88} \approx 87\ s\ m^{-1} \quad (3\text{-}5)$$

Thus, increasing CO_2 concentration from 372 to 550 ppm should increase canopy resistance of 0.12 m tall C_3 grass from 70 to 87 s m^{-1}.

Reference evapotranspiration was calculated using daily data and then aggregated to annual and summer (June to August) values, since the latter is the most important season for agriculture and irrigation purposes in the Northern Hemisphere.

3.2.4. Data evaluation

3.2.4.1. Performance indicators

The performance of the reanalysis and RCMs data was evaluated at each agrometeorological station using the root mean square error (RMSE) and the (Bias) as statistical indicators, which are calculated as follows:

$$Bias = \frac{1}{n}\sum_{i=1}^{n}(A_i - B_i) \quad (3\text{-}6)$$

$$RMSE = \sqrt{\frac{1}{n}\sum_{i=1}^{n}(A_i - B_i)^2} \quad (3\text{-}7)$$

Where '*A'* is any of the model simulated data, '*B* 'is any of the reference data, '*i'* is the day number and '*n'* the number of examined days. A small RMSE, indicates that the difference between the simulated and reference data is small and the closer the Bias is to zero indicates a good simulation.

A positive Bias means that there is an overestimation, and a negative Bias means that there is an underestimation.

3.2.4.2. RCMs bias-correction

RCM simulations are subject to possible biases that are mostly due to parameterization of sub-grid processes, limited representation of local features, incorrect boundary conditions and differences between spatial resolutions of the simulations and observations (Benestad 2010; Ehret et al. 2012). To minimize these biases, the quantile mapping technique (QM) was employed to bias-correct air temperature, wind speed, solar radiation and dew point temperature data extracted from the three Euro-Cordex RCMs, for both the historical and future period, using ERA5-Land data as reference. ET_o calculated using raw weather variables was also bias-corrected as this direct bias-correction gave slightly lower RMSE and Bias than ET_o calculated using the bias-corrected weather variables. The QM approach has become increasingly popular and widely used because of its efficiency and low computational cost (Fang et al. 2015; Sun et al. 2019; Pastén-Zapata et al. 2020; Torma et al. 2020). For this purpose, the full calibration period 1981-2005 is considered. This means that evaluation and validation period are identical, and no independent cross-validation exercise is carried out. The latter was covered by previous works e.g. (Ivanov and Kotlarski 2017; Gutiérrez et al. 2019) which revealed that QM, in general, performs well in a historical cross-validation setting with independent calibration and validation periods (Feigenwinter et al. 2018).

3.2.4.3. Taylor diagram

In addition to computing the mean Bias and RMSE, the degree of correspondence between the raw and bias-corrected RCM simulations and reanalysis outputs can be quantified and illustrated schematically in the form of a Taylor diagram (Taylor 2001). These diagrams are especially useful in evaluating multiple aspects of complex models or in gauging the relative skill of many different models (Yin et al. 2016; Tegegne and Melesse 2020; Torma et al. 2020). The performance of the different models is evaluated by comparing their correlation (R), centered root-mean-square difference (cRMSD) and the amplitude of their variations represented by their standard deviations ($StDev_o$ and $StDev_s$):

$$R = \frac{\sum_{i=1}^{N}(X_s-\overline{X_s}).(X_o-\overline{X_o})}{\sqrt{\sum_{i=1}^{N}(X_s-\overline{X_s})^2 \sum_{i}^{N}(X_o-\overline{X_o})^2}} \quad (3\text{-}8)$$

$$cRMSD = \left\{\frac{1}{N}\sum_{i=1}^{N}[(X_o - \overline{X_o}) - (X_s - \overline{X_s})]^2\right\}^{1/2} \quad (3\text{-}9)$$

$$StDev_o = \frac{1}{N}\sum_{i=1}^{N}(X_o - \overline{X_o})^2 \quad (3\text{-}10)$$

$$StDev_s = \frac{1}{N}\sum_{i=1}^{N}(X_s - \overline{X_s})^2 \quad (3\text{-}11)$$

where X_o is the observed value, X_s is the simulated value, $\overline{Xo}$ is the average of the observed value, $\overline{Xs}$ is the average of the simulated value, and N is the number of values.

For each model, the three aforementioned statistics are plotted: (1) the Pearson correlation coefficient (R), which is related to the azimuthal angle, (2) the centered RMS difference (cRMSD) in the simulated field, which is proportional to the distance from the point on the x-axis (black contours) that is identified as "observed" (represented by a black circle), and (3) the ratio of standard deviation derived from the RCM simulations against the observations, which is proportional to the radial distance from the origin (red contour). The colored symbols represent the different RCM simulations where the color refers to the RCM and the different symbols represent the raw and bias-corrected daily ET_o means. Simulations that agree well with observations will lie nearest the reference point on the x-axis.

Finally, the different steps followed by the methodology in this study are summarized in the flow chart of Figure 3-2.

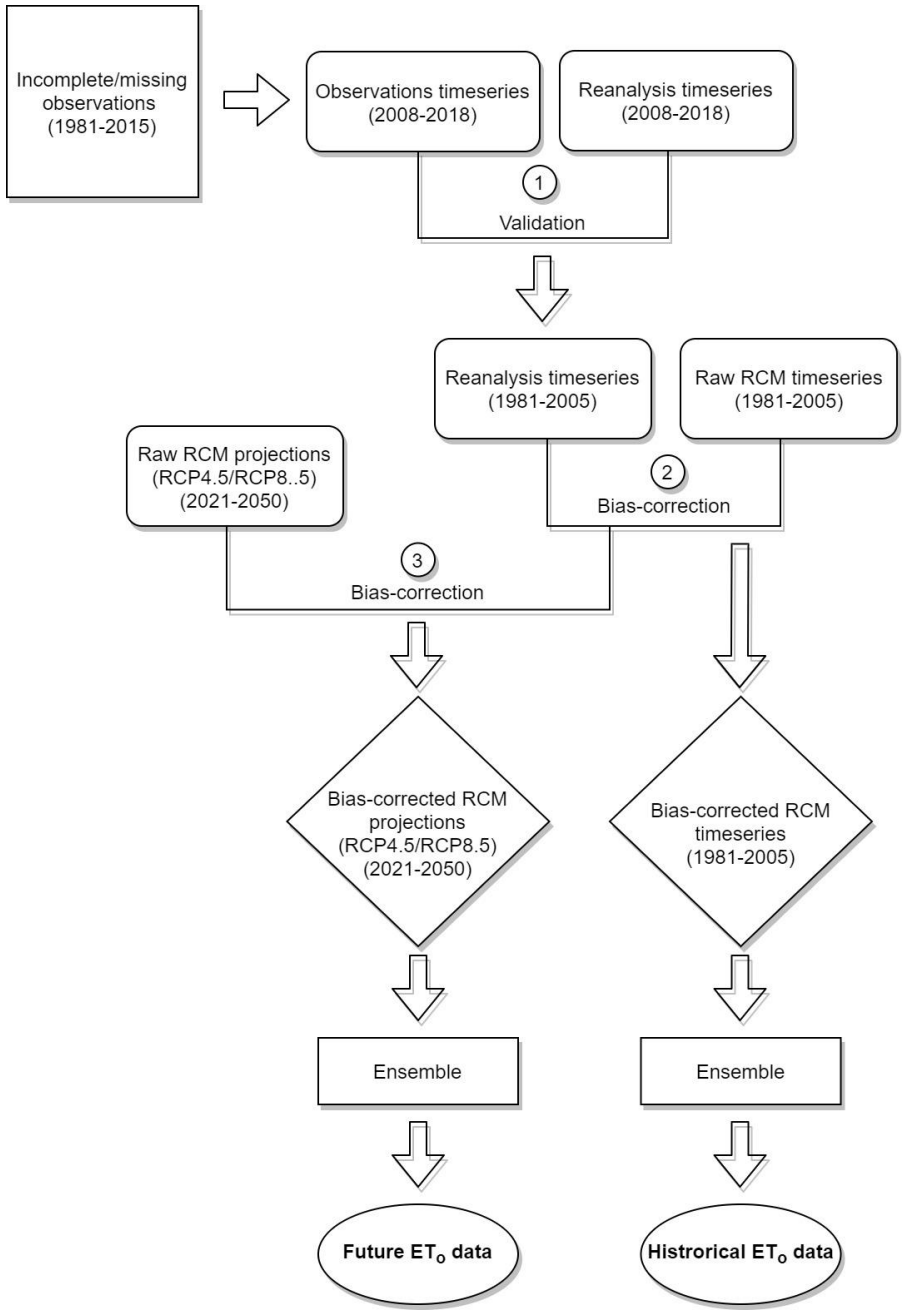

Fig. 3-2. Flowchart of the proposed methodology used to assess future reference evapotranspiration, using the FAO-PM equation and historical/future data.

3.3. Results and discussion

3.3.1. Validation of the ERA5-Land reanalysis with observed data

The performance of the reanalysis and the observed data of four climatic variables, i.e. mean air temperature (T_{mean}), solar radiation (R_s), mean dew point temperature (T_{dew}) and mean wind speed (WS), along with ET_o, calculated using these variables in the validation period 2008-2018 (4018 days), were evaluated at each agrometeorological station using the root mean square error RMSE and the Bias as statistical indicators. Results are shown in Table 3-2. For all stations, T_{mean}, T_{dew} and WS RMSE and Bias are less than 20% of the observed values and the coefficient of determination R^2 is higher than 0.5. For R_s, RMSE and Bias are slightly higher but less than 30% with a minimum R^2 of 0.8.

Looking at ET_o performance in Table 3-2, it is clear that ERA5-Land slightly underestimates ET_o in most locations, with Bias values ranging between -0.8 and 0.03 mm d^{-1}, a minimum RMSE of 0.2 mm d^{-1} and a maximum RMSE of 1.2 mmd^{-1}. This could be due mainly to the effect of the solar radiation underestimation especially because it was demonstrated that solar radiation errors have a high impact on the estimated evapotranspiration (Perera et al. 2014; Pelosi et al. 2016).

Table 3-2. Performance indices calculated for the reanalysis data with respect to observed data in the period (2008-2018).

Station	T_{mean}(°C)		T_{dew}(°C)		R_s (MJ d^{-1} m^2)		WS (m s^{-1})		ET_o (mm d^{-1})	
	RMSE	**Bias**	**RMSE**	**Bias**	**RMSE**	**Bias**	**RMSE**	**Bias**	**RMSE**	**Bias**
Cadriano	0.7	0.2	3.1	-2.7	5.9	-3.9	0.5	0.1	0.2	0.03
Martorano	0.6	0.3	1.8	-1.7	6.8	-5.8	0.2	-0.1	0.9	-0.6
San Pancrazio	0.7	-0.1	1.9	-1.7	7.5	-6.4	0.3	-0.2	1.2	-0.8
San Pietro Capofiume	1.1	1.0	2.1	-1.9	7.8	-6.7	0.3	-0.2	0.8	-0.5
Volano	1.7	1.3	2.5	-0.1	6.7	-5.7	1.2	1.1	0.6	-0.1

For all stations, both RMSE and Bias are lower than 30% of the ET_o from observations, while the minimum R^2 is around 0.8. Martins et al. (2017) considered an ET_o RMSE lower than 0.8 mm d^{-1} satisfactory when they compared ET_o from reanalysis with observed ET_o in the Iberian Peninsula.

However, the variability of the performance of ERA5-Land data could be explained by the presence of missing data in the observed time series in all stations, especially for Martorano and Volano, that could negatively affect RMSE and Bias values (Kidson and Trenberth 1988). In the latter location, it could be further explained by the fact that ERA5-land is produced by running the scheme of surface exchanges over land without taking into account the possible vicinity of the sea. Observational practice indicates that surface parameters in coastal areas may be influenced by the sea up to 5-10 km inland, as a consequence it is possible that ERA5-land may not correctly represent local climate variability in this area (Pelosi et al. 2020). The extension of the analysis to the regional level could help to understand if that effect is relevant at that level or if it is mostly a very local issue. In general, it is known that reanalysis datasets may feature a certain degree of deviations from the "true" value (Maraun et al. 2010). Overall, these results are considered acceptable and since, in our case, observed data necessary for the calculation of the FAO-PM equation for the study period 1981-2005 are not available or have large gaps, it was decided to use ERA5-Land data as a surrogate of ground observations and for the bias-correction of the different RCMs.

3.3.2. Validation and bias correction of RCMs

After this first step, reanalysis data were used to evaluate data extracted from the three RCM models for our five reference stations. As stated before, those RCMs were selected among others because they have daily data of all the variables necessary for the calculation of the FAO-PM equation. Figure 3-3 reports mean annual ET_o calculated from the reanalysis data and the three RCMs for the reference period 1981-2005, for the five agrometeorological stations considered, with and without bias-correction (described in par. 3.2.4.2). All RCMs overestimate ET_o in all locations when compared to ET_o from ERA5-Land. For all stations, the mean annual ET_o RMSE is higher and the positive Bias is more pronounced in the HIRHAM5 model simulations, while the RACMO22E model presents the lowest RMSE and Bias. Although less obvious with RACMO22E model, the performance indices also seem to be affected by the distance from the sea as San Pancrazio and Cadriano show the highest RMSE and Bias values, while Volano shows the lowest values. Taking into account all simulations, Bias varies between 13% and 65% and RMSE values range between 121 mm y^{-1} and 440 mm y^{-1}, which are unacceptable values. After applying the QM bias correction technique, the Bias present in the raw simulated annual ET_o means were almost eliminated, leading

to negligible differences between RCMs and reanalysis annual ET_o means. The new Bias varies between -0.14% and 0.04% and the new RMSE values are between 46 mm y^{-1} and 65 mm y^{-1}, which is substantially less than in the case of raw simulations.

The same observations apply also to the ET_o means over the summer season (June to August). Similarly, all RCMs overestimate ET_o in all five stations (Figure 3-4). However, the positive Bias is higher for the RCA4 model instead. It is also interesting to note that RACMO22E with and without bias correction is among the best performing RCMs at all locations and in both time frames. The effect of the distance from the sea on the performance indices is also noticed as San Pancrazio and Cadriano still have the highest RMSE and Bias values and Volano the lowest ones. In the summer season, Bias varies between 17% and 69% and RMSE values range between 14 mm/season and 43 mm/season. Applying the QM bias correction technique reduced the biases to a range between -0.07% and 0.06% and the RMSE to a range between 6 mm/season and 7 mm/season, which is negligible.

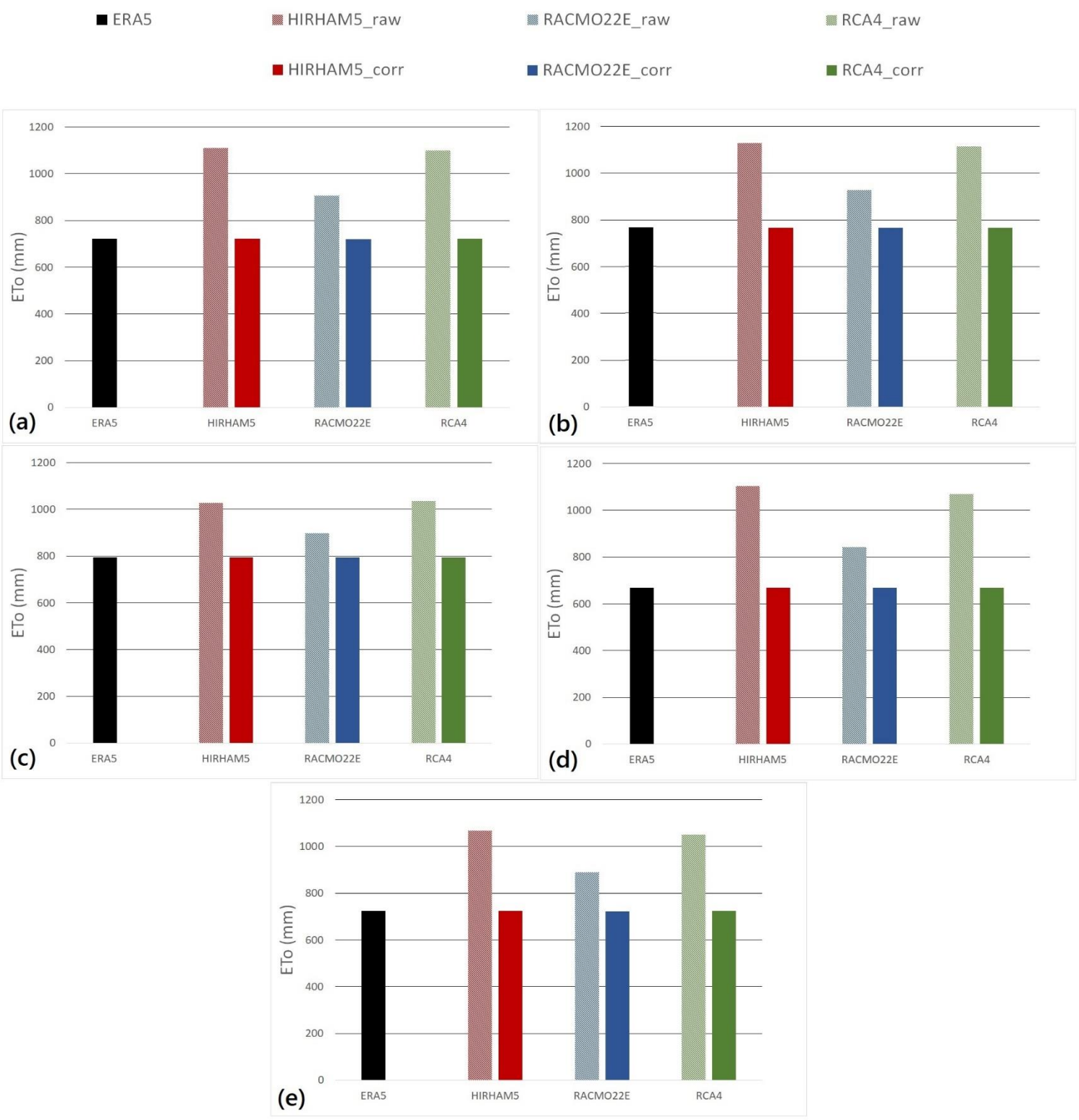

Fig. 3-3. Mean annual ET_o in Cadriano (a), Martorano (b), Volano (c), San Pancrazio (d) and San Pietro Capofiume (e) using raw (left column) and bias corrected data (right column) for all RCMs for the period 1981–2005. Reanalysis data (ERA5) are shown for comparison.

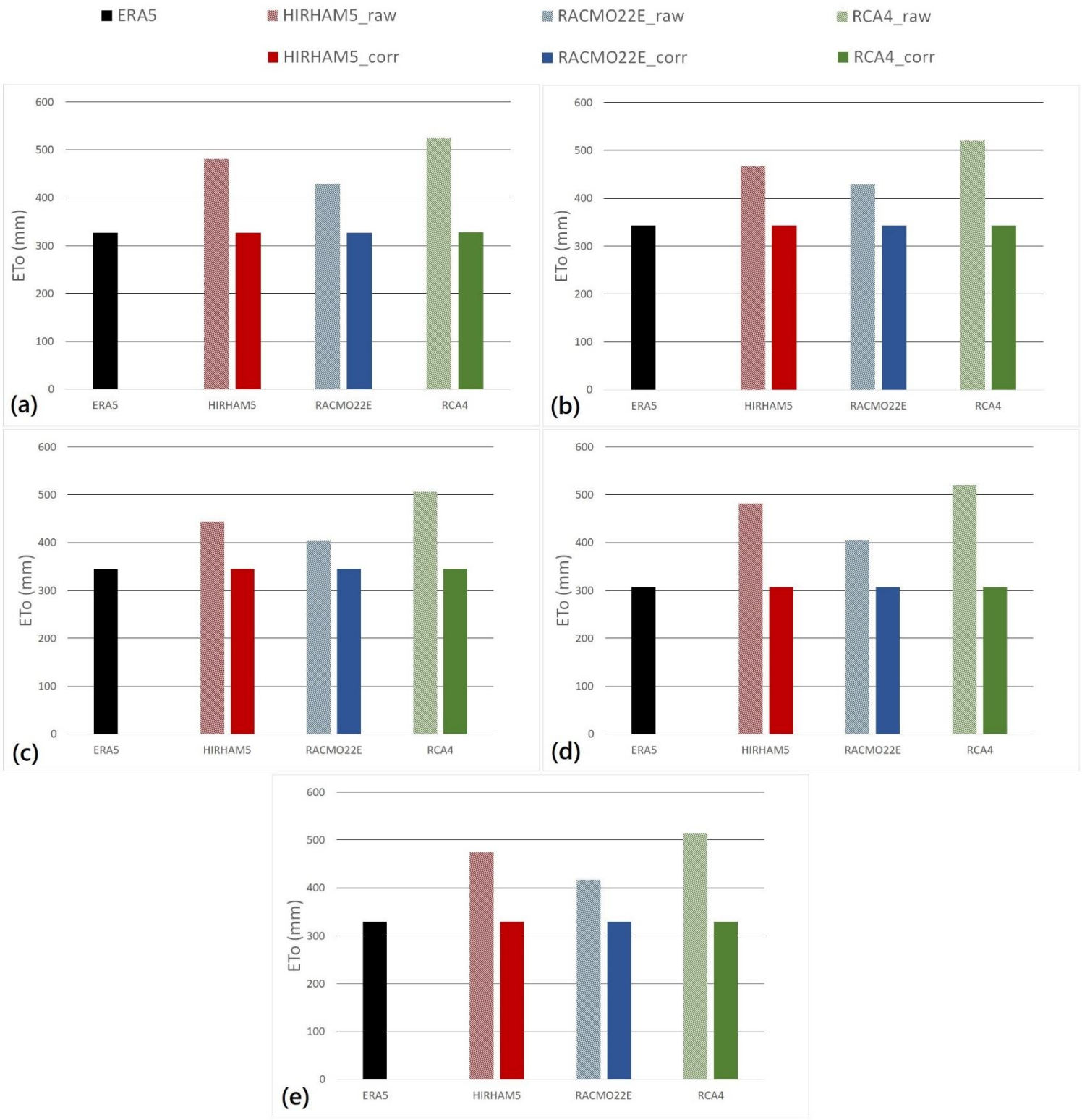

Fig. 3-4. Mean summer ET_o bias in Cadriano (a), Martorano (b), Volano (c), San Pancrazio (d) and San Pietro Capofiume (e) using raw (lesft column) and bias corrected (right column) data for all RCMs for the period 1981–2005. Reanalysis data (ERA5) are shown for comparison.

A better evaluation of model performances may be obtained using a Taylor diagram that summarizes the relative skill with which the different RCMs simulate ET_o in the five locations in comparison with the reanalysis outputs over the period 1981–2005. Looking at Figure 3-5, note that all RCM simulations whether raw or bias-corrected, exhibit high correlation coefficients (above 0.97). On the other hand, a difference is seen when looking at RMSD and the standard deviation. Those metrics are lower for the bias-corrected RCMs, hence their closeness to the reference point. In contrast to the raw RCMs symbols, those representing the bias-corrected RCMs are packed on the red arc meaning that they have the same standard deviation than the reanalysis data, which indicates that their variations is of the right amplitude. The previous observation about RACMO22E being the best performing RCM with and without bias correction for all locations is also confirmed. It is evident that the application of the bias-correction substantially improved the ET_o simulations by the different RCMs when compared to the ERA5-Land.

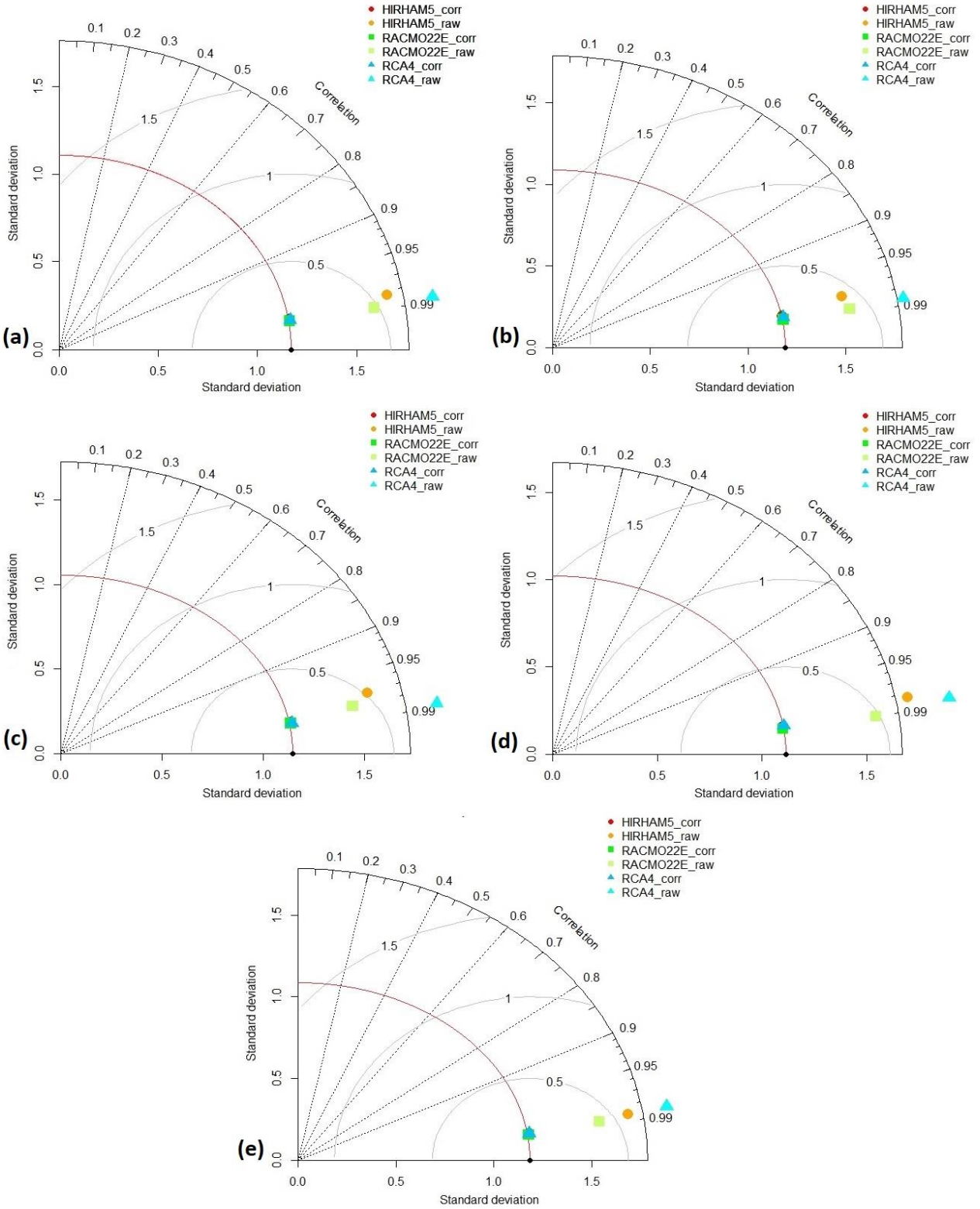

Fig. 3-5. Taylor diagrams for summarizing the statistical characteristics of RCM simulation data and the effect of bias correction for Cadriano (a), Martorano (b), Volano (c), San Pancrazio (d) and San Pietro Capofiume (e), for the period 1981-2005.

3.3.3. ET_o projections

The same approach applied to the reference period was also applied to bias-correct RCMs data for the period 2021-2050 following RCP4.5 and RCP8.5 scenarios. Then, an ensemble for each scenario from the three bias-corrected RCMs was built to study the projected ET_o changes with respect to the reference period. The combination of information provided by an ensemble approach from different RCMs simulations instead of only one specific RCM is a way to reduce further uncertainties associated with climate models projections and to produce more robust results (Christensen et al. 2010; Kendon et al. 2010; Giménez and García-Galiano 2018).

3.3.3.1. Future change in temperature

Before analyzing what may happen in different scenarios to ET_o, we want to look at what is projected for mean air temperature in the different scenarios. For the RCP4.5 scenario (Table 3-3), annual T_{mean} will range between 14.2±0.5 °C in San Pancrazio and 15.8±0.4 °C in Volano, while, in summer, it will range between a minimum of 24.4±0.9 °C in San Pancrazio and a maximum of 25.3±0.9 °C in San Pietro Capofiume. This implies a general increase of annual T_{mean} by about 1 °C in 2021-2050 with respect to the reference period 1981-2005, going up to 1.3 °C in summer. For RCP8.5 scenario, the annual average value of T_{mean} is projected to fluctuate between 14.5±0.5 °C in San Pancrazio and 16.1±0.4 °C in Volano. In summer, T_{mean} will range between 24.7±0.7 °C in San Pancrazio and 25.5±0.8 °C in San Pietro Capofiume. Compared to the reference period, the increase of the average annual value will be by around 1.2 °C in all locations, reaching 1.5 °C in summer. Similar results were found when assessing air temperature changes for the period 2021-2050 with respect to the reference period 1982-2011 in the Po river basin (Mercogliano et al. 2014; Vezzoli et al. 2016). D'Oria et al. (2018) analyzed the climate change effects on temperature over the Taro, Parma and Enza River basins, in the Emilia Romagna region, using an ensemble of 13 Regional Climate Models and the same emission scenarios (RCP4.5 and RCP8.5). At annual scale, they expected increments up to +0.75 °C in the 2016-2035 period and +1.5 °C in the 2046-2065 period under the RCP4.5, and higher, up to +1 °C in 2016-2035 and +2 °C in 2046-2065 with the RCP 8.5, using 1985-2005 as a reference period. These results are also close to the national projections that anticipate an increase in T_{mean} ranging between 1.25 °C e 1.75 °C in 2021-2050 for RCP4.5 and between 1.5 °C e 2.0 °C for RCP8.5 (Desiato et al. 2005). Overall, the magnitudes of air temperature increase for RCP4.5 and RCP8.5 are close, due to the small difference between the

two emission pathways before 2050. The same observation was made by Wang and Chen (2014) when assessing the magnitudes of temperature increase in China for the same RCP scenarios.

Table 3-3. Statistics for T_{mean} in the five agrometeorological stations for the historical and future period 2021–2050.

Station		T_{mean} (°C)					
		Reference Period (1981-2005)		RCP4.5		RCP8.5	
		Annual	Summer	Annual	Summer	Annual	Summer
Cadriano	Mean	13.8	23.7	14.8	25	15	25.2
	SD	0.4	0.7	0.4	0.9	0.4	0.7
Martorano	Mean	14.2	23.7	15.1	24.9	15.4	25.1
	SD	0.3	0.7	0.4	0.8	0.4	0.6
Volano	Mean	14.9	23.8	15.8	25.1	16	25.3
	SD	0.3	0.6	0.3	0.8	0.4	0.6
San Pancrazio	Mean	13.2	23.2	14.2	24.4	14.5	24.7
	SD	0.4	0.7	0.4	0.9	0.5	0.7
San Pietro Capofiume	Mean	14	24	15	25.3	15.3	25.5
	SD	0.37	0.78	0.4	0.9	0.5	0.8

3.3.3.2. Future changes in solar radiation, wind speed and dew point temperature

Certainly, air temperature has an important influence on evapotranspiration. However, other weather variables, involved in the FAO-PM equation, have also an effect on ET_o. Thus, it is useful to assess the future change in solar radiation, wind speed and dew point temperature for the two considered RCP scenarios.

For both RCP4.5 and RCP8.5, annual solar radiation will increase by around 1.3% in all locations during the future period 2021-2050 (Table 3-4), while summer solar radiation will increase by around 0.8% to 1.3%. However, according to Gutiérrez et al. (2020), the amplitude of the changes in surface solar radiation likely depends on the RCM and on its aerosol forcing choice, suggesting that it is important to be cautious when using CORDEX projections for solar radiation and arguing for the inclusion of aerosol forcing evolution in the next generation of CORDEX simulations. Besides, such a small increase will likely not affect much ET_o.

For wind speed (Table 3-5), annual values show an average increase of around 14% in all locations and for both RCP scenarios, with regards to the reference period 1981-2005. In the other hand, summer values will stay constant. It is known that wind speed has a positive effect on ET_o, and its increase contributes to an increase of the reference evapotranspiration (Allen et al. 1998).

Finally, an increase of around 9.2% to 12.3% in annual T_{dew} is projected for all locations during 2021-2050 in comparison with the reference period (Table 3-6). Similarly, summer T_{dew} will increase by 5.6% to 7.1%. This means an increase of the quantity of water vapor, which has the effect of decreasing evapotranspiration, offsetting, at least in part, the effect of the increase in T_{mean} and WS.

The impact on ET_o projections of the variation of all these quantities, to which an increase of the CO_2 level and consequently of the stomatal resistance is added, is studied in the following paragraphs with a particular focus on the change in air temperature as it is used often as a major argument against the effect of a change in CO_2 concentrations.

Table 3-4. Mean solar radiation at the five agrometeorological stations for the historical and future period 2021–2050

Station		R_s (MJ m^{-2} d^{-1})					
		Reference Period (1981-2005)		RCP4.5		RCP8.5	
		Annual	Summer	Annual	Summer	Annual	Summer
Cadriano	Mean	7.8	12.4	7.9	12.5	7.9	12.6
	SD	0.1	0.2	0.1	0.2	0.1	0.2
Martorano	Mean	7.9	12.5	8	12.6	8	12.6
	SD	0.1	0.2	0.1	0.2	0.1	0.2
Volano	Mean	8	12.6	8.1	12.7	8.1	12.8
	SD	0.1	0.2	0.1	0.2	0.1	0.2
San Pancrazio	Mean	7.7	12.2	7.8	12.3	7.8	12.3
	SD	0.1	0.2	0.1	0.2	0.1	0.2
San Pietro Capofiume	Mean	7.9	12.4	8	12.5	8	12.6
	SD	0.1	0.2	0.1	0.2	0.1	0.2

Table 3-5. Mean wind speed at the five agrometeorological stations for the historical and future period 2021–2050

Station		WS (m s^{-1})					
		Reference Period (1981-2005)		RCP4.5		RCP8.5	
		Annual	Summer	Annual	Summer	Annual	Summer
Cadriano	Mean	1.4	1.4	1.5	1.4	1.5	1.4
	SD	0.03	0.05	0.03	0.05	0.03	0.05
Martorano	Mean	1.5	1.6	1.7	1.6	1.7	1.6
	SD	0.05	0.06	0.03	0.06	0.03	0.06
Volano	Mean	2.4	2.6	2.7	2.6	2.7	2.6
	SD	0.06	0.11	0.06	0.10	0.05	0.08
San Pancrazio	Mean	1	1.1	1.2	1.1	1.2	1.1
	SD	0.03	0.04	0.03	0.05	0.03	0.03
San Pietro Capofiume	Mean	1.2	1.3	1.4	1.3	1.4	1.3
	SD	0.04	0.07	0.03	0.06	0.03	0.05

Table 3-6. Mean dew point temperature at the five agrometeorological stations for the historical and future period 2021–2050

Station		T_{dew} (°C)					
		Reference Period (1981-2005)		RCP4.5		RCP8.5	
		Annual	Summer	Annual	Summer	Annual	Summer
Cadriano	Mean	8	14.6	8.7	15.2	9	15.6
	SD	0.3	0.5	0.4	0.5	0.4	0.4
Martorano	Mean	8.3	14.5	9.1	15.4	9.3	15.6
	SD	0.3	0.5	0.4	0.5	0.4	0.4
Volano	Mean	9.9	17	10.6	17.9	10.9	18.1
	SD	0.3	0.5	0.4	0.6	0.4	0.4
San Pancrazio	Mean	7.5	14.2	8.3	15.1	8.6	15.3
	SD	0.3	0.5	0.4	0.5	0.4	0.5
San Pietro Capofiume	Mean	8.3	15	9.1	15.9	9.3	16
	SD	0.3	0.5	0.4	0.5	0.4	0.4

3.3.3.3. Future reference evapotranspiration scenarios

For the estimation of the future situation of the ET_o in 2021-2050, with respect to the reference period 1981-2005, four scenarios were considered: the first scenario considers RCP4.5 without changing the CO_2 concentration in the FAO-PM equation, which was about 372 ppm when it was first developed; the second scenario considers RCP8.5 without changing the future CO_2 concentration in the FAO-PM equation (372 ppm); the third scenario uses RCP4.5 with an increase of the canopy resistance to account for a CO_2 concentration of 550 ppm; and the fourth scenario considers RCP8.5 taking in consideration a future CO_2 concentration of 550 ppm. They are summarized in Table 3-7.

Table 3-7: Evapotranspiration scenarios

	RCP4.5	**RCP8.5**
CO_2 concentration 372ppm	Scenario ET_1	Scenario ET_2
CO_2 concentration 550ppm	Scenario ET_3	Scenario ET_4

Reference evapotranspiration calculated by the FAO-PM equation using future data and the four scenarios of Table 3-7, is reported in Table 3-8. The average annual ET_o in all locations is about 735 mm in the reference period 1981-2005, and it is projected to reach values ranging between 764 mm for RCP4.5 and 772 mm for RCP8.5 in 2021-2050. These findings are close to those of Nistor and Mîndrescu (2019) in Emilia-Romagna region. They showed that the annual ET_o register values between 494 and 798 mm in 1961-1990 and between 778 mm and 833 mm in 2011-2070.

The highest annual and summer ET_o values are observed in Volano for both the historical and future period, while the lowest values are observed in San Pancrazio. Based on the data available, this could be partially explained by the former location having the highest air temperature, wind speed and solar radiation. (Table 3-3, 3-4 and 3-5), while the latter location having the lowest of those values. Similar conclusions were found by Goyal (2004) and Liu and Zhang (2013) when assessing ET_o in China and India respectively.

Table 3-8. Mean annual and summertime reference evapotranspiration (ET_o) and annual ET_o change (Δ) for the four scenarios.

Station	Season	ET_o historical (mm)	Δ Scenario ET_1		Δ Scenario ET_2		Δ Scenario ET_3		Δ Scenario ET_4	
			mm	%	mm	%	mm	%	mm	%
Cadriano	Summer	328	15	4.4%	18	5.4%	4	1.3%	7	2.1%
	Annual	721	28	3.9%	37	5.1%	2	0.2%	7	1%
Martorano	Summer	343	16	4.7%	18	5.2%	6	1.7%	4	1.2%
	Annual	767	30	3.9%	39	5.1%	2	0.2%	2	0.3%
Volano	Summer	345	17	5.0%	20	5.7%	2	0.4%	5	1.4%
	Annual	794	35	4.4%	42	5.3%	-8	-1.1%	-1	-0.1%
San Pancrazio	Summer	307	11	3.5%	15	4.9%	4	1.2%	6	1.9%
	Annual	669	23	3.5%	32	4.8%	5	0.8%	8	1.1%
San Pietro Capofiume	Summer	329	15	4.7%	18	5.5%	7	2%	7	2.2%
	Annual	723	29	4.1%	37	5.1%	4	0.6%	7	1%
Average	**Summer**	**330**	**15**	**4.5%**	**18**	**5.4%**	**4**	**1.3%**	**6**	**1.7%**
	Annual	**735**	**29**	**4%**	**37**	**5.1%**	**1**	**0.1%**	**5**	**0.7%**

For scenario ET_1, an increase of annual T_{mean} by around 1 °C in all locations in 2021-2050 will contribute in increasing annual ET_o by an average of 4% ranging between 3.5% in San Pancrazio and 4.4% in Volano. An increase of summertime T_{mean} by around 1.3 °C will be followed by an increase in ET_o by an average of 4.5% with a minimum change of 3.5% in San Pancrazio and a maximum of 5% in Volano.

For scenario ET_2, an increase of annual T_{mean} by around 1.2 °C in 2021-2050 will be met by an increase in ET_o by an average of 5.1% with the minimum is San Pancrazio (4.8%) and the maximum in Volano (5.3%). The same pattern is projected in summer when an increase of around 1.5 °C in T_{mean} will help increasing ET_o by 5.3% reaching its minimum in San Pancrazio (4.9%) and its maximum in Volano (5.7%). Overall, considering both scenarios, the absolute magnitude of variation from the reference annual and summertime ET_o for all locations was between 3.5% and 5.7% for an increase of T_{mean} by 1 °C to 1.5 °C, which represent an average increase of 4% to

5.4% with regard to the reference period 1981-2005. According to Allen (2000), under well-watered conditions, evapotranspiration will increase about 4 to 5% per 1 °C rise in temperature. In the Mediterranean region, Saadi et al. (2015) predicted that an increase of air temperature of 1.57 ± 0.27 °C would increase annual reference evapotranspiration by 6.7%. These observations are also proportional to findings by Goyal (2004) in India where they showed that evapotranspiration will increase by 14.8% with an increase in temperature by 20%. They are also proportional to findings by Ramírez and Finnerty (1996) that indicated that a 3 °C increase in temperature induces a 14% increase in evapotranspiration rates in Colorado.

When increasing atmospheric CO2 concentration, which means increasing the canopy resistance component of the FAO-PM equation to account for a 550 ppm CO_2 concentration, the result is a counterbalance of the effect of the change in the different weather variables, with a quite small difference between actual and future ET_o, both for yearly and summer quantities. In particular, for Scenario ET_3 this means that annual ET_o will increase by only a maximum of 0.8% in San Pancrazio with regards to the reference period and it will even decrease by a maximum of 1.1% in Volano. In summertime, ET_o is anticipated to increase between 0.4% in Volano and 2% in San Pietro Capofiume.

For Scenario ET_4, the increase of CO_2 concentration is projected to have the same effect as scenario ET_3. Annual ET_o will increase by a maximum of 1.1% in San Pancrazio while it will decrease by 0.1% in Volano in comparison with the reference period. On the other hand, in summer, the increase is predicted to be between 1.2% in Martorano and 2.2% in San Pietro Capofiume. It is interesting to notice that, unlike scenario ET_1 and ET_2, the windiest location (Volano), had the least increase in both annual and summer ET_o with regards to the historical period when compared to San Pancrazio, the least windy station. This is because an increase in CO_2 concentration increases the factor 0.34 that accompanies wind speed in the denominator of Eq. (3-1) causing smaller ET_o increments compared to the situation without CO_2 variation (Moratiel et al. 2011). Similar observations were reported by Snyder (2017) when he found that, with an increase in CO_2 concentration, the annual ET_o increased slightly where there were mean wind speeds less than 1.7 $m \cdot s^{-1}$, and it decreased for wind speeds greater than 1.7 $m \cdot s^{-1}$. However, in our case, the change in ET_o does not follow a clear wind speed negative gradient, as there are also several other factors

that might affect at a certain extent the magnitude of the variation, such as dew point temperature and solar radiation.

Overall, when the effect of an increase in CO_2 concentration from 372 ppm to 550 ppm was considered in combination with the projected increase in temperature by 1 °C to 1.5 °C, changes in both annual and summer ET_o demand varied from -1.1% to 2.2% during the 2021-2050 period with regard to the reference period 1981-2005. Comparable results were obtained in Colorado by Islam et al. (2012) whose simulations showed that the effect of increase in CO_2 levels up to 450 ppm to offset the effect of about 1 °C rise in temperature, whereas a 2 °C rise in temperature was offset by a doubling of the CO_2 concentration (660 ppm). Similarly, simulations by Priya et al. (2014) concluded that the effect of 2.5 °C rise in temperature in Varanasi (India) was offset by an increase of the CO_2 concentration from 330 ppm to 660 ppm.

Accounting for the projected increase in CO_2 concentration in the FAO-PM equation should give a more realistic estimation of WUE and irrigation requirements, especially for C_3 crops such as wheat, barley, potato and sunflower, for which Emilia-Romagna is famous, as C_4 species are less responsive to increased atmospheric CO_2. This means that farmers should be able to achieve higher crop yields per unit land area with similar or less amounts of water. However, elevated carbon dioxide concentrations may have detrimental effects on agriculture, as they can affect crop quality due to reductions in nutrients, including many that are important for overall health, such as iron, zinc, and protein (Erda et al. 2005; Smith et al. 2018). Besides, they can increase the damage caused by certain pests and boost weeds prevalence, because many weedy species are C_3 plants, which are favored in an elevated carbon dioxide environment (Ramírez and Finnerty 1996; Fuhrer 2003). This is enhanced even further by increasing competitiveness and reducing herbicide sensitivity of some weed species (Matzrafi 2019). Besides, temperature increases along with CO_2, will accelerate plants maturity, and hinder pollination (Boote et al. 2005). Further, if temperatures continue to rise, the overall WUE could actually decrease due to increased water requirements in warmer climates such as that of Emilia-Romagna and to possible seed yield reductions caused by higher temperatures (Allen 2000). In fact, CO_2 fertilizing effects should decrease once optimal temperatures are exceeded for a range of processes, especially plant water use (Easterling et al. 2007; Backlund et al. 2008; Lovelli et al. 2010; Turral et al. 2011). However, even without taking in consideration the increments in CO_2 levels, the studied locations

should not imply dramatic increases in water demand with respect to the 1981-2005 period as ET_o increase does not exceed 6% with the projected increase in air temperature. Using water balance and a calibrated Hargreaves and Samani equation (Hargreaves and Samani 1982), similar conclusion was drawn by Tomei et al. (2010) for the future period 2021-2050 with respect to the 1991-2008 period. They explain that the result is mainly due to possible increase in spring precipitation, that could mitigate the impact of the further increase in temperature and evapotranspiration.

3.3.4. Uncertainties

Some uncertainties are present in this study. First, uncertainties may come from the use of reanalysis data, which stems from the general difficulty in combining heterogeneous observations onto a regular grid, the choice of the assimilation model, and the quality and distribution of the underlying observations (Reichler and Kim 2008). However, these uncertainities should be less important in the ERA5-Land climate dataset due to its high resolution and its foundation in physical laws, which makes it suitable for studying climate-vegetation interrelationships in areas with poor data availability (Zandler et al. 2020). Second, uncertainties may originate from the RCM projections due to the uncertainty of physics parameterization and lateral boundary conditions, limitations with initial conditions, imperfections of numerical equations, and various model configurations (Kim et al., 2020). To reduce the uncertainty associated with model outputs, a multi-RCM-ensemble was used in this study as recommended in the literature (Eekhout and Vente 2019; Mendez et al. 2020; Yu et al. 2020). Moreover, a statistical bias-correction technique namely quantile mapping (QM) was applied as it is proven to reduce biases in the mean, variance or the complete distribution of simulated climate variables (Pastén-Zapata et al., 2020). Besides, the increase in spatial resolution of RCMs was shown to have a significant effect on the model performance (Prein et al., 2016). Therefore, high resolution CORDEX-RCMs were selected. However, RCMs post-processing is unable to alleviate all uncertainties as climate simulations can never capture the complexities of the real system. Hence, uncertainty is unavoidable in regional climate scenarios and indeed in any geographical discipline which utilizes numerical modelling (Foley, 2010).

3.4. Summary and conclusion

The aim of this paper was to assess the effect of climate change on crop reference evapotranspiration in five locations in Emilia-Romagna region during the near future period 2021-2050, with a focus on the effects of higher CO_2 levels and agrometeorological parameters on ET_o. Since climate change studies usually need between 20 to 30 years of observed data and due to the unavailability or incompleteness of such dataset in our case, the high-resolution ERA5-Land reanalysis dataset (9 km) was evaluated to serve as an alternative. The comparison made against data observations for the period 2008-2018 gave satisfying results, allowing the reanalysis dataset to be used as a long-term reference dataset. This dataset was used to correct for systematic biases in the daily weather variables extracted from three high-resolution EURO-CORDEX RCMs (12 km), then used for the calculation of ET_o. The three-member RCM ensemble assuming a medium (RCP4.5) and a high range emission scenario (RCP8.5) was assessed for the future period 2021–2050 with respect to the reference period 1981-2005. According to the bias-corrected ensemble simulations and both RCP scenarios, mean air temperature in the five study locations is anticipated to increase by 1 °C to 1.5 °C annually and during summertime with respect to the 1981-2005 period. This increase is coincident with an increase in the other weather variables involved in the FAO-PM equation, mainly wind speed and dew point temperature. Focusing on summer season, which is important for irrigation, and maintaining the preset CO_2 concentration of 372 ppm, the FAO-PM equation predicts the increase in future summer ET_o to range between 3.5% and 5.7% in all stations. By taking into account the increase of CO_2 concentration up to 550 ppm in the ET_o calculations, the new range of summer ET_o variation will be between 0.4% to 2.2%, thus reducing the effect of an increase in the different weather variables, especially air temperature.

Overall, the results of this study favor the adoption of reanalysis data to estimate ET_o when full observation datasets are not available. Besides, they show that taking into consideration the future projected CO_2 concentrations is important to have a more accurate idea about future crop water demands and to be able to have more efficient water resources management strategies in Emilia-Romagna. Despite some uncertainties, results may provide a theoretical basis for further study of the potential impacts of climate change on local water resources and agriculture As a future step, this work could be extended to the end of the century scenario, when important increases in

temperature in all seasons are projected to occur over Emilia Romagna region (Tomozeiu et al. 2007, 2018).

Acknowledgment

This research was realized using data generated using Copernicus Atmosphere Monitoring Service information (2020) and Copernicus Climate Change Service Information (2020). Neither the European Commission nor ECMWF is responsible for any use that may be made of the Copernicus Information or data that this work contains.

Chapter 4

Evaluation of Forecast Reference Evapotranspiration (FRET) for Different Micro-climates Regions in California

The original research described in this Chapter has been submitted for publication as:

Ben Hamouda G, Zaccaria D, Bali K, Snyder RL, Ventura F. Evaluation of Forecast Reference Evapotranspiration (FRET) for Managing Irrigation Under Different Climates in California. J. Irrig. Drain. Eng. In Review

4. Evaluation of Forecast Reference Evapotranspiration (FRET) for Different Micro-climates Regions in California

Abstract

In California, daily crop evapotranspiration (ET_c) is commonly estimated using near-real-time, standardized reference evapotranspiration (ET_o) calculated from meteorological data and crop coefficient (K_c) values that adjust for the difference between ET_o and ET_c. However, using ET_o calculated from forecast rather than near-real-time meteorological data provides more timely information to growers, farm managers, irrigation practitioners, water resource planners, as well as to water purveyors and managers to anticipate the water demand for the upcoming days, which is important for water allocation and delivery planning, and for irrigation scheduling decisions. Forecast ET_o is also relevant for scientific research to develop methods and tools enabling more resource-efficient water use for agricultural production and urban landscapes. Verifying the reliability of ET_o forecast models for various climatic conditions is crucial to promote the broad adoption and use of ET_o predictions for weather-based adaptive water management and prospective irrigation scheduling. The US National Weather Service (NWS) has released the product "FRET" that provides forecasts of ET_o at 2.5-km grid resolution for the entire continental USA. In this study, comparisons were made between ET_o forecasts from FRET and the observed ET_o values from the California Irrigation Management Information System (CIMIS) for a total of 108 days during the peak irrigation water demand period of 2019, which corresponds to the mid-season period of the major crops. FRET ET_o forecasts and CIMIS ET_o observations (which are calculated from measured weather parameters) were compared for 15 CIMIS station locations to represent a variety of weather conditions of some major agricultural production and urban areas in California. Air temperature, dew point temperature, wind speed and solar radiation data were collected from NWS and CIMIS and analyzed to assess the accuracy of predicted weather variables and of FRET ET_o forecasts. The FRET data consist of 1, 3, 5, and 7-day forecasts of the weather parameters and calculated ET_o values, which were then compared with the corresponding observed daily weather and ET_o data from CIMIS to statistically evaluate FRET performance. The comparison among forecast and measured weather variables revealed good match for maximum (R^2 ranging between 0.98 and 1.00) and minimum air temperature ($R^2 > 0.91$), dew point temperature (R^2 ranging between 0.7 and 1.00) and wind speed (R^2 ranging between 0.66 and 0.99), but less accurate results

were obtained for solar radiation (R^2 ranging between 0.21 and 0.87). The analysis also showed good correlation between the FRET ET_o forecast data and observed CIMIS ET_o data (R^2 ranging between 0,93 and 1.00 and RMSE is less than 1 mm d-1) for the majority of the stations, with some differences that are likely due to the climatic conditions of specific locations. This suggests that FRET ET_o forecasts provide reliable information for predicting the near-future water demand and improving irrigation water management in California. The comparisons are promising for most of the 15 CIMIS station locations, and it is likely that the FRET model has the potential to provide accurate ET_o forecasts in similar semi-arid and sub-humid areas elsewhere. Weekly irrigation schedule examples are provided to illustrate the use of FRET ET_o forecasts along with soil properties and irrigation systems' performance for prospective irrigation scheduling of some specialty crops and urban landscape. The information provided in this article can help to improve water management efficiency of high-frequency agricultural irrigation systems and urban sprinkler irrigation systems in California and other locations with similar climates. It also offers a less expensive method to obtain ET_o data in developing countries that do not have ET_o station networks, and it offers an alternative to installing ET_o stations in agricultural and urban areas where it is difficult to find acceptable surfaces for ET_o stations.

Keywords: CIMIS; ET_o; Penman Monteith equation; Weather data; Irrigation scheduling

4.1. Introduction

Frequent water applications are required for agricultural low volume micro-irrigation and for urban high frequency sprinkler irrigation systems. Low volume micro-irrigation practices are commonly used for many crops because of better control on water distribution and fertigation through the irrigation system (Fares and Abbas 2009). These systems typically have a higher distribution uniformity and application efficiencies than surface and traditional sprinkler irrigation systems. In addition, frequent low volume micro-irrigation events often deliver higher yields and better crop quality (Madramootoo and Morrison 2013; Suryavanshi et al. 2015). Urban irrigation systems are often designed to apply water frequently and during the nighttime so that people can use and enjoy the landscapes during daytime. While near-real-time evapotranspiration (ET) information is helpful for scheduling irrigation with traditional low-frequency methods, e.g., furrow, basin, border, and impact sprinkler, using the ET-based method with ET_o information from the previous week is somewhat less efficient for scheduling high-frequency irrigation of crops where the water must be

ordered a few days in advance of the irrigation event, as well as for urban landscapes, where irrigation times are commonly programmed into a controller for the coming week (Luo et al. 2014). In the case of micro-irrigated specialty crops, scheduling irrigation for the upcoming week based on ET_o from the previous week may carry forward deficit and/or excessive water applications without the possibility to tailor irrigation events to varying weather conditions from one week to the next. In this regard, accurate ET_o forecast information becomes useful to improve irrigation efficiency and to account for weather variations (Melton et al. 2012).

Time series forecasting has gained remarkable interest from researchers in the last few decades, and ET_o forecasts are becoming important for real-time irrigation scheduling and agricultural water management (e.g. Ballesteros et al. 2016); especially in semi-arid and arid regions where supplemental or full irrigation is often needed to produce crops. This is mainly due to important advances in weather forecasting methods based on statistical and numerical weather prediction (NWP) models (Bauer et al. 2015), which provide a solid proof of the suitability of ET_o forecasts as a substitute to weather stations measurements (Cai et al. 2007; Perera et al. 2014; Luo et al. 2015; Traore et al. 2016; Ballesteros et al. 2016; Yang et al. 2016; Manikumari et al. 2017; Liu et al. 2020). Moreover, the ability to forecast ET_o and the accuracy of predictions are projected to improve in the future and the forecast uncertainties will decline as the performance of the statistical and NWP models increase or systematic errors are minimized from the forecast weather variables. Using forecast ET_o has advantages in that it helps farmers making optimal irrigation decisions by enabling them to schedule water applications on the basis of expected weather conditions rather than on intuitions or past weather data (Vanella et al. 2020). According to Ballesteros et al. (2016), the forecasting methodology should allow for accurate predictions for the period of high crop water requirements, because failures in the determination of crop requirements could strongly affect crop yield, if underestimated, and water usage, if overestimated. This in turn increases farm profits from higher yields, lower water and energy usage, and/or greater irrigation and energy productivity. In addition, reliable ET_o forecasts can reduce costs by eliminating the need for automated weather networks, or decreasing the number of weather stations, while providing ET_o data in a timely fashion for irrigation scheduling purposes (Duce et al. 2000). Since ET_o forecast models have the capacity to produce spatially distributed data, having forecast ET_o is relevant for assessments and studies at regional scale, unlike in-situ observations obtained from weather stations in heterogeneous landscapes (e.g., Cruz-Blanco et al. 2014; Tomas-Burguera et al. 2018). Similar

limitations in obtaining accurate spatial ET_o information are experienced with remote sensing techniques because of coarse temporal resolution due to infrequent satellites overpasses and/or gaps in imagery acquisition due to cloud cover (Ju and Roy 2008). Forecast model outputs, however, are usually available to the scientific community but not to the public, as they are difficult to analyze and interpret for non-professionals (Yang et al. 2016). These limitations fostered the development of free and user-friendly models to produce daily ET_o forecast data and make them accessible to the public. In California, early in the development of the CIMIS network, it was discovered that newspapers, radio, and TV media generally refused to disseminate ET_o information from a State-run ET_o station network to the public because they felt that the State was an unreliable source for information. On the other hand, the news media were open to disseminating information from the NWS, which is considered a reliable source of information.

In this context, an ET_o forecast product (FRET) was originally developed in California to help improve irrigation scheduling and management of high frequency agricultural and urban irrigation systems and to encourage the adoption and use of ET-based scheduling. The FRET model to forecast ET_o was developed jointly by the University of California Agriculture and Natural Resources (UC ANR), the California Department of Water Resources (CDWR), and the US National Weather Service (NWS). Nationwide, FRET ET_o forecasts up to 7-day lead are updated twice a day and they are disseminated through an internet website. The NWS daily forecast weather data are generated with the Global Forecast System (GFS) mesoscale model and output to a gridded map. The GFS is a weather forecast model produced by the National Centers for Environmental Prediction (NCEP). The model is described online (NOAA 2021). The 7-days forecast of weather and ET_o data are found by selecting a location on variable-specific gridded map. To obtain the data, the user selects a point on the map, and uses a selection bar to choose days 1-7 to retrieve the forecast variable and ET_o. Note that day 1 is the current day forecast and days 2-7 are for the following six days. The NWS forecast data includes all of the variables used to calculate ET_o except solar radiation, which is not forecast but estimated from forecast daily cloud cover.

The FRET model was tested in California and afterwards extended by the NWS to provide ET_o forecasts for the entire continental USA. FRET forecasts of daily ET_o are freely disseminated over the 48 continental states daily via a dedicated website (https://digital.weather.gov/). Note that it is

possible to display several variables on the map, so "Daily FRET (in.)" is selected from a dropdown menu above the map to display the daily ET_o map.

The NWS calculates FRET ET_o in metric units, but it converts the ET_o rates to inches per day for use by irrigators within the USA. FRET was developed to help improve irrigation management of high frequency agricultural micro-irrigation systems and high application frequency urban sprinkler systems. For high frequency micro-irrigation systems, there is an advantage in using forecast ET_o as it offers irrigators the ability to adjust irrigation schedules by matching irrigation applications to actual soil water depletion and plant water status. It is also of practical use by farm managers and irrigators who use automation hardware and controllers to manage irrigation and adjust for weather changes. Considering that farmers make decisions on the timing and amount of water to apply a few days before the actual irrigation events, forecast weather information can potentially increase productivity by optimizing irrigation applications and energy usage during low-peak rate times.

CIMIS is a large network of automated weather stations operated by the CDWR that provides free near-real-time ET_o data to California growers, urban landscape managers and various other professionals and stakeholders to support irrigation planning and management decisions (https://cimis.water.ca.gov), as well as to inform pest control practices. For information on CIMIS and its applications see Cohen-Vogel et al. (1998), Eching (2002), Hart et al. (2009) and Snyder et al. (2015). The CIMIS network encompasses about 150 automated weather stations that are mostly located over well-watered, cool-season grass fields as recommended by the United Nations-Food and Agriculture Organization (UN-FAO) (Allen et al. 1998) and by the American Society of Civil Engineers-Environmental Water Resources Institute (ASCE-EWRI) (TCSRE 2005).

The CIMIS network stations collect hourly weather data over large well-watered grass fields and hourly ET_o is calculated following Allen et al. (2006). CIMIS daily ET_o is computed from the 24-hourly ET_o calculations. The NWS and CIMIS provide respectively forecast and observed values of air temperature and relative humidity at 1.5 m height. The NWS provides forecast wind speed values at 10 m above the ground, whereas CIMIS measures wind speed at 2 m height. For the purpose of the present study, the NWS wind speed forecast data at 10 m height were adjusted to estimate wind speed at 2 m height prior to comparing with CIMIS data using Equation 4-1:

$$u_2 = u_z \left(\frac{4.87}{\ln(67.8\, z_w - 5.42)} \right) \quad (4\text{-}1)$$

where u_2 and u_z are wind speeds (m s^{-1}) at heights of 2 m and z_w m, respectively, above the ground level. FRET ET_o forecasts were previously compared to ET_o values calculated from measured weather variables for 42 locations in Florida, and results showed that forecasts were similar to calculated data (Migliaccio et al. 2017). Additional information on FRET is available from Hobbins (2010).

Our assumption is that a good match between FRET forecast and CIMIS observed daily ET_o for a specific CIMIS station validates the utility of the NWS FRET ET_o forecast model in the micro-climate of that station. Therefore, the NWS FRET model should provide an accurate ET_o forecast in other states or countries having a similar micro-climate as the specified CIMIS station.

The main objective of this research is evaluating the accuracy of predicting daily ET_o using 1-, 3-, 5-, and 7-day NWS model weather forecast data and a daily ET_o equation (Allen et al. 1989) by comparing with observed CIMIS ET_o computed as the sum of 24 hourly ET_o calculations (Allen et al. 2006). Assessing how accurate the ET_o predictions are in various Californian microclimates is crucial to provide reliable data for improving irrigation management. Some sample irrigation schedules were developed using FRET ET_o information and they are provided to illustrate the use of forecast ET_o along with soil hydraulic properties and irrigation system's performance parameters for prospective irrigation decisions on specialty crops and urban landscape.

4.2.Materials and Methods

4.2.1. Study area

Since meteorological variables are non-homogeneous over large areas and have variable effects on ET_o, it is important to evaluate FRET performance for a range of microclimatic conditions. In order to represent different microclimatic conditions, 15 CIMIS stations were considered for this study and selected from different counties within the state of California. Figure 4-1 illustrates the CIMIS station locations, and the climatic information for each selected station are presented in Table 4-1. The ET_o zones refer to the California ET_o zone map (CIMIS 2012), which divides California into 18 ET_o zones on the basis of long-term ET_o averages.

Fig. 4-1. Map of California with the location (red dots) of the 15 CIMIS stations considered for the present study.

4.2.2.FRET ET_o

The daily ET_o equation from the UN-FAO Irrigation and Drainage Handbook No. 56 (Allen et al. 1998), also endorsed by ASCE-EWRI in TCSRE (2005), was selected as the most widely accepted equation. All the variables except solar radiation that are required to calculate ET_o with this equation are forecast by the NWS. Daily solar radiation is estimated as a function of fraction cloud cover based on an equation from Doorenbos and Pruitt (1977). The daily standardized reference evapotranspiration equation for short canopies is based on the original Penman-Monteith (PM) equation (Monteith 1965) except for the fact that it was modified from an instantaneous ET_o equation to a daily ET_o equation by changing some of the variables and estimating the daily mean canopy resistance as $r_c = 70$ s m^{-1} and the aerodynamic resistance as $r_a = 208/u_2$ s m^{-1}, where u_2 is the mean daily wind speed measured at 2 m height above the ground.

Table 4-1. Location, ET_o zone and climate class of the 15 CIMIS stations selected for the present study.

Station ID	ET_o Zone	Station name	Climate Class [a]	Latitude[b]	Longitude[b]	Elevation (m)
2	16	Five Points South West	Semi-arid, steppe (BSk)	36.3820	-120.2298	82.30
5	15	Shafter	Arid low latitude desert (BWh)	35.5325	-119.2817	109.73
6	14	Davis	Mediterranean/hot summer (Csa)	38.5356	-121.7763	18.29
13	13	Camino	Mediterranean/hot summer (Csa)	38.7531	-120.733	847.34
35	14	Bishop	Semi-arid, steppe (BSk)	37.3585	-118.4055	1271.02
39	12	Parlier	Semi-arid, steppe (BSk)	36.5974	-119.5040	102.72
64	3	Santa Ynez	Mediterranean/cool summer (Csb)	34.5831	-120.0792	149.35
75	4	Irvine	Semi-arid, steppe (BSk)	33.6884	-117.7211	124.97
77	8	Oakville	Mediterranean/cool summer (Csb)	38.4284	-122.4102	57.91
78	9	Pomona	Mediterranean/hot summer (Csa)	34.5658	-117.8130	222.504
87	18	Meloland	Arid low latitude desert (BWh)	32.8061	-115.4462	-15.24
90	7	Alturas	Cool continental/dry summer (Dsb)	41.4382	-120.4803	1342.64
171	6	Union City	Mediterranean/cool summer (Csb)	37.5987	-122.0532	4.88
173	1	Torrey Pines	Semi-arid, steppe w/summer fog (BSkn)	32.9018	-117.2504	102.108
211	10	Gilroy	Mediterranean/cool summer (Csb)	37.0150	-121.5370	56.388

[a] The explanation of each letter symbol can be found in Arnfield (2020).

[b] In decimal degrees (DD)

Both the UN-FAO Irrigation and Drainage Handbook No. 56 (Allen et al. 1998) and the report by ASCE-EWRI (Allen et. al 2005) explain in detail the daily ET_o equation and the recommended procedures to measure and calculate variables that are inputs in that equation. The daily standardized reference evapotranspiration is calculated as indicated in Equation 4-2:

$$ET_o = \frac{0.408\Delta(R_n - G) + \gamma\left(\frac{900}{T_m+273}\right)u_2(e_s - e_d)}{\Delta + \gamma(1 + 0.34u_2)} \quad (4\text{-}2)$$

where R_n (MJ m^{-2} d^{-1}) is the net radiation, G (MJ m^{-2} d^{-1}) is the ground heat flux, T_m (°C) is the mean daily temperature, u_2 (m s^{-1}) is the mean daily wind speed, e_s (kPa) is the saturation vapor pressure at T_m, and e_d (kPa) is the vapor pressure at the mean daily dew point temperature T_d (°C). Note that Δ (kPa °C^{-1}) is the slope of the saturation vapor pressure at T_m and γ (kPa °C^{-1}) is the psychrometric constant. The estimate of the ratio of crop surface

resistance (r_c) to aerodynamic resistance (r_a) included in the standardized surface (Allen et al. 1998; TCSRE 2005) has the form indicated hereafter:

$$0.34u_2 = \frac{r_c}{r_a} \approx \frac{70\ s\ m^{-1}}{\frac{208}{u_2} s\ m^{-1}} \tag{4-3}$$

The numeric value of 900 is a product of several fixed values and the 0.408 converts the (R_n - G) from MJ m^{-2} d^{-1} to mm d^{-1}. Note that daily R_n is computed from daily solar radiation (R_s), elevation (E), latitude (deg.), day of the year (i = 1-365), solar constant G_{SC} = 0.082 MJ m^{-2} min^{-1}, saturation vapor pressure at maximum [$e_s(T_x)$] and minimum [$e_s(T_n)$] daily air temperature, and mean daily dew point temperature [$e_d = e_s(T)$]. Details on the calculation of R_n are presented in (Allen et al. 1998; TCSRE 2005).

The NWS forecasts all the necessary variables except solar radiation, which is a key input into the daily ET_o equation. The NWS, however, employs a daily fraction cloud cover forecast to estimate daily solar radiation R_s rather than directly using a R_s forecast using the approach published in the UN-FAO Irrigation and Drainage Handbook No. 24 (Doorenbos and Pruitt 1977). The daily fraction cloud cover (C_c) is used to estimate the daily ratio of actual to potential sunshine hours (n/N) using Equation 4-4.

$$\frac{n}{N} = -0.0083\ C_c + 0.9659 \tag{4-4}$$

Then, the daily solar radiation (R_s) is calculated from n/N using Equation 4-5 and extraterrestrial radiation (R_a), which is a function of the latitude and the day of the year.

$$R_s = \left(0.25 + 0.5\ \frac{n}{N}\right) \cdot R_a \tag{4-5}$$

The calculation of daily R_a is described in (Allen et al. 1998; TCSRE 2005).

The NWS forecasts are made available to the public and are updated twice per day. Every day, forecasts for the next seven days can be retrieved from the NWS digital forecast map (https://digital.weather.gov/). Please note that the FRET forecast data are not archived, so for the specific purpose of the present study, the 1-.3-, 5-, and 7-day forecasts of weather and ET_o data were downloaded and archived on every working day during the data collection phase. Specifically, data were downloaded daily from the 2nd of June to the 17th of September 2019, for a total of 108 days.

4.2.3.CIMIS ET_o

CIMIS stations measure weather data each minute and ET_o is calculated with an hourly time-step using R_s (MJ m^{-2} h^{-1}), mean air temperature (T_m, ^oC), mean dew point temperature (T_d, ^oC) and mean wind speed (u_2, m s^{-1}), using the hourly ET_o equation as described in (TCSRE 2005; Allen et al. 2006). Note that the hourly ET_o equation was modified from that in Allen et al. (1998) to better account for stomata closure during nighttime. The equations for daylight hours (Equation 4-6) and for nighttime hours (Equation 4-7) are employed by CIMIS to compute hourly ET_o based on TCSRE (2005) and Allen et al. (2006):

$$ET_o = \frac{0.408\Delta\,(R_n - G) + \gamma\left(\frac{37}{T_m+273}\right)u_2(e_s - e_d)}{\Delta + \gamma(1 + 0.24u_2)} \quad (4\text{-}6)$$

$$ET_o = \frac{0.408\Delta\,(R_n - G) + \gamma\left(\frac{37}{T_m+273}\right)u_2(e_s - e_d)}{\Delta + \gamma(1 + 0.96u_2)} \quad (4\text{-}7)$$

The hourly ET_o equation differs from the daily ET_o equation in that the value of 900 in Eq. 4-2 is replaced by 37 = 900/24 and the r_c from Eq. 4-2 is changed from 70 s m^{-1} to 50 s m^{-1} during daylight hours and to 200 s m^{-1} during nighttime. The aerodynamic resistance r_a is still calculated as $208/u_2$, so the numeric value of 0.34 in Eq. 4-2 is changed to r_c = 50/208=0.24 during daylight (Eq. 4-6) and r_c = 200/208 = 0.96 during nighttime (Eq. 4-7). The transition between daytime and nighttime is determined using the day of the year and the latitude and longitude. The methodology to compute hourly ET_o is thoroughly explained in TCSRE (2005) and Allen et al. (2006). The CIMIS daily ET_o is calculated as the sum of the midnight to midnight 24 hourly ET_o values. All collected and computed CIMIS data are archived and are made available online to the public.

4.2.4.Model evaluation

To evaluate the FRET model's performance, specific statistical indices were used, as suggested by Wilks (2005):

i. Coefficient of determination, R^2 (Equation 4-8)

ii. Root Mean Square Error, RMSE (Equation 4-9);

iii. Mean Absolute Error, MAE (Equation 4-10);

iv. Residual Mass Coefficient, CRM (Equation 4-11);

$$R^2 = \frac{(\sum(x_i - \hat{x})(y_i - \hat{y}))^2}{\sum(x_i - \hat{x})^2 \sum(y_i - \hat{y})^2} \quad (4\text{-}8)$$

$$RMSE = \sqrt{\frac{\sum(y_i - x_i)^2}{n}} \quad (4\text{-}9)$$

$$MAE = \frac{(\sum|y_i - x_i|}{n} \quad (4\text{-}10)$$

$$CRM = \frac{\sum_{i=1}^{n} y_i - \sum_{i=1}^{n} x_i}{\sum_{i=1}^{n} y_i} \quad (4\text{-}11)$$

where y_i is the measured value, x_i is the forecast value, $\hat{y}$ and $\hat{x}$ are the means of the data arrays of y_i and x_i, and n is the number of measured/forecasted data.

Both MAE and RMSE express average model prediction error in units of the variable of interest. The main difference between these two metrics is that RMSE gives a relatively high weight to large errors. This means that the RMSE should be more useful when large errors are particularly undesirable. The CRM is a measure of the tendency of the model to overestimate or underestimate the variable of interest. Positive values for CRM indicate that the model underestimates the variable of interest. Negative values for CRM indicate a tendency to overestimate. For a perfect fit between measured and forecasted data, values of MAE, RMSE and CRM should equal 0.0. For R^2, it should be equal to 1.0. It is worth noting that the meteorological variables were evaluated using only R^2 and RMSE, while all statistical indexes were used for ET_o since it is the main focus of this work.

4.3.Results and discussion

4.3.1. Comparison of NWS forecast data with CIMIS measured data

The comparisons between forecast weather variables used for calculating FRET ET_o and the measured weather variables used for computing CIMIS ET_o were performed with datasets relative to 108 days spanning over the period from June to September 2019. Specifically, observed CIMIS weather data for each day were compared with the corresponding weather data that was forecast 1, 3, 5, and 7 days earlier. The graphs from Figure 4-2a to Figure 4-2e show average monthly values of maximum (T_x) and minimum (T_n) air temperature, dew point temperature (T_d), wind speed (u_2) and solar radiation (R_s), for the selected 15 CIMIS stations, while Tables 4-2 through 4-6 show the RMSE and R^2 values for the comparison of measured versus forecast daily values. Figure 4-2f shows CIMIS ET_o monthly means. Note that the Oakville CIMIS ET_o data were unavailable during June due to delays in obtaining parts for a maintenance problem.

The air temperature comparison (Tables 4-2 and 4-3) shows a good agreement for forecast and observed data. For T_x, R^2 values are between 0.98 and 1.00, whereas RMSE values are between 0.7°C and 4.4°C. The 4.4 °C was associated with the Camino CIMIS station for all lead times. The higher RMSE is likely due to the effect of pine trees that are grown seasonally around the weather station for repopulating burned forest areas (Wang et al. 2015). For T_n, R^2 values are higher than 0.91, while RMSE values range between 1.3 °C and 4.7 °C. The results indicated that the forecast is better for T_x than T_n, which agrees with some previous forecast studies (Perera et al. 2014) and disagrees with other studies (Luo et al. 2015; Yang et al. 2016). With few exceptions, the T_x and T_n forecast performance decreased as the number of forecast days increased.

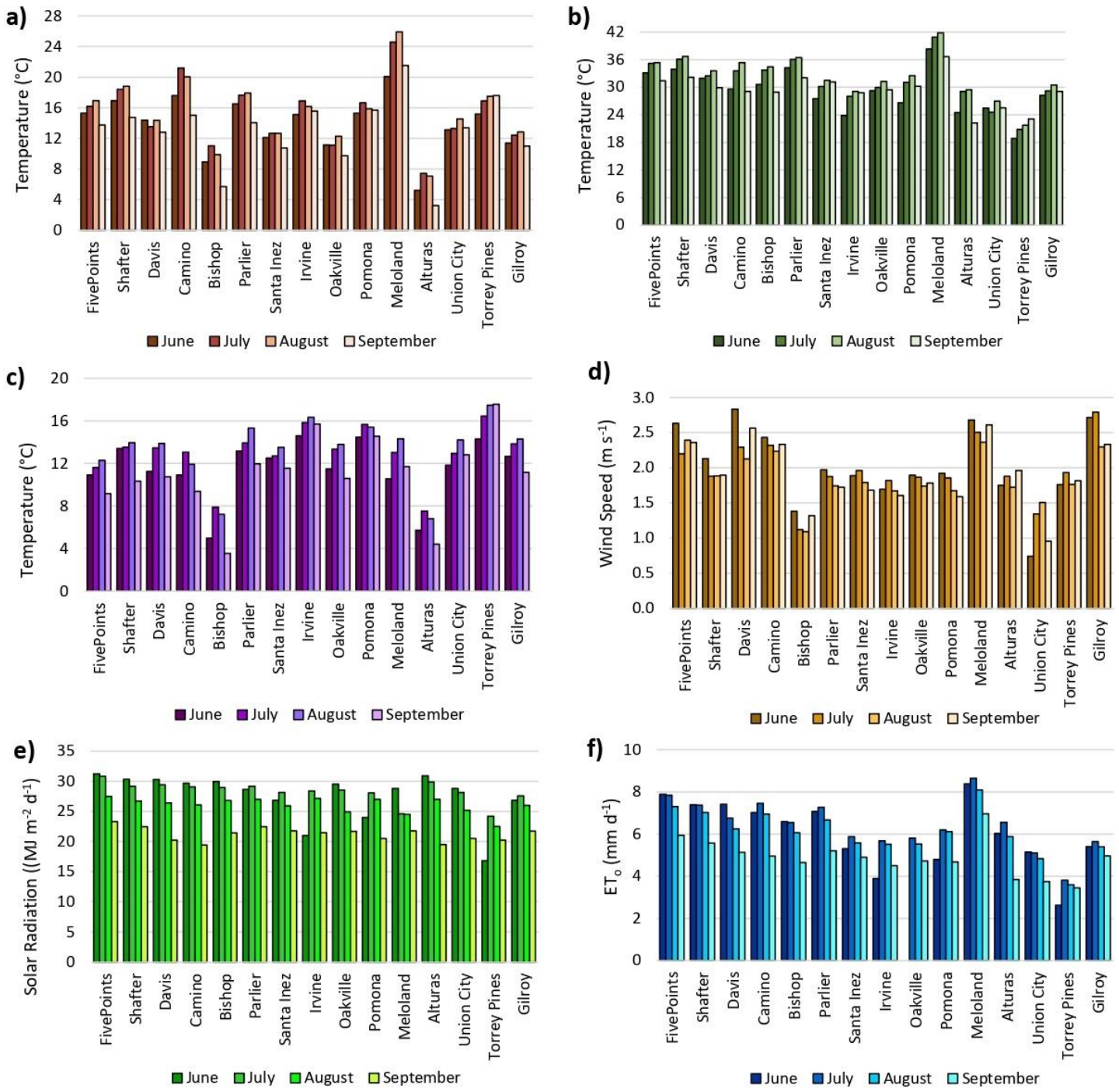

Fig. 4-2**.** a) Minimum air temperature; b) Maximum air temperature; c) Dew point temperature; d) Wind speed measured at 2 m height; e) Solar radiation; and f) ET_o. The data are monthly means for the 15 CIMIS stations considered for this study for the period of June through September 2019.

Table 4-2. Root mean square error (RMSE) and coefficient of determination (R^2) for the comparison between measured and forecast maximum air temperature (T_x)

			RMSE (°C)				R^2			
Station ID	**ET_o zone**	**Name**	**1d**	**3d**	**5d**	**7d**	**1d**	**3d**	**5d**	**7d**
2	16	Five Points	1.83	2.01	2.30	2.46	1.00	1.00	1.00	1.00
5	15	Shafter	1.09	1.25	1.59	1.84	1.00	1.00	1.00	1.00
6	14	Davis	1.15	1.41	1.73	2.18	1.00	1.00	1.00	1.00
13	13	Camino	3.85	3.74	4.07	4.43	1.00	1.00	1.00	1.00
35	14	Bishop	1.95	2.05	1.98	2.21	1.00	1.00	1.00	1.00
39	12	Parlier	0.74	0.91	1.39	2.02	1.00	1.00	1.00	1.00
64	3	Santa Ynez	2.42	2.83	3.40	3.99	0.99	0.99	0.99	0.98
75	4	Irvine	1.98	2.24	2.47	2.79	1.00	1.00	0.99	0.99
77	8	Oakville	2.63	2.65	2.78	3.62	0.99	0.99	0.99	0.99
78	9	Pomona	1.39	1.49	2.23	2.58	1.00	1.00	0.99	0.99
87	18	Meloland	2.61	2.95	2.63	2.84	1.00	1.00	1.00	1.00
90	7	Alturas	1.92	2.13	2.83	3.38	1.00	1.00	0.99	0.99
171	6	Union City	2.05	2.18	2.71	3.30	0.99	0.99	0.99	0.98
173	1	Torrey Pines	1.53	1.56	1.62	1.78	1.00	1.00	1.00	0.99
211	10	Gilroy	2.07	2.17	2.91	3.34	1.00	1.00	0.99	0.99

Table 4-3. Root mean square error (RMSE) and coefficient of determination (R^2) for the comparisons between measured and forecasted minimum air temperature (T_n)

			RMSE (°C)				R^2			
Station ID	**ET_o zone**	**Station name**	**1d**	**3d**	**5d**	**7d**	**1d**	**3d**	**5d**	**7d**
2	16	Five Points	3.67	2.58	2.90	3.11	0.97	0.99	0.98	0.98
5	15	Shafter	1.29	1.37	1.53	1.83	1.00	0.99	0.99	0.99
6	14	Davis	1.84	1.84	1.99	2.03	0.99	0.99	0.99	0.99
13	13	Camino	3.21	3.36	3.53	3.95	0.99	0.99	0.99	0.98
35	14	Bishop	4.02	4.20	4.40	4.66	0.97	0.97	0.96	0.96
39	12	Parlier	1.28	1.39	1.60	1.93	1.00	0.99	0.99	0.99
64	3	Santa Ynez	1.45	1.78	1.54	1.60	0.99	0.98	0.99	0.99
75	4	Irvine	1.77	2.17	2.32	2.18	0.99	0.99	0.99	0.99
77	8	Oakville	3.04	2.84	3.07	3.24	0.98	0.98	0.98	0.97
78	9	Pomona	2.04	2.45	2.32	2.41	0.99	0.99	0.99	0.99
87	18	Meloland	2.75	3.33	3.64	4.13	0.99	0.98	0.98	0.97
90	7	Alturas	1.98	2.19	2.48	2.82	0.95	0.94	0.92	0.91
171	6	Union City	1.63	1.86	1.93	1.89	0.99	0.99	0.99	0.99
173	1	Torrey Pines	1.71	1.74	1.82	1.96	1.00	1.00	0.99	0.99
211	10	Gilroy	1.87	2.28	2.52	2.54	0.98	0.97	0.97	0.96

For T_d, the R^2 values fall between 0.70 and 1.00 and RMSE values range between 1.0 °C and 5.4 °C (Table 4-4). The 5-day forecasting performance is worse than for other forecast periods, and T_d tends to have lower R^2 and higher RMSE at stations with higher elevation, i.e. the weather stations at Camino (847 m a.s.l), Bishop (1271 m a.s.l) and Alturas (1343 m a.s.l.). The Torrey Pines station is located on the Pacific Coast and it "is affected by the movement of the marine layer across the site" as indicated in the station description on the CIMIS web site (https://cimis.water.ca.gov/Stations.aspx). The Torrey Pines station has one of the best T_d forecasts of all the 15 stations in this study.

Table 4-4. Root mean square error (RMSE) and coefficient of determination (R^2) for the comparisons between measured and forecast dew point temperature (T_d).

			RMSE (°C)				R^2			
Station ID	**ET_o zone**	**Station name**	**1d**	**3d**	**5d**	**7d**	**1d**	**3d**	**5d**	**7d**
2	16	Five Points	1.62	2.62	3.42	3.28	0.98	0.96	0.92	0.93
5	15	Shafter	2.39	3.17	3.27	3.34	0.98	0.96	0.97	0.97
6	14	Davis	1.68	1.49	1.97	1.83	0.99	0.99	0.98	0.98
13	13	Camino	4.21	3.52	5.44	5.32	0.97	0.96	0.85	0.88
35	14	Bishop	2.71	3.85	4.38	4.27	0.79	0.77	0.70	0.74
39	12	Parlier	1.66	2.67	2.68	3.17	0.99	0.97	0.98	0.96
64	3	Santa Ynez	1.49	2.38	3.41	2.68	0.99	0.98	0.97	0.97
75	4	Irvine	1.05	0.95	2.07	1.30	1.00	1.00	0.99	1.00
77	8	Oakville	2.04	2.61	3.08	3.29	0.98	0.98	0.98	0.98
78	9	Pomona	1.04	1.32	2.22	2.01	1.00	0.99	0.99	0.99
87	18	Meloland	4.08	3.98	3.74	4.01	0.95	0.93	0.93	0.93
90	7	Alturas	2.29	2.54	2.67	2.64	0.72	0.87	0.85	0.86
171	6	Union City	2.70	1.62	2.83	1.88	0.99	0.99	1.00	1.00
173	1	Torrey Pines	1.45	1.17	1.32	1.50	1.00	1.00	0.98	0.98
211	10	Gilroy	2.35	2.99	3.02	3.12	0.99	0.99	0.97	0.96

Forecasting wind speed is more complicated than other weather variables, due to the intermittent and unstable nature of the wind (Tascikaraoglu and Uzunoglu 2014; Wang et al. 2014; Wang et al. 2017). However, the wind speed results are good (Table 4-5) with R^2 values ranging between 0.66 and 0.98 and RMSE values ranging from 0.6 to 3.7 m s^{-1}. The wind speed forecast performance was variable for the different lead times and no clear trend with forecast time appears from the data analysis. Interestingly, the 1-day wind speed forecast was worst of the four forecast periods.

Table 4-5. Root mean square error (RMSE) and coefficient of determination (R^2) for the comparisons between measured and forecast 2-m wind speed (u_2).

			RMSE (m s^{-1})				R^2			
Station ID	**ET_o zone**	**Station name**	**1d**	**3d**	**5d**	**7d**	**1d**	**3d**	**5d**	**7d**
2	16	Five Points	0.92	1.26	0.82	0.74	0.91	0.85	0.93	0.94
5	15	Shafter	0.79	1.13	1.12	1.13	0.92	0.82	0.87	0.89
6	14	Davis	1.13	1.17	0.90	0.79	0.87	0.86	0.91	0.92
13	13	Camino	0.76	0.70	0.60	0.71	0.94	0.95	0.98	0.95
35	14	Bishop	2.58	1.04	1.05	1.03	0.80	0.83	0.83	0.83
39	12	Parlier	0.79	1.04	0.91	0.94	0.87	0.82	0.85	0.87
64	3	Santa Ynez	2.54	1.29	0.91	0.95	0.89	0.77	0.73	0.71
75	4	Irvine	0.94	1.13	1.21	1.20	0.90	0.77	0.73	0.71
77	8	Oakville	2.12	1.42	0.62	0.61	0.75	0.71	0.92	0.91
78	9	Pomona	1.87	0.92	1.19	1.17	0.87	0.83	0.68	0.87
87	18	Meloland	1.41	1.32	1.54	1.63	0.81	0.85	0.79	0.74
90	7	Alturas	2.24	0.78	1.25	1.27	0.81	0.87	0.66	0.68
171	6	Union City	3.73	1.41	0.83	0.82	0.75	0.70	0.78	0.77
173	1	Torrey Pines	1.64	0.91	0.89	1.05	0.96	0.86	0.87	0.78
211	10	Gilroy	1.19	1.59	1.73	1.82	0.88	0.73	0.90	0.89

The solar radiation (R_s) comparisons are summarized in Table 4-6. The NWS does not forecast solar radiation, but they do forecast cloud cover, which is then used to estimate solar radiation R_s. The R_s analysis show large variability with R^2 values ranging between 0.21 and 0.87 and RMSE between 1.5 and 6.7 MJ m^{-2} d^{-1}.

Overall, comparisons between measured and forecast weather parameters are satisfactory with a slight overestimation of T_x and T_n and a slight underestimation of T_d and R_s. The u_2 shows a large variability during the entire study period.

Table 4-6. Root mean square error (RMSE) and coefficient of determination (R^2) for the comparisons between measured and forecast solar radiation (R_s).

			RMSE (MJ $m^{-2}d^{-1}$)				R^2			
Station ID	**ET_o zone**	**Station name**	**1d**	**3d**	**5d**	**7d**	**1d**	**3d**	**5d**	**7d**
2	16	Five Points	2.88	2.60	3.01	3.01	0.53	0.59	0.51	0.58
5	15	Shafter	2.83	2.40	2.13	2.69	0.44	0.51	0.55	0.51
6	14	Davis	2.71	2.41	2.04	1.51	0.46	0.55	0.71	0.87
13	13	Camino	2.11	1.99	1.63	2.06	0.59	0.65	0.76	0.72
35	14	Bishop	3.37	3.32	2.57	3.24	0.55	0.52	0.72	0.62
39	12	Parlier	2.31	2.08	2.15	2.63	0.45	0.48	0.52	0.49
64	3	Santa Ynez	4.98	4.76	5.38	5.18	0.37	0.42	0.44	0.37
75	4	Irvine	5.82	5.98	6.12	5.73	0.49	0.48	0.49	0.46
77	8	Oakville	2.71	2.68	2.74	2.64	0.44	0.46	0.50	0.45
78	9	Pomona	3.91	3.46	3.39	3.91	0.34	0.42	0.56	0.44
87	18	Meloland	4.50	4.77	5.52	4.48	0.30	0.26	0.29	0.28
90	7	Alturas	3.96	4.10	3.69	3.26	0.49	0.48	0.62	0.65
171	6	Union City	4.06	4.59	4.11	3.79	0.32	0.35	0.52	0.49
173	1	Torrey Pines	6.38	6.22	6.67	6.39	0.21	0.38	0.40	0.27
211	10	Gilroy	2.85	2.91	3.10	3.00	0.35	0.35	0.34	0.36

4.3.2.Comparison of daily and 24 hourly ET_o using CIMIS data

Because FRET employs a daily equation for ET_o and CIMIS uses an hourly equation and sums the 24 hourly ET_o calculations to compute daily ET_o, a comparison between daily ET_o computed from both hourly and daily CIMIS data was conducted to determine how much difference in ET_o might be due to using the hourly and daily equations. The results are summarized in Table 4-7. The R^2 values for CIMIS data from using hourly versus daily data are between 0.83 and 0.98 and the RMSE values are between 0.2- and 0.5-mm d^{-1} for all stations except the station in Meloland, which has an R^2 = 0.6 and an RMSE of 1.3 mm d^{-1}. This station is located below sea level in the Low Desert region within a large irrigated area having variable wind speeds and a high chance of advection. The extreme local environment makes it difficult to accurately estimate ET_o with the PM equation (e.g., Irmak et al. 2005). Across all the 15 selected stations, the R^2 and RMSE values are quite good considering the ET_o values ranged between 1- and 14-mm d^{-1}. The good results obtained from this comparison indicate that a daily equation can provide ET_o values that are

comparable to ET_o computed as the sum of 24 hourly ET_o calculations. Therefore, if the NWS forecast weather data are accurate, accurate ET_o forecasting is also possible.

Table 4-7. Root mean square error (RMSE) and coefficient of determination (R^2) for the comparisons between sum-of-hourly ET_o and daily ET_o values from CIMIS.

Station ID	ET_o zone	Station name	RMSE (mm d^{-1})	R^2
2	16	Five Points	0,27	0.91
5	15	Shafter	0,26	0.91
6	14	Davis	0,22	0.96
13	13	Camino	0,19	0.97
35	14	Bishop	0,50	0.96
39	12	Parlier	0,26	0.89
64	3	Santa Ynez	0,20	0.94
75	4	Irvine	0,29	0.97
77	8	Oakville	0,47	0.94
78	9	Pomona	0,35	0.95
87	18	Meloland	1,52	0.60
90	7	Alturas	0,52	0.89
171	6	Union City	0,31	0.95
173	1	Torrey Pines	0,18	0.98
211	10	Gilroy	0,42	0.83

4.3.3.Comparison of ET_o from FRET with ET_o from CIMIS

The daily FRET ET_o forecast values provided by the NWS were compared with sums of 24-hourly ET_o values retrieved from CIMIS. Figure 4-3 shows plots of FRET vs. CIMIS ET_o for the month of July for all the forecast periods. July is usually the warmest month in California and the one with the highest crop irrigation requirements. The graphs show that there is a good agreement for all the 15 selected stations, ranging from low (Torrey Pines), to moderate (Oakville), and high (Meloland) evapotranspiration demand. Despite the variability in wind speed and solar radiation forecasts, the comparisons between the ET_o values from FRET and CIMIS showed a good match. The results indicate that the FRET daily ET_o equation is robust and smooths out errors related to the input variables. Figure 4-3 also shows that the 7-day ET_o forecast was nearly as good as the 1-day forecast, and the 3-day and 5-day forecasts were slightly better. This contrasts with the findings of Perera et al. (2014) who indicated a declining accuracy of ET_o forecasts for longer lead-times in

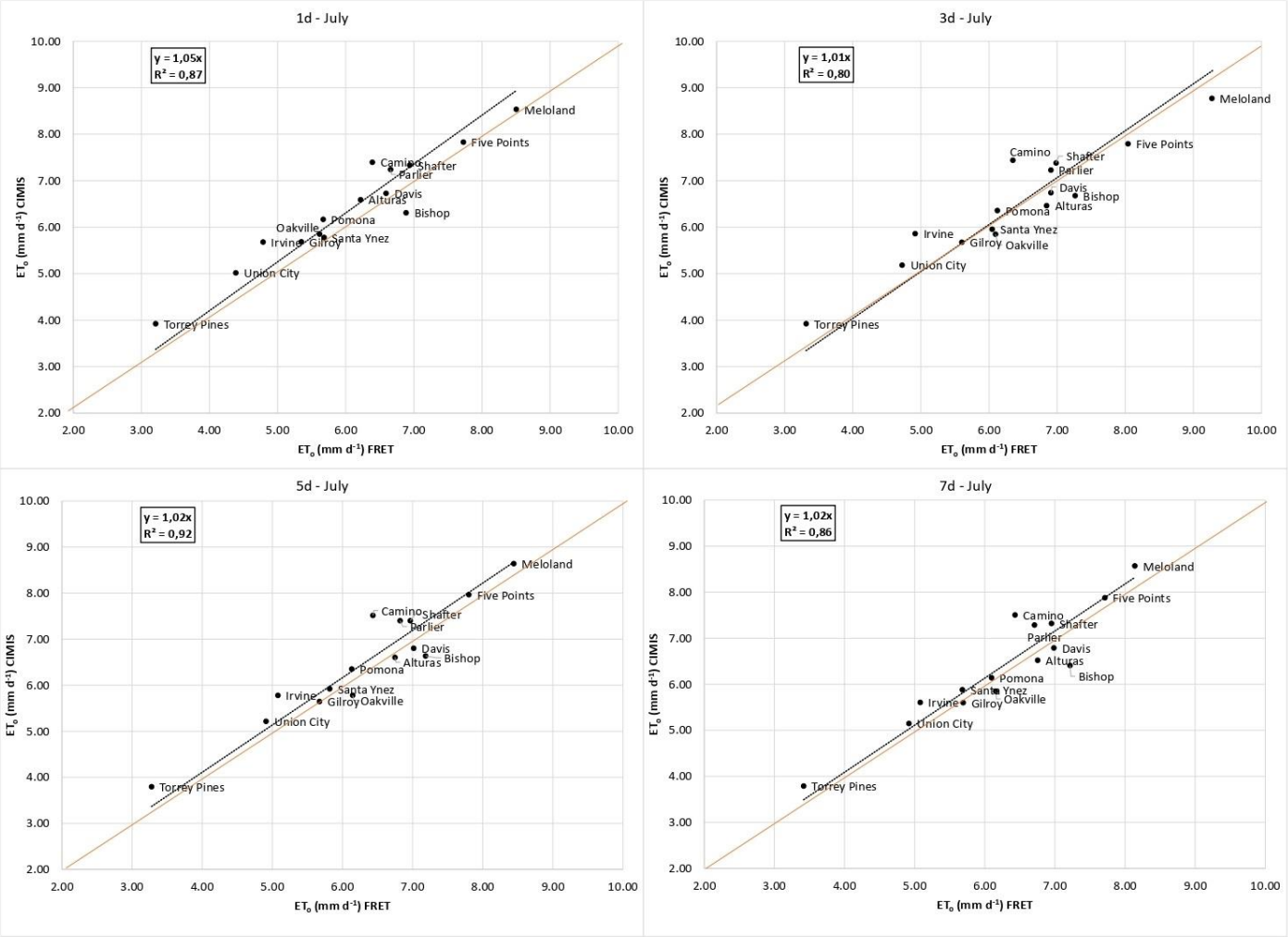

Fig. 4-3. Comparison between the FRET ET_o and the CIMIS ET_o, for all the 15 selected CIMIS stations in July 2019. The four graphs refer to different lead-times, i.e., 1, 3, 5 and 7- day, respectively.

Australia. This might be due to more predictable summer weather in California. Table 4-8 shows the slope of the least square regression line and R^2 for the comparisons between CIMIS ET_o and FRET ET_o for all months. The R^2 and RMSE values are similar to those for July (Fig. 4-3). Appendix A shows plots of FRET vs. CIMIS ET_o for the months of June and August for all the forecast periods. Tables 4-9 and 4-10 show the statistical indicators considering all the data together for each station and lead-time.

Table 4-8. Slope of the regression line and coefficient of determination (R^2) for the comparisons between CIMIS ET_o and FRET ET_o.

Month	**1d**		**3d**		**5d**		**7d**	
	slope	**R^2**	**slope**	**R^2**	**slope**	**R^2**	**slope**	**R^2**
June	1.03	0.94	1.01	0.94	1.02	0.92	1.06	0.90
July	1.05	0.87	1.01	0.80	1.02	0.92	1.02	0.86
August	1.05	0.81	0.996	0.75	1.03	0.83	1.01	0.82

Table 4-9. Root mean square error (RMSE) and coefficient of determination (R^2) for the comparisons between CIMIS ET_o and FRET ET_o.

			RMSE (mm d^{-1})				**R^2**			
Station ID	**ET_o zone**	**Station name**	**1d**	**3d**	**5d**	**7d**	**1d**	**3d**	**5d**	**7d**
2	16	Five Points	0.62	0.65	0.60	0.60	0.99	0.99	0.99	0.99
5	15	Shafter	0.78	0.81	0.84	0.92	0.99	0.99	0.99	0.99
6	14	Davis	0.54	0.67	0.70	0.77	0.99	0.99	0.99	0.99
13	13	Camino	1.07	1.13	1.13	1.24	1.00	1.00	1.00	1.00
35	14	Bishop	0.97	1.18	1.03	1.13	0.99	0.98	0.98	0.98
39	12	Parlier	0.72	0.68	0.96	0.77	0.99	0.99	0.98	0.98
64	3	Santa Ynez	0.66	0.69	0.78	0.93	0.99	0.99	0.98	0.97
75	4	Irvine	1.13	1.01	1.04	0.96	0.96	0.97	0.97	0.97
77	8	Oakville	0.54	0.63	0.61	0.57	0.99	0.99	0.99	0.99
78	9	Pomona	0.77	0.64	0.75	0.82	0.99	0.99	0.98	0.99
87	18	Meloland	1.52	1.48	1.66	1.45	0.97	0.97	0.96	0.97
90	7	Alturas	0.64	0.82	0.65	0.74	0.99	0.98	0.99	0.98
171	6	Union City	0.65	0.65	0.60	0.65	0.98	0.98	0.99	0.98
173	1	Torrey Pines	0.89	1.09	0.94	0.83	0.95	0.94	0.93	0.95
211	10	Gilroy	0.63	0.76	0.85	0.97	0.99	0.98	0.98	0.97

The coefficient of determination R^2 ranges between 0.9 and 1.0, while RMSE is mostly less than 1 mm d^{-1}. The poorest results were obtained for the station located in Meloland (Low Desert region in southern California), with RMSE around 1.5-1.7 mm d^{-1}, and ET_o ranging from 2 to 12 mm d^{-1}. The MAE (Table 4-10) has values lower than the RMSE (Table 4-9), but the values are well correlated between the two statistics and both indicate that the FRET forecast ET_o error is generally small relative to the magnitude of the measured ET_o. The Coefficient of Residual Mass (CRM) is positive and nearing zero on most times. A positive value of CRM indicates the tendency of the

Table 4-10. Statistical indices Mean Absolute Error, (MAE) and Residual Mass Coefficient (CRM) for the comparisons between CIMIS ET_o and FRET ET_o.

			MAE (mm d^{-1})				CRM			
Station ID	**ET_o zone**	**Station name**	**1d**	**3d**	**5d**	**7d**	**1d**	**3d**	**5d**	**7d**
2	16	Five Points	0.46	0.47	0.47	0.48	0.04	-0.01	0.03	0.02
5	15	Shafter	0.65	0.65	0.67	0.73	0.08	0.06	0.08	0.09
6	14	Davis	0.39	0.50	0.52	0.52	0.03	-0.01	0.01	0.00
13	13	Camino	1.01	1.04	1.02	1.11	0.15	0.15	0.14	0.15
35	14	Bishop	0.73	0.94	0.77	0.87	-0.10	-0.13	-0.10	-0.13
39	12	Parlier	0.61	0.54	0.69	0.66	0.08	0.05	0.07	0.09
64	3	Santa Ynez	0.54	0.55	0.62	0.72	0.03	-0.02	0.00	0.03
75	4	Irvine	0.96	0.83	0.80	0.74	0.09	0.09	0.08	0.09
77	8	Oakville	0.40	0.50	0.49	0.45	-0.38	-0.46	-0.35	-0.30
78	9	Pomona	0.63	0.47	0.55	0.60	0.06	0.01	0.00	0.01
87	18	Meloland	0.90	0.84	1.11	1.04	0.02	-0.03	0.03	0.03
90	7	Alturas	0.50	0.58	0.49	0.58	0.06	-0.04	0.00	-0.01
171	6	Union City	0.50	0.52	0.46	0.49	0.06	0.03	0.04	0.03
173	1	Torrey Pines	0.74	0.83	0.81	0.71	0.11	0.06	0.07	0.07
211	10	Gilroy	0.53	0.61	0.72	0.80	0.03	0.01	0.03	0.03

model to underestimate the measured data. There are only two stations with a negative CRM, namely Bishop (the mountain range site) and Oakville (Napa Valley). Bishop has the highest elevation of the 15 stations, and it consistently has the lowest T_d of any location with $T_d < 0$ °C often even during summer. It is extremely dry, and this might explain why the forecast ET_o might exceed the observed ET_o. Oakville is in the heart of Napa Valley wine county, and it has considerable weather variation from day-to-day due to its proximity to the ocean and surrounding mountains. This may lead to large variations in humidity depending on the wind direction and that might explain why the FRET forecast is exceeding the observed ET_o. While there is no clear reason for why FRET slightly underestimates the observed ET_o at most of the stations or overestimates at Bishop and Oakville, it is most likely due to the NWS forecasts not perfectly representing weather data collected over irrigated grass fields.

4.4.Sample irrigation schedules using FRET ET_o forecasts

4.4.1.Using FRET ET_o to schedule agricultural irrigation

This section provides guidelines on how to develop weekly irrigation schedules using forecast ET_o data for a micro-irrigated nut orchard and a sprinkler-irrigated vegetable field. Since irrigation

scheduling based on forecast ET_o is not a common procedure amongst specialty crop growers, this section is included in the article to illustrate the use of FRET ET_o data to plan irrigation schedules for up to seven days in the future. These sample schedules are developed by integrating ET_c estimated using forecast ET_o and crop coefficient (K_c) values with information on soil infiltration rate, water holding capacity, water application rate, distribution uniformity, and grower-defined frequency and water application set times. Sample schedules are prepared at the end of each week (Friday) to book water deliveries from an irrigation district, and the irrigation schedules are passed on to the farm irrigation crew for execution during the following seven days (Saturday through Friday).

The FRET ET_o forecast is used for calculating ET_c and estimating soil water depletion below field capacity. The required gross irrigation depth is determined from the estimated water depletion in the effective rooting zone and the system distribution uniformity to optimize the application efficiency and refill the low quarter (E_Q) after each irrigation. The amount of water to apply depends on distribution uniformity of the irrigation system (drip, micro-sprinkler, sprinkler) as well as the irrigation timing, flow rate, and set-time. E_Q represents the percentage of gross water applied that is beneficially utilized to meet the crop consumptive use. For microirrigation, E_Q is calculated as the mean low quarter volume of irrigation water per unit area infiltrated and stored in the root zone. According to Keller and Bliesner (2000), E_Q is primarily a function of the water distribution uniformity (DU), but it also depends on minor losses (runoff, leaks, filters and line flushing, and drainage), unavoidable losses to deep percolation (due to soil wetting pattern and untimely rainfall), and avoidable losses resulting from poor irrigation scheduling. For well-watered crops, adequately maintained and properly operated microirrigation systems, and accurately scheduled irrigation, E_Q approximates the system DU.

In general, dividing the soil water depletion by the DU (instead of by E_Q) provides an estimate of the water depth that will infiltrate into the low quarter of an irrigated field. In this way, the low quarter of the field will receive sufficient water to return to field capacity and maintain good production, while the remainder of the field will receive more than sufficient water to refill the soil to field capacity.

The input information needed to develop an irrigation schedule for the upcoming week and the details about irrigation timing and maximum gross water depth to apply are indicated below:

1. Weekly ET_o (mm) obtained summing up the daily forecast ET_o from FRET for the next seven days.
2. Weekly or bi-weekly values of K_c for the current time period and crop stage.
3. Available water holding capacity of the soil (W_A, mm m^{-1}) from the site-specific soil survey or from tabulated values for the identified soil type (e.g., Table 4-12).
4. Effective crop root depth, Z_E (m) (e.g., Table 4-13).
5. Maximum allowable depletion (MAD, %) for the crop (e.g., Table 4-13).
6. Basic soil infiltration rate (IR_B, mm h^{-1}) from the site-specific soil survey or from tabulated values for the identified soil type (e.g., Table 4-14).
7. Tree spacing (T_S, m^2).
8. Average application rate of the irrigation system (AR, mm h^{-1}) from the system's performance evaluation or calculated from flow measurements (flow meter) and the area irrigated, or from tabulated values (e.g., Table 4-15).
9. Maximum recommended number of operation hours for the irrigation system ($IO_{MAX} \leq 16$ hours day^{-1}).
10. Distribution uniformity (low quarter DU) of the irrigation system (%) from the system's performance evaluation.

The distribution uniformity of the low quarter (DU_{LQ}) is a measure of how evenly water soaks in across a field and infiltrates into the soil root zone. DU_{LQ} is calculated with Equation 4-12:

$$DU_{LQ} = \frac{mean\ of\ low\ quarter\ applied\ depth}{overall\ mean\ of\ applied\ depths} \quad (4\text{-}12)$$

where the *"mean of the low quarter applied depth"* is the mean of the lowest 25% of application depth measurements, and the *"overall mean of applied depths"* is the mean of all application depth measurements.

The limit of 16 hours per day for irrigation system operation provides for a few down-time hours, which are necessary for irrigators and field personnel to trouble-shoot the irrigation system when

problems occur, or in case some equipment and components malfunction, fail or get damaged, thus requiring timely fix.

Table 4-11 shows the main input data, as well as the calculated gross irrigation requirements (GIR), the gross irrigation depth (D_G), the gross volume (I_V) and the irrigation set time duration (I_D) for a dual-line drip irrigated pistachio orchard and a sprinkler irrigated onion field located in the southern portion of the San Joaquin Valley of California for viable irrigation frequencies for a sample week during mid-August 2019. The sample schedules for pistachio account for tree spacing and density (Ts, m^2), while the schedule for sprinkler irrigated onion refers to a crop canopy covering about 100% of the planted area. The sample schedule for pistachio demonstrates either two or three irrigations per week, whereas the sample schedule for onion considers three irrigations per week or daily irrigations for the 6-day working week. The pistachio and onion irrigation schedule derivations are discussed below, while the values of input parameters related to weather, soil and irrigation system's performance, as well as the calculation results are all reported in Table 4-11.

Table 4-11. Irrigation scheduling examples using FRET ET_o information for drip irrigated pistachio, sprinkler-irrigated onion, and sprinkler-irrigated turfgrass for a sample week of mid-August 2019.

Data	Acronym	Dual-line Drip Pistachio	Hand-move Sprinkler Onion	Sprinkler Turfgrass
Weekly ET_o (mm), from FRET	FRET ET_o	48.0	57.1	45.6
Weekly mean crop coefficient for the current time period (and crop stage)	K_c	0.86	1.20	0.80
Net Irrigation Requirement (mm)	NIR	41.3	68.52	36.5
Basic soil infiltration rate (mm h^{-1}) from soil survey (or from reference tables, e.g., Table 4-14)	IR_B	5.0	9.5	10.0
Soil water holding capacity (mm of water per m of soil) from soil survey (or from reference tables, e.g., Table 4-12)	W_A	183	170	193.0
Effective crop root depth (m) (e.g. Table 4-13)	Z_E	1.5	0.45	0.5 – 1.0
Maximum allowable depletion for the crop (%) (e.g. Table 4-13)	MAD	50	30	50
Percentage wet area by the irrigation system (%)	P_W	40	100	100
Tree spacing (m^2)	T_S	6 x 5	-	-
Average application rate of the irrigation system, (mm h^{-1}) from the irrigation system's performance evaluation (or from reference tables e.g. Table 4-14 and Table 4-15)	AR	1.27	3.20	11.00
Distribution uniformity of the low quarter of the irrigation system (%) from the system's performance evaluation	DU_{LQ}	0.92	0.80	0.75
Gross Irrigation Requirement (mm)	GIR	45.0	85.6	48.6
Volume of water to apply per tree per week (l $tree^{-1}$ $week^{-1}$)	V_W	1350	-	-
THREE IRRIGATION EVENTS PER WEEK				
Gross depth of water to apply per irrigation (mm)	$D_{G\ (2\text{-}day)}$	15.0	28.5	-
Irrigation Volume per tree per irrigation (l $tree^{-1}$)	$I_{V\ (2\text{-}day)}$	450	-	-
Irrigation duration (h)	$I_{D\ (2\text{-}day)}$	12	9	-
TWO IRRIGATION EVENTS PER WEEK				
Gross depth of water to apply per irrigation (mm)	$D_{G\ (3\text{-}day)}$	22.5	-	-
Irrigation Volume per tree per irrigation (l $tree^{-1}$)	$I_{V\ (3\text{-}day)}$	675	-	-
Irrigation duration (h)	$I_{D\ (3\text{-}day)}$	17.5	-	-
TWO IRRIGATION CYCLES PER DAY				
Gross depth of water to apply for the 2-cycles frequency (mm)	$D_{G\ (2\text{-}cycles)}$	-	-	3.5
Irrigation duration (min)	$I_{D\ (2\text{-}cycles)}$	-	-	21

Table 4-12. Average available water holding capacity (TAW) for various soil textures

Soil type		Soil water holding capacity, W_A (mm m^{-1})
General description	**Texture class**	
light, sandy	coarse sand	42
	fine sand	75
	sandy loam	100
medium, loamy	fine sandy loam	125
	loam	150
	silt loam	167
heavy, clay	clay loam	183
	clay	200
	peat/muck	500

Note: Table is modified from U.S. Bureau of Reclamation, AGRIMET Irrigation Guide website (https://www.usbr.gov/pn/agrimet/irrigation.html)

Table 4-13. Effective root depth (Z_E) and maximum allowable depletion (MAD) for different crops.

Crop	Average root depth, Z_E (m)	MAD (%)
alfalfa	2.4	55
pasture	0.8	50
turf	0.5	50
small grains	1.4	55
beans	0.9	40
corn	1.7	50
potatoes	1.1	40
sugar beets	1.2	50
cotton	1.5	55
orchards	2.4	50-65
grapes	1.8	65

Note: Table is modified from U.S. Bureau of Reclamation, Agrimet Irrigation Guide website (https://www.usbr.gov/pn/agrimet/irrigation.html)

Table 4-14. Suggested maximum irrigation application rates (AR) for average soil, slope, and tilth.

Soil type	Maximum water application rate (mm h^{-1}) at slope ($AR \leq IR_B$)		
	0-5%	5-8%	8-12%
Coarse sandy soil	38.1 - 50.8	25.4 - 38.1	19.1 - 25.4
Light sandy soil	19.1 - 25.4	12.7 - 20.3	10.2 - 15.2
Silt loam	7.6 - 12.7	6.4 - 10.2	3.8 - 7.6
Clay loam, clay	3.8	2.5	2.0

Note: Table is taken from NRCS (1984)

Table 4-15. Average water application rates (AR) of different irrigation systems

System	Average Application Rate, AR (mm h^{-1}) *
Surface Irrigation	10-11
Sprinkler Irrigation	3.0-3.8
Micro-sprinkler	0.75-1.27
Drip Irrigation	0.25-0.75

* Values of application rates are taken from technical catalogs of irrigation manufacturers.

4.4.1.1.Sample irrigation schedule for a dual-line drip irrigated pistachio orchard

The following example describes a stepwise procedure for preparing an irrigation schedule for a dual-line drip irrigated pistachio orchard near Hanford, California (southern portion of the San Joaquin Valley) using the information from Table 4-11. The procedure also applies to other irrigation systems.

a) Max gross depth of water per irrigation ($D_{G\,MAX}$), calculated with Equation 4-13:

$$D_{G\,MAX} = \frac{MAD \times W_A \times P_W \times Z_E}{E_Q} = \frac{0.50 \times 183 \times 0.40 \times 1.5}{0.92} = 59.7 \text{ mm} \cong 60 \text{ mm} \qquad (4\text{-}13)$$

where P_W is the percentage of the ground area wetted by the dual drip system (40%) and E_Q is the water application efficiency for the low quarter. For well-water conditions, the DU_{LQ} value is commonly used as E_Q. If DU_{LQ} from the irrigation system's performance evaluation is not available, the use of realistic E_Q values from reference tables is recommended (e.g., Table 4-16). The maximum gross depth of water per irrigation ($D_{G\,MAX}$) is a limit value that should not be

exceeded when scheduling irrigations, as it represents the maximum depth of applied water that the effective root zone can store and make available for tree water use. Any applied water above this maximum limit may result in deep percolation and water loss, which will make irrigation less efficient and thus decrease the water productivity. To irrigate efficiently, during the irrigation season it is highly recommended to apply irrigation water in amounts less or equal than $D_{G\,MAX}$.

Table 4-16. Ranges of potential application efficiency of the low quarter (E_Q) for well-designed and well-managed irrigation systems

Irrigation method/system	Potential Low-quarter Application Efficiency, E_Q (%)
Sprinkler	
LEPA	80-90
Linear move	75-85
Center pivot	75-90
Travelling gun	65-75
Side-roll	65-85
hand-move	65-85
Solid-set	70-85
Surface	
Furrow (conventional)	45-65
Furrow (surge)	55-75
Furrow (with tailwater reuse)	60-80
Basin	60-75
Precision level basin	65-80
Drip	
Bubbler (low head)	80-90
Microspray	85-90
Micro-point source	85-90
Micro-line source	85-90
Surface drip	85-95
Subsurface drip	90-95

Note: Table is taken from Howell (2003)

b) Recommended irrigation set time or duration ($I_{D\,REC}$)

The recommended set time ($I_{D\,REC}$) is calculated based on the maximum gross depth of water to apply per irrigation ($D_{G\,MAX}$) and the basic soil infiltration rate (IR_B), according to Equation 4-14. In other terms, the recommended irrigation duration is the time required to infiltrate the maximum gross depth of applied water per irrigation, considering application rates by the irrigation system

that are lower than or equal to the basic soil infiltration rate, in order to avoid water logging and runoff.

$$I_{D\,REC} = \frac{D_{G\,MAX}}{IR_B} = \frac{60}{5.0} = 12 \text{ h} \quad (4\text{-}14)$$

$I_{D\,REC}$ indicates the limit set time that should be considered when irrigating, as it represents the irrigation duration compatible with the capacity of the soil to infiltrate and store water, and the maximum irrigation water that should be applied per irrigation to pursue resource-efficient water management.

It is important to ensure that the application rate (AR) of the irrigation system is less than the soil basic infiltration rate (IR_B). This guarantees that the entire amount of irrigation water applied by the irrigation system is infiltrated into the effective root zone, thus avoiding inefficiency. In this specific example, the application rate of the irrigation system (AR = 1.27 mm h^{-1}) is much lower than the soil basic infiltration rate (IR_B = 5.0 mm h^{-1}). This is a good configuration and indicates a careful design of the drip irrigation system. It also means that the actual duration of irrigation events can easily be extended longer than $I_{D\,REC}$. However, even when AR is much lower than IR_B, it is important not to exceed 16 hours of irrigation system operation per day in order to leave a few down-time hours for trouble-shooting and repairs.

c) Computation of weekly net (NIR) and gross irrigation requirements (GIR).

The NIR and GIR are calculated using the Equations 4-15 and 4-16:

$$NIR = ET_c - R_{eff} \quad (4\text{-}15)$$

$$GIR = \frac{NIR}{E_Q} \quad (4\text{-}16)$$

where ET_c is crop evapotranspiration and R_{eff} is effective rainfall.

Since there was no rain for the considered period, R_{eff} = 0. Hence, $NIR = ET_c$ and $GIR = NIR/E_Q = ET_c/E_Q$, where $ET_c = ET_o \, x \, K_c$. The bi-weekly values of K_c for mature micro-irrigated pistachio, which are reported in Table 4-17, were developed from a recent study on evapotranspiration of well-watered micro-irrigated pistachio conducted by researchers from the University of California between 2016 and 2019 (unpublished data).

Table 4-17. Bi-weekly values of K_c for mature micro-irrigated pistachio from the UC research study of 2016-2019 (unpublished data)

Period	K_c pistachio
1-15 Apr	0.37
16-30 Apr	0.59
1-15 May	0.79
16-31 May	0.82
1-15 Jun	0.89
15-30 Jun	0.89
1-15 Jul	0.90
15-31 Jul	0.84
1-15 Aug	0.86
15-31 Aug	0.86
1-15 Sep	0.82
15-30 Sep	0.78
1-15 Oct	0.62
16-31 Oct	0.59

Since the sample irrigation schedule refers to mid-August, a value of K_c = 0.86 was used along with FRET ET_o = 48 mm, which led to an estimated ET_c value of 41.3 mm. Given that in this case NIR is assumed equal to ET_c and $E_Q \sim DU_{LQ}$, considering DU_{LQ} = 0.92 from the irrigation system's performance evaluation, then GIR = 41.3 mm/0.92 = 44.9 mm, which can be rounded up to 45.0 mm. It is worth noting that in this specific case GIR is lower than D_G max (45.0 mm < 59.7 mm). Thus, the GIR amount could be applied in a single irrigation event or with multiple irrigations over the course of the seven days following the schedule development, according to the grower's preference.

d) Calculation of volume of water to apply per tree per week (V_w)

The weekly volume of water to apply per tree equals is calculated with Equation 4-17, i.e., it is obtained from the product of the weekly gross irrigation requirement (GIR) and the tree spacing product (T_S) in square meters. In this example, T_S = 6 m × 5 m = 30 m^2:

$$V_w = GIR \times T_S = 45.0 \times 30 = 1350 \text{ L tree}^{-1} \text{ week}^{-1} \quad (4\text{-}17)$$

e) Selection of the irrigation frequency (I_F) and calculation of the actual irrigation duration (I_D) or set time

Typically, the grower or farm manager decides on a suitable irrigation frequency (I_F) based on labor availability, shifts of the irrigators, and on availability of water supply. Field personnel are necessary to operate the irrigation system and oversee the correct execution of the irrigation schedule. Generally, farm personnel work six days a week, so the weekly irrigation schedule must be completed within six workdays. In this example, it is considered that the water amount corresponding to the weekly gross irrigation requirement (GIR) of pistachio (45.0 mm) can be applied in three irrigations (one irrigation every two days) or in two irrigations (one irrigation every three days). In both cases, the weekly GIR can be applied within the six workdays of the week.

Three irrigations per week

The total weekly GIR = 45.0 mm is divided in three equal irrigation events, during which a gross irrigation depth of $D_{G\ (2\text{-}day)}$ = 15 mm is applied. This corresponds to a volume per tree of: $I_{V\ (2\text{-}day)}$ = 15 mm x 6 m x 5 m = 450 L tree^{-1}. The duration (I_D) of each irrigation event (one every two days) is calculated considering the total amount of water to apply per irrigation (15 mm) and the application rate (AR) of the dual-dripline irrigation system (1.27 mm h^{-1}) as: $I_{D\ (2\text{-}day)}$ = 15 mm /1.27 mm h^{-1}= 12 h. In summary, one irrigation of 12 hours is necessary every two days to apply the weekly GIR of 45.0 mm, which is necessary to meet the trees' evapotranspiration needs.

Two irrigations per week

In this case, the total weekly GIR = 45.0 mm is divided in two equal irrigation events, during which a gross irrigation depth of $D_{G\ (3\text{-}day)}$ = 22.5 mm is applied. This corresponds to a volume per tree of: $I_{V\ (3\text{-}day)}$ = 22.5 mm x 6 m x 5 m = 675 L tree^{-1}. The duration (I_D) of each irrigation event (one every three days) is calculated considering the total amount of water to apply per irrigation (22.5 mm) and the application rate (AR) by the dual-dripline irrigation system (1.27 mm h^{-1}) as: $I_{D\ (3\text{-}day)}$ = 22.5 / 1.27 mm h^{-1} = 17.7 h, which can be rounded down to 17.5 h. In summary, one irrigation of 17.5 hours is necessary every three days to apply the weekly GIR of 45.0 mm to meet the trees' evapotranspiration needs.

The calculations above indicate that the irrigation frequency of three days (one irrigation every three days) requires 17.5 hours of irrigation system operation per each irrigation event, which slightly exceeds the 16-hour maximum irrigation operation per day recommendation. Adjustments to I_F and operating hours (I_D) are possible based on information from soil moisture monitoring and tree water status. For instance, if the soil moisture sensors show that soil has some residual moisture from the last irrigation, then the farm manager may decide to postpone the first irrigation of next week by a day or two. Alternatively, the farm manager can split the total gross irrigation requirement (GIR) of 45.0 mm into two non-equal irrigation events and apply a smaller amount of water with the first irrigation, and a larger amount of water with the second irrigation, or vice versa, thus tailoring irrigation amounts to the actual soil water and/or tree water status.

4.4.1.2.Sample irrigation schedule for a hand-move sprinkler-irrigated onion field

This example illustrates an irrigation schedule prepared for an onion field located in Five Points, California (southwestern portion of the San Joaquin Valley) using input information from Table 4-11, for a week of early August 2019. In this field, onions are grown on a silt loam soil (W_A = 170 mm m^{-1}; IR_B = 9.5 mm h^{-1}) with a hand-move solid-set sprinkler system. The hand-move system consists of sprinklers set at the regular spacing of 9 m by 12 m that wet 100% of the cropped area, with an average application rate AR = 3.2 mm h^{-1} and DU_{LQ} = 0.80, which are both determined from the irrigation system's performance evaluation.

The sample schedule considers a weekly FRET ET_o forecast of 57.1 mm, and a K_c value of 1.20 for early August from a UC study (unpublished data), which results in NIR = 68.5 mm for the next 7 days.

a) Max gross depth of water per irrigation ($D_{G\,MAX}$):

$$D_{G\,MAX} = \frac{MAD \times W_A \times P_W \times Z_E}{E_Q} = \frac{0.30 \times 170 \times 1.0 \times 0.45}{0.80} = 28.7 \text{ mm} \qquad (4\text{-}18)$$

Any irrigation water application above 28.7 mm may result in deep percolation and water loss, making irrigation less efficient. Generally, during an irrigation season, it is highly recommended to apply irrigation water in amounts less than or equal to $D_{G\,MAX}$.

b) Recommended irrigation set time or duration ($I_{D\,REC}$)

Given that $D_{G\ MAX}$ = 28.7 mm and the silt loam soil has a basic soil infiltration rate IR_B = 9.5 mm h^{-1}, the recommended irrigation duration ($I_{D\ REC}$) is calculated according to Equation 4-19 below:

$$I_{D\ REC} = \frac{D_{G\ MAX}}{IR_B} = \frac{28.7}{9.5} = 3.0 \text{ h} \quad (4\text{-}19)$$

An irrigation set time of 3 hours is compatible with the capacity of the silt loam soil to infiltrate and store water, with a basic soil infiltration rate of 9.5 mm h^{-1}, and the application of maximum gross water depth of 28.7 mm in order to achieve efficient water management.

In this specific case, the sprinkler system has an application rate AR = 3.2 mm h^{-1}, which is considerably lower than the soil basic infiltration rate IR_B = 9.5 mm h^{-1}. This ensures that the total water applied by the irrigation system is infiltrated into the root zone, which minimizing inefficiencies and water loss.

c) Computation of weekly gross irrigation requirements (GIR)

Assuming that no rain is expected within the next 7 days, Reff = 0 and Equation 4-20 is used for calculating the weekly gross irrigation requirement:

$$GIR = \frac{NIR}{E_Q} = \frac{68.5}{0.80} = 85.6 \text{ mm} \quad (4\text{-}20)$$

where $NIR = ET_c - R_{eff}$

Since no rain is expected, $NIR = ET_c$ and $GIR = NIR/ E_Q = ET_c/E_Q$. Because $NIR = ET_c$ and $E_Q \sim DU_{LQ}$, if DU_{LQ} = 0.80 from the irrigation system performance evaluation, then GIR = 68.5 mm/0.80 = 85.6 mm.

It is worth noting that, in this specific case, the weekly GIR is larger than $D_{G\ MAX}$ (85.6 mm > 28.7 mm). Consequently, a single GIR application is not recommended. Instead, multiple irrigations over the course of the next seven days are needed to avoid wasteful water application.

d) Selection of the irrigation frequency (I_F) and calculation of the actual Irrigation Duration (I_D) or set time

In this example, the water amount corresponding to the weekly GIR of sprinkler-irrigated onion (85.6 mm) is applied in three equal irrigation events (one irrigation every two days) over the six workdays of the week. At each event, a gross irrigation depth of $D_{G\ (2\text{-}day)}$ = 28.5 mm is applied,

which is compatible (slightly lower) with the calculated maximum gross irrigation depth ($D_{G\ MAX}$ = 28.7 mm).

The duration (I_D) of each irrigation event is calculated considering the total amount of water to apply per irrigation (28.5 mm) and the application rate (AR) of the hand-move sprinkler irrigation system (3.2 mm h^{-1}) as: $I_{D\ (2\text{-}day)}$ = 28.5 mm /3.2 mm h^{-1} = 8.9 h ≈ 9 h. In summary, one irrigation of 9 hours is necessary every two days to apply the weekly GIR of 85.6 mm that meets the onion field evapotranspiration needs.

In this case, the grower can tailor the timing and frequency of irrigations on the basis of soil moisture monitoring instead of irrigating at regular 2-day intervals of equal application depths. Alternatively, the grower can opt to irrigate six times per week with a D_G = 14.3 mm and I_D = 4.5 h for each irrigation. Choosing daily irrigation over the course of a 6-day working week would probably lead to higher soil evaporation as a consequence of the frequent, light irrigation, which would decrease the irrigation efficiency and water productivity.

4.4.2. Using FRET ET_o to schedule urban landscape irrigation

The last column of Table 4-11 shows information for sprinkler irrigation scheduling for turfgrass in urban environment (gardens, sport facilities). Many management aspects are similar for agricultural and urban irrigation scheduling. However, differences in plant materials, micro-climates and irrigation systems make urban management somewhat more complicated (Glenn et al. 2015; Kjelgren et al. 2016).

Turfgrass is one of the more common urban landscape plants, and considerable water resources are used to maintain turfgrass for its pleasant appearance and utility as a surface for athletic activities and recreation (Monteiro 2017). Proper irrigation management of turfgrass can contribute significantly to reducing unrecoverable water and energy losses (Leinauer et al. 2010). One of the biggest problems in urban irrigation is to have a good estimate of ET_o, which represents the atmospheric water demand for the prevailing climate conditions and affects the actual water consumption for the evapotranspiration process. Urban areas generally have considerably more micro-climates than agricultural areas, and it is often difficult to find a site that provides the conditions needed to determine a representative ET_o, and it is even more difficult to represent microclimates within the urban areas (Litvak and Pataki 2016). One advantage from using FRET

is that a reasonably accurate estimate of ET_o is possible in an urban setting where it is difficult to find a good weather station location to quantify ET_o. In fact, as indicated in previous sections, FRET ET_o is estimated from weather forecasts rather than from typical weather stations. Hence, ET_o forecasts come from an already established service, which lowers considerably the costs related to installation and maintenance of weather stations.

Commercial irrigation sprinklers for turfgrass are designed to apply water with high volume and high frequency, which allows for irrigation that is typically applied every one to four days with high application rates so that the entire landscape is irrigated in a relatively short period of time (Leinauer and Smeal 2012). Commonly, turfgrass is irrigated at night or in the morning around sunrise when wind speeds tend to be low and human landscape use is minimal. Information needed to schedule turfgrass irrigation is similar to that necessary for agricultural irrigation, and includes: 1) representative ET_o data; 2) accurate crop coefficient (K_c) values, which differ mainly for the grass types; 3) the available soil water holding capacity (W_A); 4) the effective root depth (Z_E); 5) the maximum allowable depletion (MAD); 6) the basic soil infiltration rate (IR_B); 7) the distribution uniformity of the low quarter (DU_{LQ}) of the sprinkler system; and 8) the irrigation application rate (AR).

When using ET_o data from a near-real-time network for frequent turfgrass scheduling, it is necessary to input the sprinkler zone set times into a controller after midnight when the daily ET_o rate from the previous day becomes available. This is inconvenient for a turfgrass superintendent who really needs a forecast ET_o for the current day to accurately set the controller and replace the current day water loss on the following morning. Also, turfgrass superintendents typically do not reset their controllers daily, but rather set them for several days in advance by anticipating daily water losses based on observed ET_o rates from previous days or from climate data. Daily ET_o rates can change dramatically from week-to-week in some areas, so using forecast ET_o should improve irrigation management in climates with variable ET_o rates. Clearly, knowing the forecast daily ET_o rates for a few days in advance will allow superintendents to set their controller(s) for irrigating sprinkler zones more efficiently with adequate water to maintain good quality turfgrass and a high application efficiency. If the ET_o forecast is accurate, it should lead to better irrigation management.

Table 4-18 provides an example for how to schedule daily irrigation using FRET ET_o where the turfgrass is wetted twice each day (two cycles) to give the most efficient irrigation. Table 4-19 shows the fixed cycle set times required for two irrigation cycles per day on 1, 2, 3, 4, 5, and 6 days per week so that the total applied water is the same as for the daily irrigation shown in Table 4-18. Table 4-18 shows a sample irrigation schedule for cool season turfgrass with $K_c = 0.80$ and seven days of FRET ET_o. The days 0-6 correspond to forecast days 1-7 from FRET since the ET_o for the current day is the first forecast day and 6 days later is the seventh forecast day. Typical mid-summer values for ET_o (mm d^{-1}) from an arid climate are input into the second column. The K_c is listed in the third column with the calculated daily crop $ET_c = ET_o \times K_c$ (mm d^{-1}) in the fourth column. This example assumes a distribution uniformity value for sprinkler system of $DU_{LQ} = 0.75$ and the daily gross water depth to apply (D_G) is calculated as $D_G = ET_c/DU_{LQ}$ (assuming no rain occurs) and expressed in mm d^{-1}. Dividing ET_c by the DU_{LQ} leads to a mean depth of water equal to ET_c being applied to the low quarter of the irrigated field so that the low quarter can receive sufficient water to refill the soil water depletion back to field capacity at each irrigation. Most of the field will receive more water than needed to refill the soil. This example assumes an application rate of AR = 11 mm h^{-1}, and the daily set times (hours) are computed as $I_D = D_G/AR$.

Turfgrass irrigation systems are often operated to cycle through all of the sprinkler zones multiple times. This practice allows for applied water to soak into the soil in-between wetting of each zone. This is done to reduce surface runoff onto hardscapes and to maintain the application efficiency (and DU_{LQ}) as high as possible. In this example, two cycles were applied on each day in Table 4-18 and Table 4-19, and it is assumed that total time for all cycles within a day is equal to the total set time for the day. Therefore, a day that requires 42 min runtime to refill the low quarter would need two 21-minute cycles. Clearly, increasing the number of cycles decreases the cycle set times. Therefore, the number of required cycles is determined by increasing the number of cycles, which decreases the cycle set time, until a cycle set time is reached where there is minimal runoff. Depending on the available irrigation controller, it is possible to vary the water application in response to differences in daily ET_c as shown in this example. For optimal scheduling, the procedure is used to develop a forecast daily schedule from the 7-day FRET ET_o forecast. Because FRET ET_o typically improves for shorter forecast periods, it is advisable to input updated FRET forecast data as the week progresses to improve accuracy.

Table 4-18. An example of a cool season turfgrass daily irrigation schedule with 2 cycles per day using FRET ET_o.

Day	Forecast ET_o (mm)	Projected K_c	Forecast ET_c (mm)	Cumulated ET_c (mm)	DU_{LQ}	Daily D_G (mm)	Cumulated D_G (mm)	AR (mm h^{-1})	Daily set time, I_D (h)	Daily set time, I_D (min)	Cycle per day	Set time per cycle (h)	Set time per cycle (min)	Cumulated set time (h)
0	6.3	0.80	5.0	5.0	0.75	6.7	6.7	11.0	0.61	37	2	0.31	18	0.61
1	7.3	0.80	5.8	10.9	0.75	7.8	14.5	11.0	0.71	42	2	0.35	21	1.32
2	6.6	0.80	5.3	16.2	0.75	7.0	21.5	11.0	0.64	38	2	0.32	19	1.96
3	5.2	0.80	4.2	20.3	0.75	5.5	27.1	11.0	0.50	30	2	0.25	15	2.46
4	5.9	0.80	4.7	25.0	0.75	6.3	33.4	11.0	0.57	34	2	0.29	17	3.04
5	7.0	0.80	5.6	30.6	0.75	7.5	40.9	11.0	0.68	41	2	0.34	20	3.71
6	7.3	0.80	5.8	36.5	0.75	7.8	48.6	11.0	0.71	42	2	0.35	21	4.42

Table 4-19. An example of a cool season turfgrass irrigation schedule for a fixed number of days per week with 2 cycles per day on 1 through 6 days per week using FRET ET_o so that the total AW is the same as for the Table 4-18 daily schedule.

Days per week	ET_o per irrigation (mm)	Projected K_c	ET_c per irrigation (mm)	DU_{LQ}	D_G per irrigation (mm)	AR (mm h^{-1})	Daily set time, I_D (h)	Daily set time, I_D (min)	Cycles per day	Set time per cycle (h)	Set time per cycle (min)	Weekly set time (h)
6	7.6	0.80	6.1	0.75	8.1	11.0	0.74	44	2	0.37	22	4.42
5	9.1	0.80	7.3	0.75	9.7	11.0	0.88	53	2	0.44	27	4.42
4	11.4	0.80	9.1	0.75	12.2	11.0	1.11	66	2	0.55	33	4.42
3	15.2	0.80	12.2	0.75	16.2	11.0	1.47	88	2	0.74	44	4.42
2	22.8	0.80	18.2	0.75	24.3	11.0	2.21	133	2	1.11	66	4.42
1	45.6	0.80	36.5	0.75	48.6	11.0	4.42	265	2	2.21	133	4.42

It is a common practice for turfgrass superintendents to delay irrigation and then apply more water to force plant roots deeper in the soil to reduce the chance of water stress adversely impacting the grass appearance. While Table 4-18 shows the development of a daily irrigation schedule with two cycles on each day, Table 4-19 shows how to determine a schedule based on FRET ET_o by using the same weekly total D_G as in the daily schedule but applying irrigation on fewer days. Table 4-19 shows the calculation of a fixed set time for the input number of cycles and number of days per week (left-hand column) so that it has the same weekly D_G on fewer days. When using Table 4-19, it is important to check the set time per cycle (min.) for each of the number of days per week to determine if the set time is likely to result in wasteful runoff or not. For example, the set time per cycle of Table 4-19 shows 22 minutes for six days of irrigation and two cycles per day. If 22 minutes is unlikely to result in runoff, it is common to use six days and two cycles per day. For five days per week, the cycle runtime is 27 minutes, which might result in runoff, which will make it unacceptable. Likewise, few days with two cycles per day would all likely have runoff. Increasing from two to three cycles per day would decrease the set time per cycle to 22 minutes or less for four, five, and six irrigation days, so using three cycles per day would be adequate to minimize runoff of four-six irrigation days. If the schedule was changed to four cycles per day, then using three irrigation days per week or more would be adequate to minimize runoff. Having fewer than three irrigation days per week would require more than four cycles per day, so irrigation on one or two days per week is likely to be inefficient.

4.5.Conclusion

The main objective of this work was to evaluate the accuracy of using daily weather forecast data provided by the NWS to estimate reference evapotranspiration (ET_o) in California for irrigation scheduling purposes. FRET ET_o data were compared against data from 15 CIMIS stations sited in locations characterized by different microclimatic conditions. The selection of the 15 CIMIS stations was based on California ET_o zone map and Köppen classification.

The first step was the evaluation of the quality of the meteorological data forecasted from NWS and used for the calculation of ET_o as compared with the data measured by the CIMIS agrometeorological stations. Overall, the results were good for maximum and minimum air temperature, dew point temperature and wind speed, while less accurate results were obtained for solar radiation.

The second step was evaluating the quality of the FRET ET_o forecasts with 1, 3, 5, and 7-day lead-times. The comparison with CIMIS ET_o showed that the Penman-Monteith equation is rather robust as it decreased the errors resulting from inaccurate solar radiation estimation and the effect of wind speed variability. These results demonstrate that FRET provides a good alternative to using near-real-time weather station networks. The statistical indices utilized revealed that the model performed well, as the errors are of the same magnitude of ET_o estimation error in most of the stations and microclimates considered for this study. Errors are larger mainly when the measurement station is located in mountain areas, where the prediction of solar radiation is more complicated than other parameters.

Finally, some sample irrigation schedules developed using FRET ET_o were provided to illustrate the use of forecast ET_o alongside with soil hydraulic properties and irrigation system's performance parameters to optimize water applications for specialty crops and urban landscape. Using FRET can improve water scheduling at the field level and water management at the irrigation district level by producing site-specific irrigation schedules and allowing to predict the irrigation water demand for the next 7 days ahead. This will help to prevent crop water stress and over irrigation caused by the use of weather data from the current CIMIS weather stations, as well as the possible mismatch between water demand and deliveries. In addition, it is easy for farmers, irrigation practitioners, water resource planners and managers, to obtain and use FRET ET_o data. Since the NWS provides FRET data free to the public, the cost is greatly reduced relative to developing and maintaining a network of weather stations to provide near-real time ET_o data. The service provided by NWS via FRET is reliable and it is easy to extend the use of FRET ET_o to other agricultural production regions and urban regions characterized by similar climatic conditions as those considered in this research. Further work is needed to evaluate the accuracy of FRET in climatic conditions not similar to California.

Sample irrigation schedules using FRET ET_o are presented for a pistachio orchard with dual-line drip irrigation, onions with hand move sprinklers, and turfgrass with frequent high application rate popup sprinklers. The procedures to determine the weekly ET_c from FRET ET_o were presented for the crops and turfgrass, and the steps needed to compute the number of sets and set runtimes based on distribution uniformity and soil properties were discussed. Using FRET improves the ability to adjust irrigation for variations in ET_o and for actual soil and plant water status, and the sample schedules present the methodology to make these improvements.

Appendix A

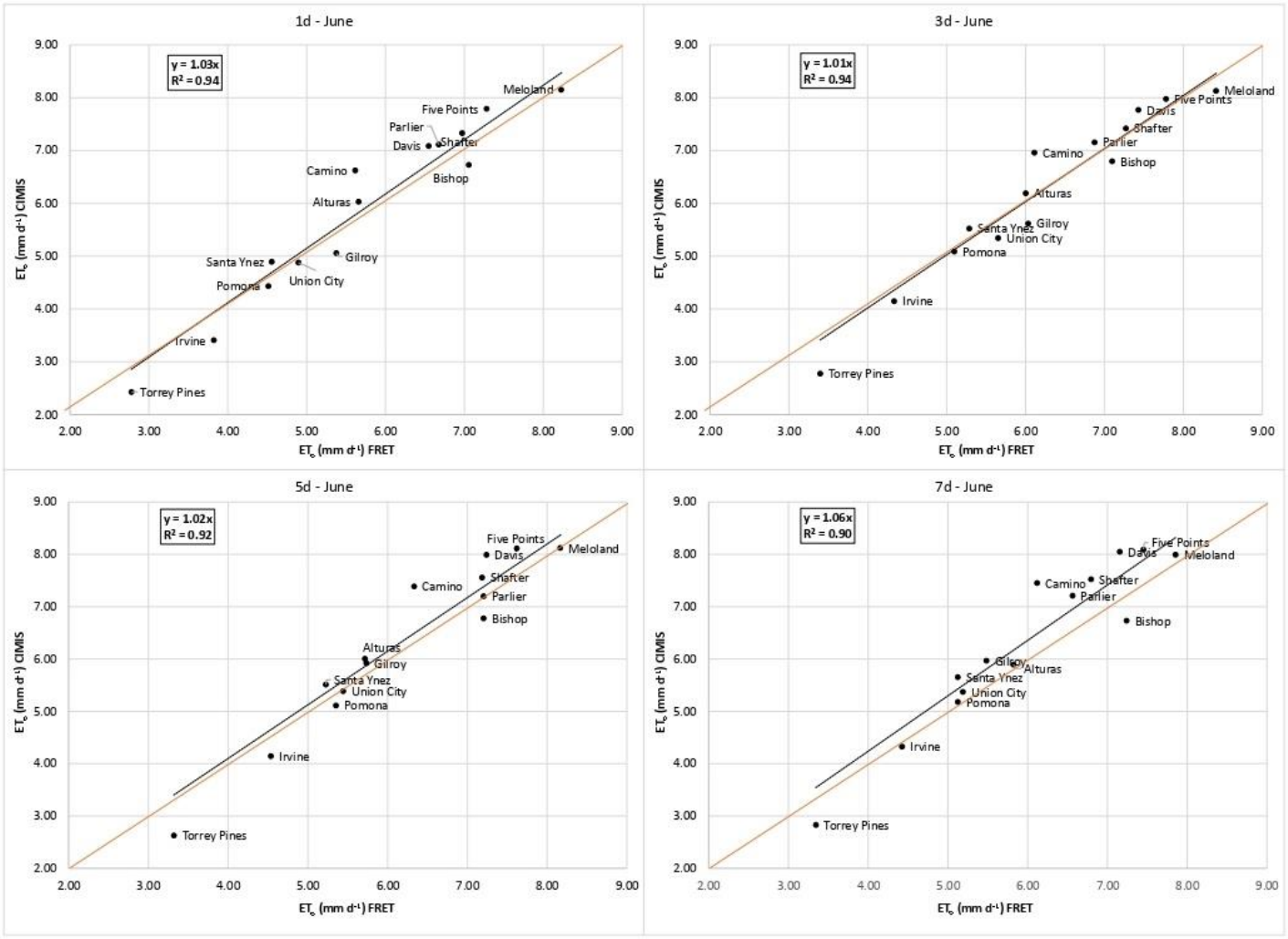

Fig. A1. Comparison between the FRET ET_o and the CIMIS ET_o, for all the 15 selected CIMIS stations in June 2019. The four graphs refer to different lead-times, i.e., 1, 3, 5 and 7- day, respectively.

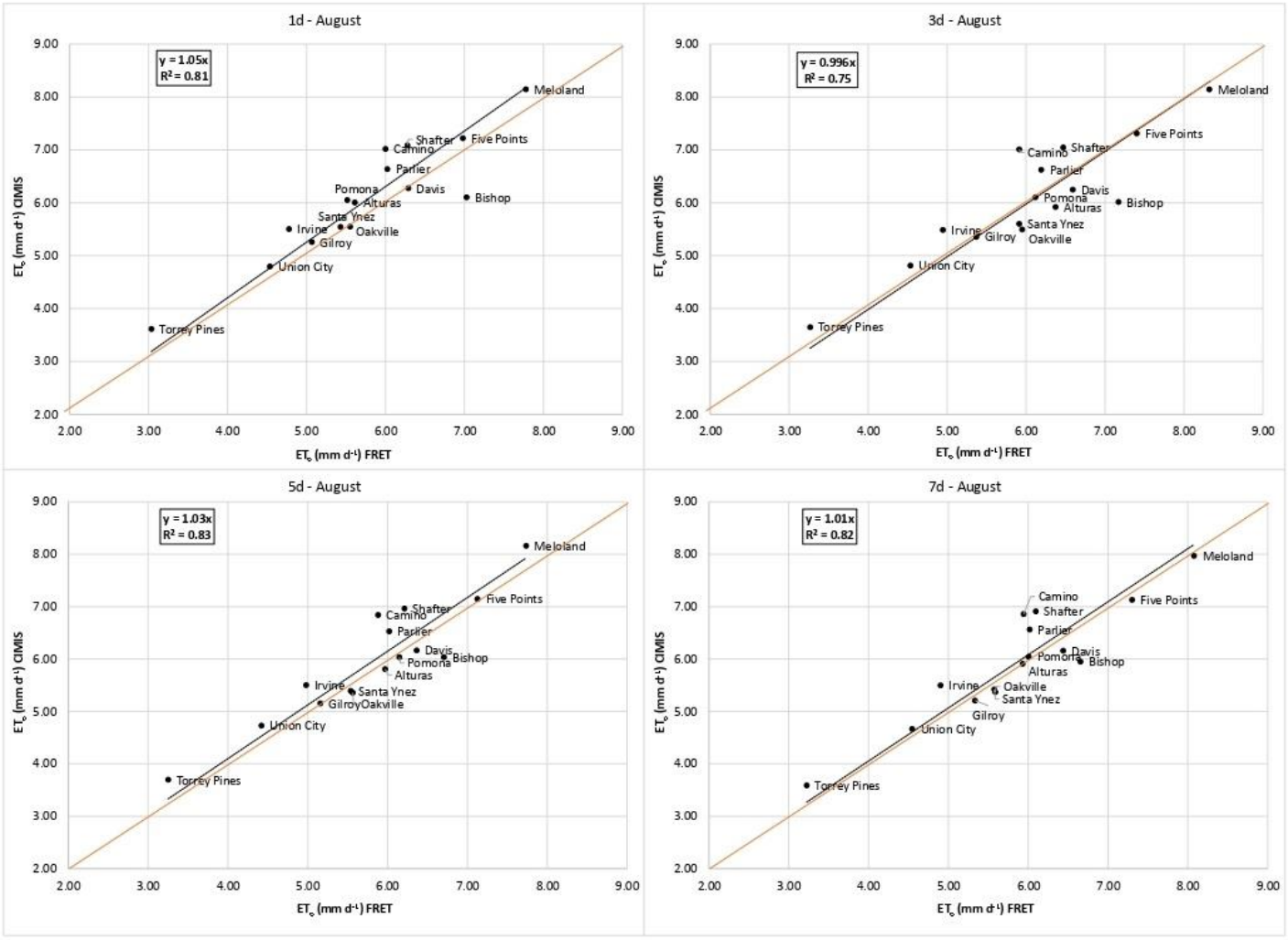

Fig. A2. Comparison between the FRET ET_o and the CIMIS ET_o, for all the 15 selected CIMIS stations in August 2019. The four graphs refer to different lead-times, i.e., 1, 3, 5 and 7- day, respectively.

5. General Conclusion

Evapotranspiration (ET) is a key process in the hydrological cycle, yet its determination is prone to many uncertainties due mainly to the physiology and structure of plants, weather conditions and data quality and availability. These uncertainties affect the accuracy and reliability of crop water demand estimations, necessary for irrigation scheduling and hydrological modeling purposes. A key objective of the thesis has been to provide insights into some challenges of evapotranspiration estimation, mainly the performance of ET_o forecasts and the importance of modeling the effect of changes in CO_2 levels on reference evapotranspiration. These challenges have been identified through literature review in Chapter 1 and in more detail in the introduction section of the respective chapters.

Chapter 2 showed the knowledge gaps in the ET modelling when it comes to accounting and the effect of the continuous increase in CO_2 levels due to climate change. The review explored different attempts to module this particular phenomenon and discussed their different advantages and disadvantages.

Subsequently, Chapter 3 describes a case study that was conducted in different locations in Emilia-Romagna in northern Italy, using a modification of the canopy resistance component of the FAO-PM equation. Results demonstrated that the fertilization effect of CO_2 was able to attenuate to a certain extent the effect of increasing air temperature on ET_o in the studied locations. The case study also showed that the recurrent data availability issue related to the FAO-PM equation could be solved using climate reanalysis as an alternative data source. As a future step, this work could be replicated in other regions of Italy or the world and extended to the "end of the century" scenario, when important increases in temperature are projected to occur over Emilia-Romagna and globally. The use of reanalysis data could also allow mapping evapotranspiration in the region, which is useful for agricultural, ecological and water resources management studies.

Finally, Chapter 4 assessed weather forecasts from the California National Weather Services (NWS), specifically ET_o (FRET) and weather variables used for its calculation. Overall, the comparison with measurements from weather stations of the California Irrigation Management Information System (CIMIS) gave good results with different performances, according to the location and microclimate of the considered weather station. Results were good particularly for the comparison of ET_o demonstrating that FRET provides a viable alternative to using near-real-time

weather station networks. The findings of Chapter 4 are important to farmers and water managers as they present an easier and more economical solution for irrigation management that could be applied in different microclimates, similar to those shown in this study. Since the evaluation was done only during summer, a possible next step would be testing the NWS forecasts during other seasons. The study could also be replicated in other US states or in different countries with similar or even different microclimate types as those present in California. Since one of the objectives of this work was to introduce FRET to a wider public, a natural next phase would be to apply FRET in Emilia-Romagna and Italy.

The findings of this thesis are important in better understanding the soil-plant-water-atmosphere relationships necessary for reliable ET estimation in hydrological and water resources studies. The observations and conclusions obtained from the research delineate some of the underlying issues in the estimation of evapotranspiration. Resolving these issues needs further improvement and implementation of strategies for the collection of critical information on ET and increasing monitoring capabilities, from local to global scale. Despite some unavoidable uncertainties, the approaches used in this work are a potential contribution to decision support tools for decision makers in the agricultural water management and policy fields, particularly in the Emilia-Romagna and similar other regions where the scarcity of data is forcing researchers to use empirical equations rather than the FAO-PM to estimate ET_o (Villani et al. 2011; Nistor and Porumb 2015; Nistor et al. 2016; Cervi and Nistor 2018; Nistor and Mîndrescu 2019). Indeed, the approaches employed can be a valuable, affordable and reliable source of data for irrigation planning and climate change impact assessment, since they provide meteorological variables at a high resolution of around 10 km and less, which is the resolution required to use hydrological models without resorting to downscaling (Boé 2007), thus excluding an additional source of uncertainties. Moreover, high spatial and temporal resolution ET_o data in irrigated fields, when associated with land-use maps can be useful for determining irrigation needs for large areas and evaluating the efficiency of water allocation plans. In addition, ET_o projections can help assessing regional climate change scenarios particularly relative to droughts and floods.

Finally, it is important to state that this work does not advocate for the replacement of observed data from weather stations by products such as reanalysis and NWP models. Weather stations will continue to provide the best estimate of surface weather data at the local and regional scales and

there are many fundamental reasons to keep on supporting a strong network of quality weather stations. The results provided in this study using ERA5-Land and FRET show that models have likely reached the point where they can reliably complement observations from weather stations and provide reliable proxies, at least in California and Emilia-Romagna regions.

References

Abrishambaf O, Faria P, Gomes L, Vale Z (2020) Agricultural irrigation scheduling for a crop management system considering water and energy use optimization. Energy Reports. 6:133–139. https://doi.org/10.1016/j.egyr.2019.08.031

Adeboye OB, Osunbitan JA, Adekalu KO, Okunade DA (2009) Evaluation of FAO-56 Penman-Monteith and Temperature Based Models in Estimating Reference Evapotranspiration Using Complete and Limited Data, Application to Nigeria. Agricultural Engineering International: CIGR Journal. 0(0):1–25. Retrieved from: https://cigrjournal.org/index.php/Ejounral/article/viewFile/1291/1243

Adeniran KA. Amodu MF, Amodu MO, Adeniji FA (2010) Water Requirements of Some Selected Crops in Kampe Dam Irrigation Project (Engineering Collection) - Informit. Australian Journal of Agricultural Engineering. 1(4):119–125. Retrieved from https://search.informit.com.au/documentSummary;dn=554779067855667;res=IELENG

Ainsworth EA, Long SP (2004) What have we learned from 15 years of free-air CO_2 enrichment (FACE)? A meta-analytic review of the responses of photosynthesis, canopy properties and plant production to rising CO_2. New Phytologist. 165(2):351–372. https://doi.org/10.1111/j.1469-8137.2004.01224.x

Akbarpour S, Niksokhan MH (2018) Investigating effects of climate change, urbanization, and sea level changes on groundwater resources in a coastal aquifer: an integrated assessment. Environmental Monitoring and Assessment. 190(10):1–16. https://doi.org/10.1007/s10661-018-6953-3

Alcamo J, Flörke M, Märker M (2007) Future long-term changes in global water resources driven by socio-economic and climatic changes. Hydrological Sciences Journal. 52(2):247–275. https://doi.org/10.1623/hysj.52.2.247

Alcamo J, van Vuuren D, Cramer W, Alder J, Bennett E, Carpenter S, Christensen V, Foley J, Maerker M, Masui T, Morita T, O'Neill B, Peterson G, Ringler C, Rosegrant M, Schulze K, Bouwman L, Eickhout B, Floerke M, Lal R, Takahashi, K. (2005). Changes in Ecosystem Services and Their Drivers across the Scenarios. In Sinh BT, Hammond A, Field C (Eds.).

Scenarios of the millennium ecosystem assessment. 297–373. Retrieved from https://www.millenniumassessment.org/documents/document.333.aspx.pdf

Alexandratos N, Bruinsma J (2012) World Agriculture towards 2030/2050: the 2012 revision. ESA Working paper No. 12-03. Rome, FAO. Retrieved from http://www.fao.org/3/a-ap106e.pdf

Allen LH (1990) Plant responses to rising carbon dioxide and potential interactions with air pollutants. Journal of Environmental Quality. 19(1):15–34. https://doi.org/10.2134/jeq1990.00472425001900010002x

Allen LH (2000) Evapotranspiration Responses of Plants and Crops to Carbon Dioxide and Temperature. Journal of Crop Production. 2(2):37–70. https://doi.org/10.1300/J144v02n02_02

Allen LH, Pan D, Boote KJ, Pickering NB, Jones JW (2003) Carbon dioxide and temperature effects on evapotranspiration and water use efficiency of soybean. Agronomy Journal. 95(4):1071–1081. https://doi.org/10.2134/agronj2003.1071

Allen MR, Dube OP, Solecki W, Aragón-Durand F, Cramer W, Humphreys S, Kainuma M, Kala J, Mahowald N, Mulugetta Y, Perez R, Wairiu M, Zickfeld, K (2018) Framing and Context. In Masson-Delmotte V, Zhai P, Pörtner H-O, Roberts D, Skea J, Shukla PR, Pirani A, Moufouma-Okia W, Péan C, Pidcock R, Connors S, Matthews JBR, Chen Y, Zhou X, Gomis MI, Lonnoy E, Maycock T, Tignor M. Waterfield T (Eds.). Global Warming of 1.5°C. Retrieved from https://www.ipcc.ch/site/assets/uploads/sites/2/2019/05/SR15_Chapter1_Low_Res.pdf

Allen RG, Jensen ME, Wright JL, Burman RD (1989) Operational Estimates of Reference Evapotranspiration. Agronomy Journal. 81:650–662. https://doi.org/10.2134/agronj1989.00021962008100040019x

Allen RG, Pereira LS, Raes D, Smith M (1998) Crop evapotranspiration-Guidelines for computing crop water requirements-FAO Irrigation and drainage paper 56. Rome, Italy. Retrieved from: http://www.fao.org/3/X0490E/X0490E00.htm

Allen RG, Pruitt WO, Wright JL, Howell TA, Ventura F, Snyder R, Itenfisu D, Steduto P,

Berengena J, Yrisarry JB, Smith M, Pereira LS, Raes D, Perrier A, Alves I, Walter I, Elliott, R (2006) A recommendation on standardized surface resistance for hourly calculation of reference ET_o by the FAO56 Penman-Monteith method. Agricultural Water Management. 81(1–2):1–22. https://doi.org/10.1016/J.AGWAT.2005.03.007

Allen RG, Smith M, Pereira LS, Perrier A (1994) An update for the calculation of reference evapotranspiration. ICID Bulletin. 43(2):35–92. Retrieved from https://www.researchgate.net/publication/322699162_An_update_for_the_calculation_of_reference_evapotranspiration

Allen RG, Smith M, Perrier A, Pereira LS (1994) An Update for the Definition of Reference Evapotranspiration. ICID Bulletin, 43(2). 1–34. Retrieved from https://www.researchgate.net/publication/237049120_An_Update_for_the_Definition_of_Reference_Evapotranspiration

Alves I, Perrier A, Pereira LS (1998) Aerodynamic and surface resistances of complete over crops: how good in the '"big leaf"' approach? Transactions of the ASAE. 41(2):345–351. https://doi.org/10.13031/2013.17184

Alves I, Pereira LS (2000) Modelling surface resistance from climatic variables? Agricultural Water Management. 42(3):371–385. https://doi.org/10.1016/S0378-3774(99)00041-4

AQUASTAT (n.d.) FAO's Information System on Water and Agriculture. Retrieved February 2, 2019, from http://www.fao.org/nr/water/aquastat/main/index.stm

Arnfield AJ (2020) Koppen climate classification. In Encyclopædia Britannica. Retrieved from https://www.britannica.com/science/Koppen-climate-classification

Backlund P, Janetos A, Schimel D (2008) The Effects of Climate Change on Agriculture, Land Resources, Water Resources, and Biodiversity in the United States: Synthesis and Assessment Product 4.3. Report by the U.S. Climate Change Science Program and the Subcommittee on Global Change Research. Retrieved from https://www.fs.fed.us/rm/pubs_other/rmrs_2008_backlund_p003.pdf

Ball JT, Woodrow IE, Berry JA (1987) A Model Predicting Stomatal Conductance and its Contribution to the Control of Photosynthesis under Different Environmental Conditions. In

Progress in Photosynthesis Research. 221–224. https://doi.org/10.1007/978-94-017-0519-6_48

Ballesteros R, Ortega JF, Moreno MA (2016) FORETo: New software for reference evapotranspiration forecasting. J. Arid Environ. 124:128–141. https://doi.org/10.1016/j.jaridenv.2015.08.006

Balsamo G, Albergel C, Beljaars A, Boussetta S, Brun E, Cloke H, Dee D, Dutra E, Muñoz-Sabater J, Pappenberger P, de Rosnay P, Stockdale T, Vitart F (2015) ERA-Interim/Land: a global land surface reanalysis data set. Hydrology and Earth System Sciences. 19(1):389–407. https://doi.org/10.5194/hess-19-389-2015

Bargaoui ZK (2012) Estimation of Evapotranspiration Using Soil Water Balance Modelling. In Irmak A (Ed.), Evapotranspiration - Remote Sensing and Modeling. 147–178. https://doi.org/10.5772/18124

Bauer P, Thorpe A, Brunet G (2015) The quiet revolution of numerical weather prediction. Nature. 525(7567):47–55. https://doi.org/10.1038/nature14956

Ben Hamouda G, Pavan V, Antolini G, Botarelli L, Ventura F (2019) Comparison and Validation of Daily Meteorological Data From Era5 Reanalysis With Observational Surface Data, for the Emilia-Romagna Region. AXXII Convegno Nazionale Di Agrometeorologia - Ricerca Ed Innovazione per La Gestione Del Rischio Meteo - Climatico in Agricoltura. 101–105. Retrieved from http://amsacta.unibo.it/6175/1/Atti_XXII_AIAM_2019.pdf

Ben Hamouda G, Ventura F. (2020) Evaluation of some evapotranspiration estimation models under CO_2 increasing concentrations: A review. Italian Journal of Agrometeorology. 2020(1):85–98. https://doi.org/10.13128/ijam-831

Benestad RE (2010) Downscaling precipitation extremes. Theoretical and Applied Climatology. 100(1):1–21. https://doi.org/10.1007/s00704-009-0158-1

Berengena J, Gavilán P (2005) Reference Evapotranspiration Estimation in a Highly Advective Semiarid Environment. Journal of Irrigation and Drainage Engineering. 131(2):147–163. https://doi.org/10.1061/(asce)0733-9437(2005)131:2(147)

Bernacchi CJ, Kimball BA, Quarles DR, Long SP, Ort DR (2007) Decreases in stomatal

conductance of soybean under open-air elevation of [CO_2] are closely coupled with decreases in ecosystem evapotranspiration. Plant Physiology. 143(1):134–144. https://doi.org/10.1104/pp.106.089557

Betts RA, Boucher O, Collins M, Cox PM, Falloon PD, Gedney N, Hemming DL, Huntingford C, Jones CD, Sexton DMH, Webb MJ (2007) Projected increase in continental runoff due to plant responses to increasing carbon dioxide. Nature. 448(7157):1037–1041. https://doi.org/10.1038/nature06045

Beutler AM, Keller AA (2005) Implementation of FAO-56 Penman-Monteith Evapotranspiration in a Large Scale Irrigation Scheduling Program. Impacts of Global Climate Change. 1–11. https://doi.org/10.1061/40792(173)538

Bhattacharya T, Khare D, Arora M (2019) A case study for the assessment of the suitability of gridded reanalysis weather data for hydrological simulation in Beas river basin of North Western Himalaya. Applied Water Science. 9(4):3. https://doi.org/10.1007/s13201-019-0993-x

Bie W, Casper MC, Reiter P, Vohland M (2015) Surface resistance calibration for a hydrological model using evapotranspiration retrieved from remote sensing data in Nahe catchment forest area. IAHS-AISH Proceedings and Reports. 368:81–86. https://doi.org/10.5194/piahs-368-81-2015

Blanco G, Gerlagh R, Suh S, Barrett J, de Coninck HC, Diaz Morejon CF, Mathur R, Nakicenovic N, Ofosu Ahenkora A, Pan J, Pathak H, Rice J, Richels R, Smith SJ, Stern DI, Toth, FL, Zhou, P (2014) Drivers, Trends and Mitigation. In Edenhofer O, Pichs-Madruga R, Sokona Y, Farahani E, Kadner S, Seyboth K, Adler A, Baum I, Brunner S, Eickemeier P, Kriemann B, Savolainen J, Schlömer S, von Stechow C, Zwickel T, Minx JC (Eds.), Climate Change 2014: Mitigation of Climate Change. Contribution of Working Group III to the Fifth Assessment Report of the Intergovernmental Panel on Climate Change. Retrieved from https://www.ipcc.ch/site/assets/uploads/2018/02/ipcc_wg3_ar5_chapter5.pdf

Boé J, Terray L. Habets F, Martin, E. (2007). Statistical and dynamical downscaling of the Seine basin climate for hydro-meteorological studies. International Journal of Climatology, 27(12), 1643–1655. https://doi.org/10.1002/joc.1602

Boehlert B, Strzepek KM, Gebretsadik Y, Swanson R, McCluskey A, Neumann JE, McFarland J, Martinich, J (2016) Climate change impacts and greenhouse gas mitigation effects on U.S. hydropower generation. Applied Energy. 183:1511–1519. https://doi.org/10.1016/j.apenergy.2016.09.054

Boote KJ, Allen LH, Prasad PVV, Baker JT, Gesch RW, Snyder AM, Pan D, Thomas JMG (2005) Elevated Temperature and CO_2 Impacts on Pollination, Reproductive Growth, and Yield of Several Globally Important Crops. Journal of Agricultural Meteorology. 60(5):469–474. https://doi.org/10.2480/agrmet.469

Bøssing Christensen O, Drews M, Hesselbjerg Christensen J, Dethloff K, Ketelsen K, Hebestadt, I, Rinke A (2007) The HIRHAM Regional Climate Model. Version 5 (beta). Retrieved from https://orbit.dtu.dk/en/publications/the-hirham-regional-climate-model-version-5-beta

Bouraima AK, Weihua Z, Chaofu W (2015) Irrigation water requirements of rice using Cropwat model in Northern Benin. International Journal of Agricultural and Biological Engineering. 8(2):58–64. https://doi.org/10.3965/j.ijabe.20150802.1290

Bunce JA (2004) Carbon dioxide effects on stomatal responses to the environment and water use by crops under field conditions. Oecologia. 140(1):1–10. https://doi.org/10.1007/s00442-003-1401-6

Burek P, Satoh Y, Fischer G, Kahil MT, Scherzer A, Tramberend, S, Nava LF, Wada Y, Eisner S, Flörke M, Hanasaki N, Magnuszewski P, Cosgrove B, Wiberg, D (2016) Water Futures and Solution - Fast Track Initiative (Final Report). Retrieved from http://pure.iiasa.ac.at/id/eprint/13008/

Burney JA, Davis SJ, Lobell DB (2010) Greenhouse gas mitigation by agricultural intensification. Proceedings of the National Academy of Sciences of the United States of America. 107(26):12052–12057. https://doi.org/10.1073/pnas.0914216107

Cai J, Liu Y, Lei T, Pereira LS (2007) Estimating reference evapotranspiration with the FAO Penman-Monteith equation using daily weather forecast messages. Agricultural and Forest Meteorology. 145(1–2):22–35. https://doi.org/10.1016/j.agrformet.2007.04.012

California Irrigation Management Information System (CIMIS) (2012) CIMIS

Evapotranspiration Zones. Retrieved from https://cimis.water.ca.gov/Content/pdf/CimisRefEvapZones.pdf

Calvet J-C, Noilhan J, Roujean J-L, Bessemoulin P, Cabelguenne M, Olioso A, Wigneron J-P (1998) An interactive vegetation SVAT model tested against data from six contrasting sites. Agricultural and Forest Meteorology. 92(2):73–95. https://doi.org/10.1016/S0168-1923(98)00091-4

Carvalho FP (2006) Agriculture, pesticides, food security and food safety. Environmental Science and Policy. 9(7–8):685–692. https://doi.org/10.1016/j.envsci.2006.08.002

Celestin S. Qi F, Li R, Yu T, Cheng W (2020) Evaluation of 32 Simple Equations against the Penman–Monteith Method to Estimate the Reference Evapotranspiration in the Hexi Corridor, Northwest China. Water. 12(10):2772. https://doi.org/10.3390/w12102772

Chávez JL, López-Urrea R (2019) One-step approach for estimating maize actual water use: Part I. Modeling a variable surface resistance. Irrigation Science. 37(2):123–137. https://doi.org/10.1007/s00271-018-0606-8

Cheng L, Zhang L, Wang Y-P, Canadell JG, Chiew FHS, Beringer J, Li L, Miralles DG, Piao S, Zhang, Y (2017) Recent increases in terrestrial carbon uptake at little cost to the water cycle. Nature Communications. 8(1). https://doi.org/10.1038/s41467-017-00114-5

Chiew FHS, Kamaladasa NN, Malano HM, McMahon TA (1995) Penman-Monteith, FAO-24 reference crop evapotranspiration and class-A pan data in Australia. Agricultural Water Management. 28(1):9–21. https://doi.org/10.1016/0378-3774(95)01172-F

Christensen J, Kjellström E, Giorgi F, Lenderink G, Rummukainen M (2010) Weight assignment in regional climate models. Climate Research. 44(2–3):179–194. https://doi.org/10.3354/cr00916

Cervi F, Nistor MM (2018). High Resolution of Water Availability for Emilia-Romagna Region over 1961-2015. Advances in Meteorology, 2018. https://doi.org/10.1155/2018/2489758

Cohen-Vogel DR, Osgood DE, Parker DD, Zilberman D (1998) The California Irrigation Management Information System (CIMIS): Intended and unanticipated impacts of public investment. Choices (third quarter). 20–25.

https://ageconsearch.umn.edu/record/132087/files/CIMIS.pdf

Córdova M, Carrillo-Rojas G, Crespo P, Wilcox B, Célleri R (2015) Evaluation of the Penman-Monteith (FAO 56 PM) Method for Calculating Reference Evapotranspiration Using Limited Data. Mountain Research and Development. 35(3):230. https://doi.org/10.1659/mrd-journal-d-14-0024.1

Cruz-Blanco M, Gavilán P, Santos C, Lorite IJ (2014) Assessment of reference evapotranspiration using remote sensing and forecasting tools under semi-arid conditions. International Journal of Applied Earth Observation and Geoinformation. 33:280–289. https://doi.org/10.1016/j.jag.2014.06.008

D'Oria M, Cozzi C, Tanda MG (2018) Future precipitation and temperature changes over the Taro, Parma and Enza River basins in Northern Italy. Italian Journal of Engineering Geology and Environment. 2018(Special Issue):49–63. https://doi.org/10.4408/IJEGE.2018-01.S-05

Damour G, Simonneau T, Cochard H, Urban L (2010) An overview of models of stomatal conductance at the leaf level. Plant, Cell and Environment. 33(9). https://doi.org/10.1111/j.1365-3040.2010.02181.x

de Carvalho LG, Evangelista AWP, Oliveira KMG, Silva BM, Alves MDC, de Sá Júnior A, Miranda WL (2013) FAO Penman-Monteith equation for reference evapotranspiration from missing data. Idesia. 31(3):39–47. https://doi.org/10.4067/S0718-34292013000300006

de Fraiture C, Wichelns D (2010) Satisfying future water demands for agriculture. Agricultural Water Management. 97(4):502–511. https://doi.org/10.1016/j.agwat.2009.08.008

Dee D, Fasullo J, Shea D, Walsh J, National Center for Atmospheric Research Staff (2016) The Climate Data Guide: Atmospheric Reanalysis: Overview and Comparison Tables. https://doi.org/10.1175/BAMS-D-13-00043.1

Department of Agriculture, Natural Resources and, and Conservation Service (NRCS) (1984) Sprinkler Irrigation. in National Engineering Handbook. Chapter 11. Part 623. Washington, DC: National Technical Information Service. https://directives.sc.egov.usda.gov/OpenNonWebContent.aspx?content=39754.wba

Desiato F, Fioravanti G, Fraschetti P, Perconti W, Piervitali E (2005) Il Clima Futuro in Italia: Analisi delle Proiezioni dei Modelli Regionali. In Stato dell 'Ambiente 58. Retrieved from https://www.isprambiente.gov.it/files/pubblicazioni/statoambiente/SA_58_15.pdf

Djaman K, Balde AB, Sow A, Muller B, Irmak S, N'Diaye MK, Manneh B, Moukoumbi YD, Futakuchi K, Saito, K (2015) Evaluation of sixteen reference evapotranspiration methods under sahelian conditions in the Senegal River Valley. Journal of Hydrology: Regional Studies. 3:139–159. https://doi.org/10.1016/j.ejrh.2015.02.002

Döll P (2002) Impact of climate change and variability on irrigation requirements: A global perspective. Climatic Change. 54(3):269–293. https://doi.org/10.1023/A:1016124032231

Dong Q, Ding Y, Fu J (2020) The response of reference evapotranspiration to climate change in Xinjiang, China : Historical changes, driving forces, and future projections. 235–254. https://doi.org/10.1002/joc.6206

Dong Q, Wang W, Shao Q, Xing W, Ding Y, Fu J (2020) The response of reference evapotranspiration to climate change in Xinjiang, China: Historical changes, driving forces, and future projections. International Journal of Climatology. 40(1):235–254. https://doi.org/10.1002/joc.6206

Doorenbos J, Pruitt WO (1977) Crop water requirements: FAO Irrigation and drainage paper No. 24. Rome. Retrieved from: http://www.fao.org/3/a-f2430e.Pdf

Duce P, Snyder RL, Soong ST, Spano D (2000 Forecasting reference evapotranspiration. Acta Horticulturae. 537:135–141. https://doi.org/10.17660/ActaHortic.2000.537.13

Easterling WE, Aggarwal PK, Batima P, Brander KM, Erda L, Howden SM, Kirilenko A, Morton J, Soussana J-F, Schmidhuber J, Tubiello FN (2007) Food, fibre and forest products. In Parry ML, Canziani OF, Palutikof JP, van der Linden PJ, Hanson CE (Eds.). Climate Change 2007: Impacts, Adaptation and Vulnerability. Contribution of working Group II to the Fourth Assessment Report of the Intergovernmental Panel on Climate Change. 273–313. Cambridge, UK: Cambridge University Press. Retrieved from: https://www.ipcc.ch/site/assets/uploads/2018/02/ar4-wg2-chapter5-1.pdf

Easterling WE, Rosenberg NJ, McKenney MS, Jones CA, Dyke PT, Williams JR (1992)

Preparing the erosion productivity impact calculator (EPIC) model to simulate crop response to climate change and the direct effects of CO_2. Agricultural and Forest Meteorology. 59(1–2):17–34. https://doi.org/10.1016/0168-1923(92)90084-H

Eching S (2002) Role of technology in irrigation advisory services: The CIMIS experience. in: 18th Congress and 53rd IEC Meeting of the International Commission on Irrigation and Drainage (ICID). FAO/ICID International Workshop on Irrigation Advisory Services and Participatory Extension Management. Montreal, Canada. http://www.ipcinfo.org/fileadmin/user_upload/faowater/docs/ias/paper24.pdf

Eekhout JPC, Vente J (2019). The implications of bias correction methods and climate model ensembles on soil erosion projections under climate change. Earth Surface Processes and Landforms, 44(5), 1137–1147. https://doi.org/10.1002/esp.4563

Ehleringer JR, Cerling T, Dearing MD (2005) A History of Atmospheric CO_2 and Its Effects on Plants, Animals, and Ecosystems.1(177). https://doi.org/10.1007/b138533

Ehret U, Zehe E, Wulfmeyer V, Warrach-Sagi K, Liebert J (2012) HESS Opinions "Should we apply bias correction to global and regional climate model data?" Hydrology and Earth System Sciences. 16(9):3391–3404. https://doi.org/10.5194/hess-16-3391-2012

Eitzinger J, Trnka M, Semerádová D, Thaler S, Svobodová E, Hlavinka P, Siska B, Takac J, Malatinska L, Novakova M, Dubrovský M, Zalud Z (2013) Regional climate change impacts on agricultural crop production in Central and Eastern Europe – hotspots, regional differences and common trends. The Journal of Agricultural Science. 151(06):787–812. https://doi.org/10.1017/S0021859612000767

Erda L, Wei X, Hui J, Yinlong X, Yue L, Liping B, Liyong X (2005) Climate change impacts on crop yield and quality with CO_2 fertilization in China. Philosophical Transactions of the Royal Society B: Biological Sciences. 360(1463):2149–2154. https://doi.org/10.1098/rstb.2005.1743

Essou GRC, Brissette F, Lucas-Picher P (2017) The use of reanalyses and gridded observations as weather input data for a hydrological model: Comparison of performances of simulated river flows based on the density of weather stations. Journal of Hydrometeorology. 18(2):497–513. https://doi.org/10.1175/JHM-D-16-0088.1

Estrela T, Pérez-Martin MA, Vargas E (2012) Impacts of climate change on water resources in Spain. Hydrological Sciences Journal. 57(6):1154–1167. https://doi.org/10.1080/02626667.2012.702213

Evenson RE, Gollin D (2003) Assessing the impact of the Green Revolution, 1960 to 2000. Science. 300(5620):758–762. https://doi.org/10.1126/science.1078710

Ewaid SH, Abed SA, Al-Ansari N (2019) Crop Water Requirements and Irrigation Schedules for Some Major Crops in Southern Iraq. Water. 11(4):756. https://doi.org/10.3390/w11040756

Exner-Kittridge MG, Rains MC (2010) Case Study on the Accuracy and Cost/Effectiveness in Simulating Reference Evapotranspiration in West-Central Florida. Journal of Hydrologic Engineering. 15(9):696–703. https://doi.org/10.1061/(asce)he.1943-5584.0000239

Fang GH, Yang J, Chen YN, Zammit C (2015) Comparing bias correction methods in downscaling meteorological variables for a hydrologic impact study in an arid area in China. Hydrology and Earth System Sciences. 19(6):2547–2559. https://doi.org/10.5194/hess-19-2547-2015

FAO (2011) The state of the world's land and water resources for food and agriculture (SOLAW) – Managing systems at risk. Retrieved from http://www.fao.org/3/i1688e/i1688e.pdf

FAO (2013) Statistical Yearbook of the Food And Agricultural Organization for the United Nations. Retrieved from http://www.fao.org/3/i3107e/i3107e.pdf

FAO (2017) The Future of Food and Agriculture Trends and Challenges. Retrieved from http://www.fao.org/3/a-i6881e.pdf

FAO (2020) World Food and Agriculture - Statistical Yearbook 2020. Retrieved from: https://doi.org/10.4060/cb1329en

FAOSTAT (2020) FAOSTAT Database. Retrieved from http://www.fao.org/faostat/en/#data

Fares A Abbas F (2009) Irrigation Systems and Nutrient Sources for Fertigation. Soil and Crop Management. (25):1–4. Retrieved from https://www.haifa-group.com/sites/default/files/article/SCM-25.pdf

Fares A, Awal R, Fares S, Johnson AB, Valenzuela H (2015) Irrigation water requirements for

seed corn and coffee under potential climate change scenarios. Journal of Water and Climate Change. 7(1), jwc2015025. https://doi.org/10.2166/wcc.2015.025

Feely RA, Wanninkhof R, Carter BR, Landschützer P, Sutton AJ, Cosca C, Triñanes JA (2019) Global ocean carbon cycle. In State of the Climate in 2018. 9(100):94–99). https://doi.org/10.1175/2019BAMSStateoftheClimate.1

Feigenwinter I, Kotlarski S, Casanueva A, Fischer A, Schwierz C, Liniger MA (2018) Exploring quantile mapping as a tool to produce user tailored climate scenarios for Switzerland. Technical Report MeteoSwiss. 270. Retrieved from https://www.meteoschweiz.admin.ch/content/dam/meteoswiss/en/service-und-publikationen/publikationen/doc/MeteoSchweiz_Fachbericht_270_final.pdf

Fenner W, Dallacort R, Junior CAF, Freitas PSLD, Queiroz TMD, Santi A (2019) Development, calibration and validation of weighing lysimeters for measurement of evapotranspiration of crops. Revista Brasileira de Engenharia Agricola e Ambiental. 23(4):297–302. https://doi.org/10.1590/1807-1929/agriambi.v23n4p297-302

Ficklin DL, Luo Y, Luedeling E, Zhang M (2009) Climate change sensitivity assessment of a highly agricultural watershed using SWAT. Journal of Hydrology. 374(1–2):16–29. https://doi.org/10.1016/J.JHYDROL.2009.05.016

Fischer G, Tubiello FN, van Velthuizen H, Wiberg DA (2007) Climate change impacts on irrigation water requirements: Effects of mitigation, 1990-2080. Technological Forecasting and Social Change. 74(7):1083–1107. https://doi.org/10.1016/j.techfore.2006.05.021

Foley AM (2010). Uncertainty in regional climate modelling: A review. Progress in Physical Geography: Earth and Environment, 34(5), 647–670. https://doi.org/10.1177/0309133310375654

França FM, Benkwitt CE, Peralta G, Robinson JPW, Graham NAJ, Tylianakis JM, Berenguer E, Lees AC, Ferreira J, Louzada J, Barlow J (2020) Climatic and local stressor interactions threaten tropical forests and coral reefs. Philosophical Transactions of the Royal Society B: Biological Sciences. 375(1794). https://doi.org/10.1098/rstb.2019.0116

Fuglie KO, Wang SL, Ball VE (2012) Productivity growth in agriculture: An international

perspective. In Productivity growth in Agriculture: An International Perspective. Vol. 40. https://doi.org/10.1093/erae/jbt013

Fuhrer J (2003) Agroecosystem responses to combinations of elevated CO_2, ozone, and global climate change. Agriculture, Ecosystems and Environment. 97(1–3):1–20. https://doi.org/10.1016/S0167-8809(03)00125-7

Fuka DR, Walter MT, Macalister C, Degaetano AT, Steenhuis TS, Easton ZM (2014) Using the Climate Forecast System Reanalysis as weather input data for watershed models. Hydrological Processes. 28(22):5613–5623. https://doi.org/10.1002/hyp.10073

Garcia M, Raes D, Allen R, Herbas C (2004) Dynamics of reference evapotranspiration in the Bolivian highlands (Altiplano). Agricultural and Forest Meteorology. 125(1–2):67–82. https://doi.org/10.1016/J.AGRFORMET.2004.03.005

Gharsallah O, Facchi A, Gandolfi C (2013) Comparison of six evapotranspiration models for a surface irrigated maize agro-ecosystem in Northern Italy. Agricultural Water Management. 130:119–130. https://doi.org/10.1016/J.AGWAT.2013.08.009

Giménez PO, García-Galiano SG (2018) Assessing Regional Climate Models (RCMs) Ensemble-driven reference evapotranspiration over Spain. Water. 10(9):1–13. https://doi.org/10.3390/w10091181

Giorgi F, Lionello P 2008 Climate change projections for the Mediterranean region. Glob. Planet. Change. 63:90–104. https://doi.org/10.1016/j.gloplacha.2007.09.005

Gleick PH, Palaniappan M (2010) Peak water limits to freshwater withdrawal and use. Proceedings of the National Academy of Sciences of the United States of America. 107(25):11155–11162. https://doi.org/10.1073/pnas.1004812107

Glenn DT, Endter-Wada J. Kjelgren R, Neale CMU (2015) Tools for evaluating and monitoring effectiveness of urban landscape water conservation interventions and programs. Landscape and Urban Planning. 139:82–93. https://doi.org/10.1016/j.landurbplan.2015.03.002

Glenn KC, Alsop B, Bell E, Goley M, Jenkinson J, Liu B, Martin C, Parrott W, Souder C, Sparks O, Urquhart W, Ward JM, Vicini JL (2017) Bringing New Plant Varieties to Market: Plant Breeding and Selection Practices Advance Beneficial Characteristics while Minimizing

Unintended Changes. Crop Science. 57(6):2906–2921. https://doi.org/10.2135/cropsci2017.03.0199

Goyal RK (2004) Sensitivity of evapotranspiration to global warming: A case study of arid zone of Rajasthan (India). Agricultural Water Management. 69(1):1–11. https://doi.org/10.1016/j.agwat.2004.03.014

Greve P, Roderick ML, Ukkola AM, Wada Y (2019) The aridity Index under global warming. Environmental Research Letters. 14(12):124006. https://doi.org/10.1088/1748-9326/ab5046

Grismer ME, Orang M, Snyder R, Matyac R (2002) Pan Evaporation to Reference Evapotranspiration Conversion Methods. Journal of Irrigation and Drainage Engineering. 128(3):180–184. https://doi.org/10.1061/(asce)0733-9437(2002)128:3(180)

Guerra E, Ventura F, Snyder RL (2016) Crop coefficients: A literature review. Journal of Irrigation and Drainage Engineering. 142(3):1–5. https://doi.org/10.1061/(ASCE)IR.1943-4774.0000983

Gutiérrez C, Somot S, Nabat P, Mallet M, Corre L, Van Meijgaard E, Perpiñán O, Gaertner M 2020 Future evolution of surface solar radiation and photovoltaic potential in Europe: investigating the role of aerosols. Environ. Res. Lett. 15:034035. https://doi.org/10.1088/1748-9326/ab6666

Gutiérrez JM, Maraun D, Widmann M, Huth R, Hertig E, Benestad R, Roessler O, Wibig J, Wilcke R, Kotlarski S, San Martín D, Herrera S, Bedia J, Casanueva A, Manzanas R, Iturbide M, Vrac M, Dubrovsky M, Ribalaygua J, Pórtoles J, Räty O, Räisänen J, Hingray B, Raynaud D, Casado MJ, Ramos P, Zerenner T, Turco M, Bosshard T, Štěpánek P, Bartholy J, Pongracz R, Keller DE, Fischer AM, Cardoso RM, Soares PMM, Czernecki B, Pagé C (2019) An intercomparison of a large ensemble of statistical downscaling methods over Europe: Results from the VALUE perfect predictor cross-validation experiment. International Journal of Climatology. 39(9):3750–3785. https://doi.org/10.1002/joc.5462

Haddeland I, Heinke J, Biemans H, Eisner S, Flörke M, Hanasaki N, Konzmann M, Ludwig F, Masaki Y, Schewe J, Stacke T, Tessler ZD, Wada Y, Wisser D (2014) Global water resources affected by human interventions and climate change. Proceedings of the National Academy of Sciences of the United States of America. 111(9):3251–3256.

https://doi.org/10.1073/pnas.1222475110

Hamza YG, Ameta SK, Tukur A, Usman A (2020) Overview on Evidence and Reality of Climate Change. IOSR Journal of Environmental Science Toxicology and Food Technology. 14(7):17–26. https://doi.org/10.9790/2402-1407021726

Hanan NP, Prince SD (1997) Stomatal conductance of West-Central Supersite vegetation in HAPEX-Sahel: Measurements and empirical models. Journal of Hydrology. 188–189(1–4):536–562. https://doi.org/10.1016/S0022-1694(96)03192-7

Hargreaves GH, Samani ZA (1982) Estimating Potential Evapotranspiration. Journal of the Irrigation and Drainage Division. 108(3):225–230.

Hart QJ, Brugnach M, Temesgen B, Rueda C, Ustin SL, Frame K. (2009) Daily reference evapotranspiration for California using satellite imagery and weather station measurement interpolation. Civ Eng Environ Syst. 26:19–33. https://doi.org/10.1080/10286600802003500

Hatch U, Jagtap S, Jones J, Lamb M (1999) Potential effects of climate change on agricultural water use in the Southeast U.S. Journal of the American Water Resources Association. 35(6):1551–1561. https://doi.org/10.1111/j.1752-1688.1999.tb04237.x

Heath OVS, Russel J (1954) Studies in Stomatal Behaviour. Journal of Experimental Botany. 5(2):269–292. https://doi.org/10.1093/jxb/5.2.269

Hewitson B, Janetos AC, Carter TR, Giorgi F, Jones RG, Kwon W-T, Mearns LO, Schippe ELF, van Aalst M (2014) Regional context. In Barros VR, Field CB, Dokken DJ, Mastrandrea MD, Mach KJ, Bilir TE, Chatterjee M, Ebi KL, Estrada YO, Genova RC, Girma B, Kissel ES, Levy AN, MacCracken S, Mastrandrea PR, White LL (Eds.). Climate Change 2014: Impacts, Adaptation, and Vulnerability. Part B: Regional Aspects. Contribution of Working Group II to the Fifth Assessment Report of the Intergovernmental Panel on Climate Change. 1133–1197. Retrieved from https://www.ipcc.ch/site/assets/uploads/2018/02/WGIIAR5-PartB_FINAL.pdf

Hobbins M (2010) What are evapotranspiration and forecast reference crop evapotranspiration (FRET)? Retrieved from https://www.researchgate.net/publication/334046335_What_are_Evapotranspiration_and_F

orecast_Reference_Crop_Evapotranspiration_FRET

Hossain MB, Yesmin S, Maniruzzaman M, Biswas JC (2017) Irrigation Scheduling of Rice (Oryza sativa L.) Using CROPWAT Model in the Western Region of Bangladesh. The Agriculturists. 15(1):19–27. https://doi.org/10.3329/agric.v15i1.33425

Hou LG, Zou, SB, Xiao HL, Yang YG (2013) Sensitivity of the reference evapotranspiration to key climatic variables during the growing season in the Ejina oasis northwest China. SpringerPlus. 2(1):11–15. https://doi.org/10.1186/2193-1801-2-S1-S4

Howell TA (2003) Irrigation Efficiency. In Stewart BA, Howell TA (Eds.). Encyclopedia of water science. 467–472. Retrieved from https://www.researchgate.net/publication/43256707_Irrigation_Efficiency

Huntington JL, Morton CG, McEvoy D, Bromley M, Hedgewisch K, Allen R, Gangopadhyay S (2016) Historical and Future Irrigation Water Requirements for Select Reclamation Project Areas, Western U.S. https://doi.org/10.13140/RG.2.2.23078.93761

Hussein ASA (1999) Grass ET Estimates Using Penman-Type Equations in Central Sudan. Journal of Irrigation and Drainage Engineering. 125(6):324–329. https://doi.org/10.1061/(asce)0733-9437(1999)125:6(324)

Iglesias A, Quiroga S, Diz A (2011) Looking into the future of agriculture in a changing climate. European Review of Agricultural Economics. 38(3):427–447. https://doi.org/10.1093/erae/jbr037

Immerzeel WW, Droogers P (2008) Calibration of a distributed hydrological model based on satellite evapotranspiration. Journal of Hydrology. 349(3–4):411–424. https://doi.org/10.1016/j.jhydrol.2007.11.017

IPCC (2013) Climate Change 2013: The Physical Science Basis. In Stocker TF, Qin D, Plattner G-K, Tignor M, Allen SK, Boschung J, Nauels A, Xia Y, Bex V, Midgley PM (Eds.), Contribution of Working Group I to the Fifth Assessment Report of the Intergovernmental Panel on Climate Change (p. 1535). Cambridge, United Kingdom and New York, NY, USA: Cambridge University Press. Retrieved from https://www.ipcc.ch/site/assets/uploads/2018/02/WG1AR5_all_final.pdf

IPCC (2014a) Climate Change 2014: Synthesis Report. Contribution of Working Groups I, II and III to the Fifth Assessment Report of the Intergovernmental Panel on Climate Change. In Pachauri RK, Meyer LA (Eds.). Kristin Seyboth (USA). Retrieved from https://www.ipcc.ch/site/assets/uploads/2018/05/SYR_AR5_FINAL_full_wcover.pdf

IPCC (2014b) Climate Change 2014 Impacts, Adaptation, and Vulnerability Part A: Global and Sectoral Aspects Working Group II Contribution to the Fifth Assessment Report of the Intergovernmental Panel on Climate Change (Field CB, Barros VR, Dokken DJ, Mach KJ, Mastrandrea MD, Bilir TE, Chatterjee M, Ebi KL, Estrada YO, Genova RC, Girma B, Kissel ES, Levy AN, MacCracken S, Mastrandrea PR, White LL Eds.) Retrieved from https://www.ipcc.ch/site/assets/uploads/2018/02/WGIIAR5-PartA_FINAL.pdf

Irmak S (2008) Evapotranspiration. In Jørgensen SE, Fath BD (Eds.). Encyclopedia of Ecology. 1432–1438. https://doi.org/10.1016/B978-008045405-4.00270-6

Irmak S, Howell TA, Allen RG, Payero JO, Martin DL (2005) Standardized ASCE Penman-Monteith: Impact of sum-of-hourly vs. 24-hour timestep computations at reference weather station sites. Transactions of the American Society of Agricultural Engineers. 48(3):1063–1077. https://doi.org/10.13031/2013.18517

Irmak S, Mutiibwa D, Irmak A, Arkebauer TJ, Weiss A, Martin DL, Eisenhauer DE (2008) On the scaling up leaf stomatal resistance to canopy resistance using photosynthetic photon flux density. Agricultural and Forest Meteorology. 148(6–7):1034–1044. https://doi.org/10.1016/j.agrformet.2008.02.001

Irmak S, Mutiibwa D (2010) On the dynamics of canopy resistance: Generalized linear estimation and relationships with primary micrometeorological variables. Water Resources Research. 46(8):1–20. https://doi.org/10.1029/2009WR008484

Irmak S, Skaggs KE, Chatterjee S (2014) A Review of the Bowen Ratio Surface Energy Balance Method for Quantifying Evapotranspiration and other Energy Fluxes. Transactions of the ASABE. 57(6):1657–1674. https://doi.org/10.13031/trans.57.10686

Islam A, Ahuja LR, Garcia LA, Ma L, Saseendran AS (2012) Modeling the Effect of Elevated CO_2 and Climate Change on Reference Evapotranspiration in the Semi-Arid Central Great Plains. Transactions of the ASABE. 55(6):2135–2146. https://doi.org/10.13031/2013.42505

Islam MR, Mizan MH, Akter M, Zakaria G (2017) Assesment of Crop and Irrigation Water Requirements for Some Selected Crops in Northwestern Bangladesh. Global Journal of Science Frontier Research. 17(3). Retrieved from: https://journalofscience.org/index.php/GJSFR/article/view/2004

Ivanov MA, Kotlarski S (2017) Assessing distribution-based climate model bias correction methods over an alpine domain: added value and limitations. International Journal of Climatology. 37(5):2633–2653. https://doi.org/10.1002/joc.4870

Jacob D, Petersen J, Eggert B, Alias A, Christensen OB, Bouwer LM, Braun A, Colette A, Déqué M, Georgievski G, Georgopoulou E, Gobiet A, Menut L, Nikulin G, Haensler A, Hempelmann N, Jones C, Keuler K, Kovats S, Kröner N, Kotlarski S, Kriegsmann A, Martin E, van Meijgaard E, Moseley C, Pfeifer S, Preuschmann S, Radermacher C, Radtke K, Rechid D, Rounsevell M, Samuelsson P, Somot S, Soussana J-F, Teichmann C, Valentini R, Vautard R, Weber B, Yiou P (2014) EURO-CORDEX: New high-resolution climate change projections for European impact research. Regional Environmental Change. 14(2):563–578. https://doi.org/10.1007/s10113-013-0499-2

Jacobs JM, Satti RS (2001) Evaluation of reference evapotranspiration methodologies and AFSIRS crop water use simulation model. Retrieved from https://citeseerx.ist.psu.edu/viewdoc/download?doi=10.1.1.629.9639&rep=rep1&type=pdf

Jägermeyr J, Gerten D, Heinke J, Schaphoff S, Kummu M, Lucht W (2015) Water savings potentials of irrigation systems: global simulation of processes and linkages. Hydrol. Earth Syst. Sci. 19:3073–3091. https://doi.org/10.5194/hess-19-3073-2015

Jarvis PG (1976) The Interpretation of the Variations in Leaf Water Potential and Stomatal Conductance Found in Canopies in the Field. Philosophical Transactions of the Royal Society B: Biological Sciences. 273(927):593–610. https://doi.org/10.1098/rstb.1976.0035

Jarvis PG, McNaughton KG (1986). Stomatal Control of Transpiration: Scaling Up from Leaf to Region. Advances in Ecological Research. 15:1–49. https://doi.org/10.1016/S0065-2504(08)60119-1

Ju J, Roy DP (2008) The availability of cloud-free Landsat ETM+ data over the conterminous United States and globally. Remote Sensing of Environment. 112(3):1196–1211.

https://doi.org/10.1016/j.rse.2007.08.011

Kashyap PS, Panda RK (2001) Evaluation of evapotranspiration estimation methods and development of crop-coefficients for potato crop in a sub-humid region. Agricultural Water Management. 50(1):9–25. https://doi.org/10.1016/S0378-3774(01)00102-0

Katerji N, Perrier A, Renard D, Aissa AKO (1983) Modélisation de l'évapotranspiration réelle d'une parcelle de luzerne : rôle d'un coefficient cultural. In Agronomie. 3. Retrieved from https://prodinra.inra.fr/?locale=en#!ConsultNotice:1653

Katerji N, Rana G (2006) Modelling evapotranspiration of six irrigated crops under Mediterranean climate conditions. Agricultural and Forest Meteorology. 138(1–4):142–155. https://doi.org/10.1016/J.AGRFORMET.2006.04.006

Katerji N, Rana G (2008) Crop evapotranspiration measurements and estimation in the Mediterranean region. Retrieved from https://hal.archives-ouvertes.fr/hal-01192026

Katerji N, Rana G (2011) Crop Reference Evapotranspiration: A Discussion of the Concept, Analysis of the Process and Validation. Water Resources Management. 25(6):1581–1600. https://doi.org/10.1007/s11269-010-9762-1

Katerji N, Rana G (2014) FAO-56 methodology for determining water requirement of irrigated crops: Critical examination of the concepts, alternative proposals and validation in Mediterranean region. Theoretical and Applied Climatology: 116(3–4):515–536. https://doi.org/10.1007/s00704-013-0972-3

Katerji N, Rana G, Ferrara RM (2017) Actual evapotranspiration for a reference crop within measured and future changing climate periods in the Mediterranean region. Theoretical and Applied Climatology. 129(3–4):923–938. https://doi.org/10.1007/s00704-016-1826-6

Keller J, Bliesner RD (2000) Sprinkler and Trickle Irrigation, Caldwell, NJ: The Blackburn Press

Kendon EJ, Jones RG, Kjellström E, Murphy JM (2010) Using and designing GCM-RCM ensemble regional climate projections. Journal of Climate. 23(24):6485–6503. https://doi.org/10.1175/2010JCLI3502.1

Kidson JW, Trenberth KE (1988) Effects of Missing Data on Estimates of Monthly Mean

General Circulation Statistics. Journal of Climate 1(12):1261–1275. https://doi.org/10.1175/1520-0442(1988)001<1261:EOMDOE>2.0.CO;2

Kim G, Cha DH, Lee G, Park C, Jin CS, Lee DK, Suh MS, Ahn JB, Min SK, Kim J (2020). Projection of future precipitation change over South Korea by regional climate models and bias correction methods. Theoretical and Applied Climatology, 141(3–4), 1415–1429. https://doi.org/10.1007/s00704-020-03282-5

Kingston DG, Todd MC, Taylor RG, Thompson JR, Arnell NW (2009) Uncertainty in the estimation of potential evapotranspiration under climate change. Geophysical Research Letters. 36(20):3–8. https://doi.org/10.1029/2009GL040267

Kirschbaum MUF (2004) Direct and Indirect Climate Change Effects on Photosynthesis and Transpiration. Plant Biology. 6(3):242–253. https://doi.org/10.1055/s-2004-820883

Kisi O, Cengiz TM (2013) Fuzzy Genetic Approach for Estimating Reference Evapotranspiration of Turkey: Mediterranean Region. Water Resources Management. 27(10):3541–3553. https://doi.org/10.1007/s11269-013-0363-7

Kjelgren R, Beeson RC, Pittenger DR, Montague DT (2016) Simplified Landscape Irrigation Demand Estimation: SLIDE Rules. Applied Engineering in Agriculture. 32(4):363–378. https://doi.org/10.13031/aea.32.11307

Korner G, Schell JA, Bauer H (1979) Maximum leaf diffusive conductance in vascular plants. Photosynthetica. 13(1):45–82.

Kravtsov S, Wyatt G, Curry JA, Tsonis AA (2014) Two contrasting views of multidecadal climate variability in the twentieth century. Geophysical Research Letters. 41(19):6881–6888. https://doi.org/10.1002/2014GL061416

Kreith F, Bohn M (2001) Principles of heat transfer. New York: Brooks/Cole Eds.

Kruijt B, Witte J-PM, Jacobs CMJ, Kroon T (2008) Effects of rising atmospheric CO_2 on evapotranspiration and soil moisture: A practical approach for the Netherlands. Journal of Hydrology. 349(3–4):257–267. https://doi.org/10.1016/J.JHYDROL.2007.10.052

Kumar M, Raghuwanshi NS, Singh R, Wallender WW, Pruitt WO (2002) Estimating

Evapotranspiration using Artificial Neural Network. Journal of Irrigation and Drainage Engineering. 128(4):224–233. https://doi.org/10.1061/(ASCE)0733-9437(2002)128:4(224)

Kummu M, de Moel H, Porkka M, Siebert S, Varis O, Ward PJ (2012) Lost food, wasted resources: Global food supply chain losses and their impacts on freshwater, cropland, and fertiliser use. Science of the Total Environment. 438:477–489. https://doi.org/10.1016/j.scitotenv.2012.08.092

Lamine D, Ansoumana B, Dior D (2015) Use of atmometers to estimate reference evapotranspiration in Arkansas. African Journal of Agricultural Research. 10(48):4376–4383. https://doi.org/10.5897/ajar2015.10332

Lardy R, Bachelet B, Bellocchi G, Hill DRC (2014) Towards vulnerability minimization of grassland soil organic matter using metamodels. Environmental Modelling and Software. 52:38–50. https://doi.org/10.1016/j.envsoft.2013.10.015

Lardy R, Graux AI, Bachelet B, Hillb DRC, Bellocchi G (2012) Steady-state soil organic matter approximation model: Application to the Pasture Simulation model. IEMSs 2012 - Managing Resources of a Limited Planet: Proceedings of the 6th Biennial Meeting of the International Environmental Modelling and Software Society. 769–776.

Lawrence MG (2005) The relationship between relative humidity and the dewpoint temperature in moist air: A simple conversion and applications. Bulletin of the American Meteorological Society. 86(2):225–233. https://doi.org/10.1175/BAMS-86-2-225

Lecina S, Martínez-Cob A, Pérez PJ. Villalobos FJ, Baselga JJ (2003) Fixed versus variable bulk canopy resistance for reference evapotranspiration estimation using the Penman–Monteith equation under semiarid conditions. Agricultural Water Management. 60(3):181–198. https://doi.org/10.1016/S0378-3774(02)00174-9

Leinauer B, Sevostianova E, Serena M, Schiavon M, MacOlino S (2010) Conservation of irrigation water for urban lawn areas. In Gianquinto GP, Orsini F (Eds.). 2nd International Conference on Landscape and Urban Horticulture. 881:487–492. https://doi.org/10.17660/ActaHortic.2010.881.78

Leinauer, B, Smeal D (2012) Turfgrass Irrigation. Circular 660.

Leuning R (1995) A critical appraisal of a combined stomatal-photosynthesis model for C_3 plants. Plant, Cell and Environment. 18(4):339–355. https://doi.org/10.1111/j.1365-3040.1995.tb00370.x

Li S, Hao X, Du T, Tong L, Zhang J, Kang S (2014) A coupled surface resistance model to estimate crop evapotranspiration in arid region of northwest China. Hydrological Processes. 28(4):2312–2323. https://doi.org/10.1002/hyp.9768

Li X, Kang S, Niu J, Huo Z, Liu J (2019) Improving the representation of stomatal responses to CO_2 within the Penman–Monteith model to better estimate evapotranspiration responses to climate change. Journal of Hydrology. 572:692–705. https://doi.org/10.1016/j.jhydrol.2019.03.029

Linderholm HW (2006) Growing season changes in the last century. Agricultural and Forest Meteorology. 137(1–2):1–14. https://doi.org/10.1016/j.agrformet.2006.03.006

Litvak E, Pataki DE (2016) Evapotranspiration of urban lawns in a semi-arid environment: An in situ evaluation of microclimatic conditions and watering recommendations. Journal of Arid Environments. 134:87–96. https://doi.org/10.1016/j.jaridenv.2016.06.016

Liu B, Liu M, Cui Y, Shao D, Mao Z, Zhang L, Khan S, Luo Y (2020) Assessing forecasting performance of daily reference evapotranspiration using public weather forecast and numerical weather prediction. Journal of Hydrology. 590:125547. https://doi.org/10.1016/j.jhydrol.2020.125547

Liu G, Liu Y, Hafeez M, Xu D, Vote C (2012) Comparison of two methods to derive time series of actual evapotranspiration using eddy covariance measurements in the southeastern Australia. Journal of Hydrology. 454–455:1–6. https://doi.org/10.1016/j.jhydrol.2012.05.011

Liu X, Zhang D (2013) Trend analysis of reference evapotranspiration in Northwest China: The roles of changing wind speed and surface air temperature. Hydrological Processes. 27(26):3941–3948. https://doi.org/10.1002/hyp.9527

Liu Y, Pereira LS, Teixeira JL (1997) Update definition and computation of reference evapotranspiration comparison with former method. Journal of Hydraulic Engineering. 6:27–33.

Lobell DB, Field CB (2007) Global scale climate-crop yield relationships and the impacts of recent warming. Environmental Research Letters. 2(1). https://doi.org/10.1088/1748-9326/2/1/014002

Long SP, Ainsworth EA, Leakey ADB, Morgan PB (2005) Global food insecurity. Treatment of major food crops with elevated carbon dioxide or ozone under large-scale fully open-air conditions suggests recent models may have overestimated future yields. Philosophical Transactions of the Royal Society B: Biological Sciences. 360(1463):2011–2020. https://doi.org/10.1098/rstb.2005.1749

Long SP, Ainsworth EA, Rogers A, Ort DR (2004a) Rising Atmospheric Carbon Dioxide: Plants FACE the Future. Annual Review of Plant Biology. 55(1):591–628. https://doi.org/10.1146/annurev.arplant.55.031903.141610

López-Urrea R, Olalla FMS, Fabeiro C, Moratalla A (2006) Testing evapotranspiration equations using lysimeter observations in a semiarid climate. Agricultural Water Management. 85(1–2):15–26. https://doi.org/10.1016/J.AGWAT.2006.03.014

Lorite IJ, Ramírez-Cuesta JM, Cruz-Blanco M, Santos C (2015) Using weather forecast data for irrigation scheduling under semi-arid conditions. Irrigation Science. 33(6):411–427. https://doi.org/10.1007/s00271-015-0478-0

Lovelli S, Perniola M, Di Tommaso T, Ventrella D, Moriondo M, Amato M (2010) Effects of rising atmospheric CO_2 on crop evapotranspiration in a Mediterranean area. Agricultural Water Management. 97(9):1287–1292. https://doi.org/10.1016/j.agwat.2010.03.005

Lu J, Sun G, Mcnulty SG, Arnataya D (2005) A comparison of six potential evapotranspiration methods for regional use in the Southeastern United States. Journal of American Water Resources Association. 41(3):621-633. https://doi.org/10.1111/j.1752-1688.2005.tb03759.x

Luo B, Minnett PJ, Szczodrak M, Nalli NR, Morris VR (2020) Accuracy assessment of MERRA-2 and ERA-Interim sea-surface temperature, air temperature and humidity profiles over the Atlantic Ocean using AEROSE measurements. Journal of Climate. 33(16):6889–6909. https://doi.org/10.1175/jcli-d-19-0955.1

Luo Y, Chang X, Peng S, Khan S, Wang W, Zheng Q, Cai X (2014) Short-term forecasting of

daily reference evapotranspiration using the Hargreaves-Samani model and temperature forecasts. Agricultural Water Management. 136:42–51. https://doi.org/10.1016/j.agwat.2014.01.006

Luo Y, Traore S, Lyu X, Wang W, Wang Y, Xie Y, Jiao X, Fipps G (2015) Medium range daily reference evapotranspiration forecasting by using ann and public weather forecasts. Water Resources Management. 29(10):3863–3876. https://doi.org/10.1007/s11269-015-1033-8

Madramootoo CA, Morrison J (2013) Advances and Challenges with Micro-Irrigation. Irrigation and Drainage. 62:255–261. https://doi.org/10.1002/ird.1704

Maestre-Valero JF, Testi L, Jiménez-Bello MA, Castel JR, Intrigliolo DS (2017) Evapotranspiration and carbon exchange in a citrus orchard using eddy covariance. Irrigation Science, 35(5), 397–408. https://doi.org/10.1007/s00271-017-0548-6

Mahto SS, Mishra V (2019) Does ERA-5 Outperform Other Reanalysis Products for Hydrologic Applications in India? Journal of Geophysical Research: Atmospheres. 124(16):9423–9441. https://doi.org/10.1029/2019JD031155

Makkink GF (1957) Testing the Penman formula by means of lysimeters. Journal of the Institution of Water Engineers. 11(3):277–288.

Mall RK, Gupta A, Sonkar G (2017) Effect of Climate Change on Agricultural Crops. Current Developments in Biotechnology and Bioengineering. 23–46. https://doi.org/10.1016/B978-0-444-63661-4.00002-5

Manikumari N, Murugappan A, Vinodhini G (2017) Time Series Forecasting of Daily Reference Evapotranspiration by Neural Network Ensemble Learning for Irrigation System. IOP Conference Series: Earth and Environmental Science. 80(1):012069. https://doi.org/10.1088/1755-1315/80/1/012069

Maraun D, Wetterhall F, Ireson AM, Chandler RE, Kendon EJ, Widmann M, Brienen S, Rust HW, Sauter T, Themel M, Venema VKC, Chun KP, Goodess CM, Jones RG, Onof C, Vrac M, Thiele-Eich I 2010 Precipitation downscaling under climate change: Recent developments to bridge the gap between dynamical models and the end user. Rev. Geophys. 48. https://doi.org/10.1029/2009RG000314

Margonis A, Papaioannou G, Kerkides P, Bourazanis G (2017) Parameterization of "canopy resistance" and estimation of hourly latent heat flux over a crop. 277–283. Retrieved from: http://ewra.net/ew/pdf/EW_2017_59_37.pdf

Martin G, Felten B, Duru M (2011) Forage rummy: A game to support the participatory design of adapted livestock systems. Environmental Modelling and Software. 26(12):1442–1453. https://doi.org/10.1016/J.ENVSOFT.2011.08.013

Martins DS, Paredes P, Raziei T, Pires C, Cadima J, Pereira LS (2017) Assessing reference evapotranspiration estimation from reanalysis weather products. An application to the Iberian Peninsula. International Journal of Climatology. 37(5):2378–2397. https://doi.org/10.1002/joc.4852

Massman WJ (1992) A surface energy balance method for partitioning evapotranspiration data into plant and soil components for a surface with partial canopy cover. Water Resources Research. 28(6):1723–1732. https://doi.org/10.1029/92WR00217

Matzrafi M (2019) Climate change exacerbates pest damage through reduced pesticide efficacy. Pest Management Science. 75(1):9–13. https://doi.org/10.1002/ps.5121

Medlyn BE, Barto, CVM, Broadmeadow MSJ, Ceulemans R, De Angelis P, Forstreuter M, Freeman M, Jackson SB, Kellomäki S, Laitat E, Rey A, Roberntz P, Sigurdsson BD, Strassemeyer J, Wang K, Curtis PS, Jarvis PG (2001) Stomatal conductance of forest species after long-term exposure to elevated CO_2 concentration: A synthesis. New Phytologist. 149(2):247–264. https://doi.org/10.1046/j.1469-8137.2001.00028.x

Melton FS, Johnson LF, Lund CP, Pierce LL, Michaelis AR, Hiatt SH, Guzman A, Adhikari DD, Purdy AJ, Rosevelt C, Votava P, Trout TJ, Temesgen B, Frame K, Sheffner EJ, Nemani RR (2012) Satellite irrigation management support with the terrestrial observation and prediction system: A framework for integration of satellite and surface observations to support improvements in agricultural water resource management. IEEE Journal of Selected Topics in Applied Earth Observations and Remote Sensing. 5(6):1709–1721. https://doi.org/10.1109/JSTARS.2012.2214474

Memon AV, Jamsa S (2018) Crop Water Requirement and Irrigation scheduling of Soybean and Tomato crop using CROPWAT 8.0. International Research Journal of Engineering and

Technology. 5(9):669–671. https://doi.org/10.13140/RG.2.2.22702.77126

Mendez M, Maathuis B, Hein-Griggs D, Alvarado-Gamboa LF (2020). Performance evaluation of bias correction methods for climate change monthly precipitation projections over Costa Rica. Water (Switzerland), 12(2), 482. https://doi.org/10.3390/w12020482

Menzel A, Fabian P (1999) Growing season extended in Europe. Nature. 397(6721):659. https://doi.org/10.1038/17709

Mercogliano P, Montesarchio M, Guido R, Schiano P, Vezzoli R, Zollo NC (2014) High Resolution Climate Scenarios on Mediterranean Test Case Areas for the Hydro-Climate Integrated System. SSRN Electronic Journal. https://doi.org/10.2139/ssrn.2539008

Met Office Hadley Centre (2020) Annual Global (Land and Ocean) temperature anomalies – HadCRUT 4. Retrieved from https://www.eea.europa.eu/data-and-maps/data/external/annual-global-land-and-ocean

Migliaccio K, Shen X, Lusher R, Siddiqui S (2017) Evaluating Forecast Reference Evapotranspiration For Florida. Proceedings of 2017 Irrigation Association Technical Conference. Retrieved from https://www.irrigation.org/IA/FileUploads/IA/Resources/TechnicalPapers/2017/EvaluatingForecastReferenceEvapotranspirationForFlorida.pdf

Milly PCD, Dunne KA (2016) Potential evapotranspiration and continental drying. Nature Climate Change. 6(10):946–949. https://doi.org/10.1038/nclimate3046

Molden D (2007) A Comprehensive Assessment of Water Management in Agriculture (Molden D, Ed.). Retrieved from https://www.iwmi.cgiar.org/assessment/files_new/synthesis/Summary_SynthesisBook.pdf

Monteiro JA (2017) Ecosystem services from turfgrass landscapes. Urban Forestry and Urban Greening. 26:151–157. https://doi.org/10.1016/j.ufug.2017.04.001

Monteith JL (1965) Evaporation and environment. In Symposia of the Society for Experimental Biology. 19:205–234. Cambridge: Cambridge University Press. Retrieved from: https://repository.rothamsted.ac.uk/item/8v5v7/evaporation-and-environment

Montero D, Echeverry F, Hernández F (2018) Combination of satellite imagery with meteorological data for estimating reference evapotranspiration. Revista de Teledeteccion. 2018(51):75–86. https://doi.org/10.4995/raet.2018.7688

Moreno JM, Aguiló E, Alonso S, Álvarez Cobelas M, Anadón R, Ballester F, Benito G, Catalán J, de Castro M, Cendrero A, Corominas J, Díaz J, Díaz-Fierros F, Duarte CM, Talaya AE, Peña AE, Estrela T, Fariña AC, González AF, Galante E, Gallart F, de Jalón LDG, Gil L, Gracia C, Iglesias A, Lapieza R, Loidi J, Palomeque FL, López-Vélez R, Zafra JML, Calabuig EL, Martín-Vide J, Meneu V, Tudela MIM, Montero G, Moreno J, Saiz JCM, Nájera A, Peñuelas J, Piserra MT, Ramos MA, de la Rosa D, Mantecón AR, Sánchez-Arcilla A, L. de Tembleque LJS, Valladares F, Vallejo VR (2005) A Preliminary Assessment of the Impacts in Spain due to the Effects of Climate Change. ECCE Project-Final Report. Retrieved from https://www.miteco.gob.es/es/cambio-climatico/temas/impactos-vulnerabilidad-y-adaptacion/Full%20report_tcm30-178514.pdf

Moratiel R, Snyder RL, Durán JM, Tarquis AM (2011) Trends in climatic variables and future reference evapotranspiration in Duero Valley (Spain). Natural Hazards and Earth System Sciences. 11(6):1795–1805. https://doi.org/10.5194/nhess-11-1795-2011

Morison JI, Gifford RM (1983) Stomatal sensitivity to carbon dioxide and humidity: a comparison of two c_3 and two c_4 grass species. Plant Physiology. 71(4):789–796. https://doi.org/10.1104/PP.71.4.789

Morison JIL (1987) Intercellular CO_2 Concentration and Stomatal Response to CO_2. Stomatal Function. Stanford University Press.

Natural Resources Conservation Service (1984). Sprinkler irrigation. In National Engineering Handbook: Vol. Part 623. Retrieved from https://directives.sc.egov.usda.gov/OpenNonWebContent.aspx?content=39754.wba

Ngongondo C, Xu CY, Tallaksen LM, Alemaw B (2013) Evaluation of the FAO Penman-montheith, priestley- Taylor and hargreaves models for estimating reference evapotranspiration in southern malawi. Hydrology Research. 44(4):706–722. https://doi.org/10.2166/nh.2012.224

Nistor MM, Mîndrescu M (2019) Climate change effect on groundwater resources in Emilia-

Romagna region: An improved assessment through NISTOR-CEGW method. Quaternary International. 504:214–228. https://doi.org/10.1016/j.quaint.2017.11.018

Nistor MM, Porumb GCG (2015) How to compute the land cover evapotranspiration at regional scale? A spatial approach of Emilia-Romagna region. GEOREVIEW: Scientific Annals of Stefan Cel Mare University of Suceava. Geography Series, 25(1):38–53. https://doi.org/10.4316/GEOREVIEW.2015.25.1.268

Nistor MM, Gualtieri AF, Cheval S, Dezsi Ş, Boţan VE (2016). Climate change effects on crop evapotranspiration in the Carpathian Region from 1961 to 2010. Meteorological Applications, 23(3):462–469. https://doi.org/10.1002/met.1570

NOAA (2018) Trends in Atmospheric Carbon Dioxide. Retrieved from https://www.esrl.noaa.gov/gmd/ccgg/trends/data.html

NOAA (2021) Global Forecast System (GFS). https://www.ncdc.noaa.gov/data-access/model-data/model-datasets/global-forcast-system-gfs (accessed 02 April 2021).

Norby RJ, De Kauwe MG, Domingues TF, Duursma RA, Ellsworth DS, Goll DS, Lapola DM, Luus KA, MacKenzie AR, Medlyn BE, Pavlick R, Rammig A, Smith B, Thomas R, Thonicke K, Walker AP, Yang X, Zaehle S (2016). Model-data synthesis for the next generation of forest free-air CO_2 enrichment (FACE) experiments. New Phytologist. 209(1):17–28. https://doi.org/10.1111/nph.13593

OECD (2012). OECD Environmental Outlook To 2050: The Consequences of Inaction. https://doi.org/10.1787/9789264122246-en

Oki T, Kanae S (2006) Global hydrological cycles and world water resources. Science. 313(5790):1068–1072. https://doi.org/10.1126/science.1128845

Olesen JE, Bindi M 2002 Consequences of climate change for European agricultural productivity, land use and policy. Eur. J. Agron. 16:239–262. https://doi.org/10.1016/S1161-0301(02)00004-7

Olioso A, Huard F, Guilioni L (2010) Prise en compte des effets du CO_2 sur le calcul de l'évapotranspiration de référence. In Présentation des méthodes et des résultats du projet CLIMATOR. 66–67. Retrieved from https://hal.inrae.fr/hal-02757684/document

Pan S, Tian H, Dangal SRS, Yang Q, Yang J, Lu C, Tao B, Ren W, Ouyang Z (2015) Responses of global terrestrial evapotranspiration to climate change and increasing atmospheric CO_2 in the 21st century. Earth's Future. 3(1):15–35. https://doi.org/10.1002/2014EF000263

Parajuli PB (2010) Assessing sensitivity of hydrologic responses to climate change from forested watershed in Mississippi. Hydrological Processes. 24(26):3785–3797. https://doi.org/10.1002/hyp.7793

Parent AC, Anctil F (2012) Quantifying evapotranspiration of a rainfed potato crop in South-eastern Canada using eddy covariance techniques. Agricultural Water Management. 113:45–56. https://doi.org/10.1016/j.agwat.2012.06.014

Parker WS (2016) Reanalyses and observations: What's the Difference? Bulletin of the American Meteorological Society. 97(9):1565–1572. https://doi.org/10.1175/BAMS-D-14-00226.1

Pastén-Zapata E, Jones JM, Moggridge H, Widmann M (2020) Evaluation of the performance of Euro-CORDEX Regional Climate Models for assessing hydrological climate change impacts in Great Britain: A comparison of different spatial resolutions and quantile mapping bias correction methods. Journal of Hydrology. 584:124653. https://doi.org/10.1016/j.jhydrol.2020.124653

Pauwels VRN, Samson R (2006) Comparison of different methods to measure and model actual evapotranspiration rates for a wet sloping grassland. Agricultural Water Management. 82(1–2):1–24. https://doi.org/10.1016/J.AGWAT.2005.06.001

Pavan V, Antolini G, Agrillo G, Auteri L, Barbiero R, Bonati V, Brunier F, Cacciamani C, Cazzuli O, Cicogna A, De Luigi C, Maraldo L, Marigo G, Millini R, Panettieri E, Ratto S, Ronchi C, Saibanti S, Sulis A, Tomei F, Tomozeiu R, Torlai I, Villani, G (2013) The ARCIS project. Retrieved from: https://www.researchgate.net/publication/260487833_The_ARCIS_project

Pelosi A, Medina H, Villani P, D'Urso G, Chirico GB (2016) Probabilistic forecasting of reference evapotranspiration with a limited area ensemble prediction system. Agricultural Water Management. 178:106–118. https://doi.org/10.1016/j.agwat.2016.09.015

Pelosi A, Terribile F, D'Urso G, Chirico GB (2020) Comparison of ERA5-Land and UERRA

MESCAN-SURFEX Reanalysis Data with Spatially Interpolated Weather Observations for the Regional Assessment of Reference Evapotranspiration. Water. 12(6):1669. https://doi.org/10.3390/w12061669

Penman HL (1948) Natural evaporation from open water, bare soil and grass. Proceedings of the Royal Society of London. Series A. Mathematical and Physical Sciences. 193(1032):120–145. https://doi.org/10.1098/rspa.1948.0037

Penman HL (1963) Vegetation and Hydrology : Soil Science. 5(96). Farham Royal, UK: Commonwealth Agricultural Bureaux.

Pereira LS, Paredes P, Jovanovic N (2020) Soil water balance models for determining crop water and irrigation requirements and irrigation scheduling focusing on the FAO56 method and the dual Kc approach. Agricultural Water Management. 241:106357. https://doi.org/10.1016/j.agwat.2020.106357

Pereira LS. Perrier A, Allen RG, Alves I (1999) Evapotranspiration: Concepts and Future Trends. Journal of Irrigation and Drainage Engineering. 125(2):45–51. https://doi.org/10.1061/(asce)0733-9437(1999)125:2(45)

Perera KC, Western AW, Nawarathna B, George B (2014) Forecasting daily reference evapotranspiration for Australia using numerical weather prediction outputs. Agricultural and Forest Meteorology. 194:50–63. https://doi.org/10.1016/j.agrformet.2014.03.014

Perez PJ, Lecina S, Castellvi F, Martínez-Cob A, Villalobos FJ (2006) A simple parameterization of bulk canopy resistance from climatic variables for estimating hourly evapotranspiration. Hydrological Processes. 20(3):515–532. https://doi.org/10.1002/hyp.5919

Peterschmitt J-M, Perrier A (1991) Evapotranspiration and canopy temperature of rice and groundnut in southeast coastal India. Crop coefficient approach and relationship between evapotranspiration and canopy temperature. Agricultural and Forest Meteorology. 56(3–4):273–298. https://doi.org/10.1016/0168-1923(91)90096-9

Pfaffenzeller S, Newbold P, Rayner A (2007) A short note on updating the Grilli and Yang commodity price index. World Bank Economic Review. 21(1):151–163. https://doi.org/10.1093/wber/lhl013

Piao S, Ciais P, Huang Y, Shen Z, Peng S, Li J, Zhou L, Liu H, Ma Y, Ding Y, Friedlingstein P, Liu C, Tan K, Yu Y, Zhang T, Fang J (2010) The impacts of climate change on water resources and agriculture in China. Nature. 467(7311):43–51. https://doi.org/10.1038/nature09364

Pingali P (2007) Agricultural Mechanization: Adoption Patterns and Economic Impact. In Evenson R, Pingali P (Eds.). Handbook of Agricultural Economics. 3:2779–2805. https://doi.org/10.1016/S1574-0072(06)03054-4

Polley HW (2002) Implications of Atmospheric and Climatic Change for Crop Yield and Water Use Efficiency. Crop Science. 42(1):131–140. Retrieved from http://www.ncbi.nlm.nih.gov/pubmed/11756263

Poyen BF, Ghosh KA, Kundu P (2016) Review on Different Evapotranspiration Empirical Equations. International Journal of Advanced Engineering, Management and Science. 2(3):17–24. Retrieved from https://www.neliti.com/publications/239382/review-on-different-evapotranspiration-empirical-equations

Prein AF, Gobiet A, Truhetz H., Keuler, K., Goergen, K., Teichmann C, Fox-Maule C, van Meijgaard E, Déqué M, Nikulin G, Vautard R, Colette A, Kjellström E, Jacob D ((2016). Precipitation in the EURO-CORDEX 0.11∘ and 0.44∘ simulations: high resolution, high benefits? Climate Dynamics, 46(1–2), 383–412. https://doi.org/10.1007/s00382-015-2589-y

Priya A, Nema AK, Islam A (2014). Effect of climate change and CO_2 on reference evapotranspiration in Varanasi, India-A case study. Journal of Agrometeorology. 16(1):44–51. Retrieved from https://www.cabdirect.org/cabdirect/abstract/20143255777

Puy A, Piano SL, Saltelli A (2020) Current Models Underestimate Future Irrigated Areas. Geophysical Research Letters. 47(8). https://doi.org/10.1029/2020GL087360

Rácz C, Nagy J, Dobos AC (2013) Comparison of several methods for calculation of reference evapotranspiration. Acta Silvatica et Lignaria Hungarica. 9(1):441–467. https://doi.org/10.2478/aslh-2013-0001

Rahimikhoob A, Behbahani MR, Fakheri J (2012) An Evaluation of Four Reference Evapotranspiration Models in a Subtropical Climate. Water Resources Management.

26(10):2867–2881. https://doi.org/10.1007/s11269-012-0054-9

Ramankutty N, Mehrabi Z, Waha K, Jarvis L, Kremen C, Herrero M, Rieseberg LH (2018) Trends in Global Agricultural Land Use: Implications for Environmental Health and Food Security. Annual Review of Plant Biology. 69(1):789–815. https://doi.org/10.1146/annurev-arplant-042817-040256

Rambikur E, Chávez JL (2012) Scintillometry for evapotranspiration estimation over irrigated alfalfa and dry grassland. Hydrology Days. 109–112. https://doi.org/http://dx.doi.org/10.25675/10217/201006

Ramírez JA, Finnerty B (1996) CO_2 and Temperature Effects on Evapotranspiration and Irrigated Agriculture. Journal of Irrigation and Drainage Engineering. 122(3):155–163. https://doi.org/10.1061/(ASCE)0733-9437(1996)122:3(155)

Rana G, Katerji N, Mastrorilli M (1998) Canopy resistance modelling for crops in contrasting water conditions. Physics and Chemistry of the Earth. 23(4):433–438. https://doi.org/10.1016/S0079-1946(98)00049-4

Rana G, Katerji N, Mastrorilli M, El Moujabber M (1994) Evapotranspiration and canopy resistance of grass in a Mediterranean region. Theoretical and Applied Climatology. 50(1–2):61–71. https://doi.org/10.1007/BF00864903

Rana G, Katerji N, Perniola M (2001) Evapotranspiration of sweet sorghum: A general model and multilocal validity in semiarid environmental conditions. Water Resources Research. 37(12):3237–3246. https://doi.org/10.1029/2001WR000476

Rasul G, Mahmood A (2009) Performance Evaluation of Different Methods for Estimation of Evapotranspiration in Pakistan's Climate. Pakistan Journal of Meteorology. 5:25–36.

Regione Emilia-Romagna (2010) Retrieved June 23, 2020, from https://sasweb.regione.emilia-romagna.it/statistica/Tabella.do?tabella=193

Reichler T, Kim J (2008). Uncertainties in the climate mean state of global observations, reanalyses, and the GFDL climate model. Journal of Geophysical Research: Atmospheres, 113(D5), https://doi.org/10.1029/2007JD009278

Riahi K, Rao S, Krey V, Cho C, Chirkov V, Fischer G, Kindermann G, Nakicenovic N, Rafaj P (2011) RCP 8.5-A scenario of comparatively high greenhouse gas emissions. Climatic Change. 109(1):33–57. https://doi.org/10.1007/s10584-011-0149-y

Roderick ML, Greve P, Farquhar GD (2015) On the assessment of aridity with changes in atmospheric CO_2. Water Resources Research. 51(7):5450–5463. https://doi.org/10.1002/2015WR017031@10.1002/(ISSN)1944-7973.WRR50

Rosegrant MW, Cai X, Cline SA (2002) World water and food to 2025. Retrieved from https://www.ifpri.org/publication/world-water-and-food-2025

Rosenzweig C, Iglesias A (1998) The use of crop models for international climate change impact assessment. https://doi.org/10.1007/978-94-017-3624-4_13

Saadi S, Todorovic M, Tanasijevic L, Pereira LS, Pizzigalli C, Lionello P (2015). Climate change and Mediterranean agriculture: Impacts on winter wheat and tomato crop evapotranspiration, irrigation requirements and yield. Agricultural Water Management. 147:103–115. https://doi.org/10.1016/j.agwat.2014.05.008

Salmon-Monviola J, Moreau P, Benhamou C, Durand P, Merot P, Oehler F, Gascuel-Odoux C (2013). Effect of climate change and increased atmospheric CO_2 on hydrological and nitrogen cycling in an intensive agricultural headwater catchment in western France. Climatic Change. 120(1–2):433–447. https://doi.org/10.1007/s10584-013-0828-y

Samuelsson P, Gollvik S, Jansson C, Kupiainen M, Kourzeneva E, Van De Berg WJ (2015). The surface processes of the Rossby Centre regional atmospheric climate model (RCA4). In METEOROLOGI NR (Vol. 157). Retrieved from: https://www.smhi.se/polopoly_fs/1.89803!/Menu/general/extGroup/attachmentColHold/mainCol1/file/meteorologi_157.pdf

Schroeder ED (2003) Water Resources. In Encyclopedia of Physical Science and Technology. 3(18):721–751). https://doi.org/https://doi.org/10.1016/B0-12-227410-5/00821-8

Schubert S, Arkin P, Carton J, Kalnay E, Koster R (2008) Reanalysis of historical climate data for key atmospheric features. In Dole R, Hoerling M, Schubert S (Eds.). Reanalysis of Historical Climate Data for Key Atmospheric Features: Implications for Attribution of

Causes of Observed Change. U.S. Clima:11–46. Asheville, NC: National Oceanic and Atmospheric Administration, National Climatic Data Center. Retrieved from: http://livebettermagazine.com/eng/reports_studies/pdf/Reanalysis_Climate_Data.pdf

Shams SH, Nazemosadat SMJ, Haghighi A, Parsa SZ (2012). Effect of carbon dioxide concentration and irrigation level on evapotranspiration and yield of red bean. Journal of Science and Technology of Greenhouse Culture. 2:1–10.

Sheikh V, Mohammadi M (2013) Evaluation of Reference Evapotranspiration Equations in Semi-arid Regions of Northeast of Iran. International Journal of Agriculture and Crop Sciences. 5(5):450–456. Retrieved from https://www.researchgate.net/publication/235731352_Evaluation_of_Reference_Evapotranspiration_Equations_in_Semi-arid_Regions_of_Northeast_of_Iran

Shiklomanov IA, Rodda JC (2003) World water resources at the beginning of the 21st century. Retrieved from http://catdir.loc.gov/catdir/samples/cam034/2002031201.pdf

Shiri J, Kişi Ö, Landera G, López JJ, Nazemi AH, Stuyt LCPM (2012). Daily reference evapotranspiration modeling by using genetic programming approach in the Basque Country (Northern Spain). Journal of Hydrology. 414–415, 302–316. https://doi.org/10.1016/j.jhydrol.2011.11.004

Shiu C-J, Liu SC, Fu C, Dai A, Sun Y (2012 How much do precipitation extremes change in a warming climate? Geophysical Research Letters. 39(17). https://doi.org/10.1029/2012GL052762

Shuttleworth WJ, Gurney RJ (1990) The theoretical relationship between foliage temperature and canopy resistance in sparse crops. Quarterly Journal of the Royal Meteorological Society. 116(492):497–519. https://doi.org/10.1002/qj.49711649213

Shuttleworth WJ, Wallace JS (1985) Evaporation from sparse crops-an energy combination theory. Quarterly Journal of the Royal Meteorological Society. 111(469):839–855. https://doi.org/10.1002/qj.49711146910

Silva D, Meza FJ, Varas E (2010) Estimating reference evapotranspiration (ET_o) using numerical weather forecast data in central Chile. Journal of Hydrology. 382(1–4):64–71.

https://doi.org/10.1016/j.jhydrol.2009.12.018

Smith M, Allen RG, Monteith JL, Perrier A, Pereira LS, Segeren A (1992) Report on The Expert Consultation on Revision of FAO Methodologies for Crop Water Requirements. Retrieved from https://agris.fao.org/agris-search/search.do?recordID=XF19940075302

Smith MR, Myers SS (2018) Impact of anthropogenic CO_2 emissions on global human nutrition. Nature Climate Change. 8(9). https://doi.org/10.1038/s41558-018-0253-3

Smith MR, Thornton PK, Myers SS (2018) The impact of rising carbon dioxide levels on crop nutrients and human health. IFPRI GCAN Policy Note. Retrieved from https://www.ifpri.org/publication/impact-rising-carbon-dioxide-levels-crop-nutrients-and-human-health

Snyder RL (2017). Climate Change Impacts on Water Use in Horticulture. Horticulturae. 3(2):27. https://doi.org/10.3390/horticulturae3020027

Snyder RL, Moratiel R, Song Z, Swelam A, Jomaa I, Shapland T (2011) Evapotranspiration response to climate change. Acta Horticulturae. (922):91–98. https://doi.org/10.17660/ActaHortic.2011.922.11

Stagl J, Mayr E, Koch H, Hattermann FF, Huang S (2014) Effects of Climate Change on the Hydrological Cycle in Central and Eastern Europe. In Advances in Global Change Research. 58:31–43. https://doi.org/10.1007/978-94-007-7960-0_3

Snyder RL, Pedras C, Montazar A, Henry JM, Ackley D (2015) Advances in ET-based landscape irrigation management. Agricultural Water Management. 147:187-197. https://doi.org/10.1016/j.agwat.2014.07.024

Stannard DI (1993) Comparison of Penman-Monteith, Shuttleworth-Wallace, and Modified Priestley-Taylor Evapotranspiration Models for wildland vegetation in semiarid rangeland. Water Resources Research. 29(5):1379–1392. https://doi.org/10.1029/93WR00333

Steduto P, Caliandro A, Rubino P, Ben Mechlia N, Masmoudi M, Martínez-Cob A, Faci JM, Rana G, Mastrorilli M, El Mourid M, Karrou M, Kanber R, Kirda C, El-Quosy D, El-Askari K, Ait Ali M, Zareb D, Snyder RL (1996) Penman-Monteith Reference Evapotranspiration Estimates in the Mediterranean Region. In Camp CR, Sadler EJ, Yoder RE (Eds.).

International conference, Evapotranspiration and irrigation scheduling. 357–364. San Antonio, TX, USA: ASAE.

Steduto P, Todorovic M, Caliandro A, Rubino P (2003) Daily reference evapotranspiration estimates by the Penman-Monteith equation in Southern Italy. Constant vs. variable canopy resistance. Theoretical and Applied Climatology. 74(3–4):217–225. https://doi.org/10.1007/s00704-002-0720-6

Stockle CO, Williams JR, Rosenberg NJ, Jones CA (1992) A method for estimating the direct and climatic effects of rising atmospheric carbon dioxide on growth and yield of crops: Part I-Modification of the EPIC model for climate change analysis. Agricultural Systems. 38(3):225–238. https://doi.org/10.1016/0308-521X(92)90067-X

Strzepek KM, Major DC, Rosenzweig C, Iglesias A, Yates DN, Holt A, Hillel D (1999) New methods of modelling water availability for agriculture under climate change: the U.S. Cornbelt. Journal of the American Water Resources Association. 35(6):1639–1655. https://doi.org/10.1111/j.1752-1688.1999.tb04242.x

Suleiman AA, Hoogenboom G (2007) Comparison of Priestley-Taylor and FAO-56 Penman-Monteith for Daily Reference Evapotranspiration Estimation in Georgia. Journal of Irrigation and Drainage Engineering. 133(2):175–182. https://doi.org/10.1061/(ASCE)0733-9437(2007)133:2(175)

Sun H, Moon S, Kim E, Kang B (2019) The Assessment of Cmip5 Models in the Context of Complementary Relationship of Areal Evapotranspiration. E-Proceedings of the 38th IAHR World Congress. Panama City. Retrieved from https://static.iahr.org/34/607.pdf

Suryavanshi P, Buttar GS, Brar AS (2015) Micro irrigation for sustainable agriculture: a brief review. Indian Journal of Economics and Development. 11:147–155. https://doi.org/10.5958/2322-0430.2015.00016.5

Tabari H (2010) Evaluation of reference crop evapotranspiration equations in various climates. Water Resources Management. 24(10):2311–2337. https://doi.org/10.1007/s11269-009-9553-8

Taiz L, Zeiger E (1991) Plant physiology the benjamin. Redwood City, CA: Benjamin-

Cummings Pub Co.

Tarek M, Brissette FP, Arsenault R (2020) Evaluation of the ERA5 reanalysis as a potential reference dataset for hydrological modelling over North America. Hydrology and Earth System Sciences. 24(5):2527–2544. https://doi.org/10.5194/hess-24-2527-2020

Tascikaraoglu A, Uzunoglu M (2014) A review of combined approaches for prediction of short-term wind speed and power. Renewable and Sustainable Energy Reviews. 34:243–254. https://doi.org/10.1016/j.rser.2014.03.033

Taylor KE (2001) Summarizing multiple aspects of model performance in a single diagram. Journal of Geophysical Research Atmospheres. 106(D7):7183–7192. https://doi.org/10.1029/2000JD900719

Technical Committee on Standardization of Reference Evapotranspiration (TCSRE) (2005) The ASCE Standardized Reference Evapotranspiration Equation. In Allen RG, Walter IA, Elliott RL, Howell TA, Itenfisu D, Jensen ME, Snyder RL (Eds.). The ASCE Standardized Reference Evapotranspiration Equation. https://doi.org/10.1061/9780784408056

Tegegne G, Melesse AM (2020) Multimodel Ensemble Projection of Hydro-climatic Extremes for Climate Change Impact Assessment on Water Resources. Water Resources Management. 1–17. https://doi.org/10.1007/s11269-020-02601-9

Teixeira AHC (2010) Determining Regional Actual Evapotranspiration of Irrigated Crops and Natural Vegetation in the São Francisco River Basin (Brazil) Using Remote Sensing and Penman-Monteith Equation. Remote Sensing. 2(5):1287–1319. https://doi.org/10.3390/rs0251287

Temesgen B, Eching S, Davidoff B, Frame K (2005) Comparison of Some Reference Evapotranspiration Equations for California. Journal of Irrigation and Drainage Engineering. 131(1):73–84. https://doi.org/10.1061/(ASCE)0733-9437(2005)131:1(73)

Thomson AM, Calvin KV, Smith SJ, Kyle GP, Volke A, Patel P, Delgado-Arias S, Bond-Lamberty B, Wise MA, Clarke LE, Edmonds JA (2011) RCP4.5: A pathway for stabilization of radiative forcing by 2100. Climatic Change. 109(1):77–94. https://doi.org/10.1007/s10584-011-0151-4

Thornthwaite CW (1948) An Approach toward a Rational Classification of Climate. Geographical Review. 38(1):55. https://doi.org/10.2307/210739

Thornton PK (2010) Livestock production: Recent trends, future prospects. Philosophical Transactions of the Royal Society B: Biological Sciences. 365(1554):2853–2867. https://doi.org/10.1098/rstb.2010.0134

Tian Y, Zhang K, Xu Y-P, Gao X, Wang J (2018) Evaluation of Potential Evapotranspiration Based on CMADS Reanalysis Dataset over China. Water. 10(9):1126. https://doi.org/10.3390/w10091126

Tipple BJ, Pagani M (2007) The Early Origins of Terrestrial C_4 Photosynthesis. Annual Review of Earth and Planetary Sciences. 35(1):435–461. https://doi.org/10.1146/annurev.earth.35.031306.140150

Todorovic M (1999) Single-Layer Evapotranspiration Model with Variable Canopy Resistance. Journal of Irrigation and Drainage Engineering. 125(5):235–245. https://doi.org/10.1061/(ASCE)0733-9437(1999)125:5(235)

Tomas-Burguera M, Beguería S, Vicente-Serrano S, Maneta M (2018) Optimal Interpolation scheme to generate reference crop evapotranspiration. Journal of Hydrology. 560:202–219. https://doi.org/10.1016/j.jhydrol.2018.03.025

Tomei F, Antolini G, Tomozeiu R, Pavan V, Villani G, Marletto V (2010) Analysis of precipitation in Emilia-Romagna (Italy) and impacts of climate change scenarios. International Workshop Advances in Statistical Hydrology. Taormina, Italy. Retrieved from: https://www.researchgate.net/publication/235890887_Analysis_Of_Precipitation_in_Emilia-Romagna_Italy_and_Impacts_of_Climate_Change_Scenarios

Tomozeiu R, Agrillo G, Cacciamani C, Pavan V (2014) Statistically downscaled climate change projections of surface temperature over Northern Italy for the periods 2021-2050 and 2070-2099. Natural Hazards. 72(1):143–168. https://doi.org/10.1007/s11069-013-0552-y

Tomozeiu R, Cacciamani C, Pavan V, Morgillo A, Busuioc A (2007) Climate change scenarios for surface temperature in Emilia-Romagna (Italy) obtained using statistical downscaling models. Theoretical and Applied Climatology. 90(1–2):25–47.

https://doi.org/10.1007/s00704-006-0275-z

Tomozeiu R, Pasqui M, Quaresima S (2018). Future changes of air temperature over Italian agricultural areas: a statistical downscaling technique applied to 2021–2050 and 2071–2100 periods. Meteorology and Atmospheric Physics. 130(5):543–563. https://doi.org/10.1007/s00703-017-0536-7

Torma CZ, Kis A, Pongrácz R (2020) Evaluation of EURO-CORDEX and Med-CORDEX precipitation simulations for the Carpathian Region: Bias corrected data and projected changes. Quarterly Journal of the Hungarian Meteorological Service. 124(1):25–46. https://doi.org/10.28974/idojaras.2020.1.2

Trajkovic S, Gocic M (2010) Comparison of some empirical equations for estimating daily reference evapotranspiration. Facta Universitatis - Series: Architecture and Civil Engineering. 8(2):163–168. https://doi.org/10.2298/fuace1002163t

Trajkovic S, Kolakovic S (2009) Evaluation of reference evapotranspiration equations under humid conditions. Water Resources Management. 23(14):3057–3067. https://doi.org/10.1007/s11269-009-9423-4

Traore S, Luo Y, Fipps G (2016) Deployment of artificial neural network for short-term forecasting of evapotranspiration using public weather forecast restricted messages. Agricultural Water Management. 163:363–379. https://doi.org/10.1016/j.agwat.2015.10.009

Trenberth KE, Fasullo JT, Kiehl J (2009). Earth's Global Energy Budget. Bulletin of the American Meteorological Society. 90(3):311–324. https://doi.org/10.1175/2008BAMS2634.1

Tubiello FN, Amthor JS, Boote KJ, Donatelli M, Easterling W, Fischer G, Gifford RM, Howdenh M, Reilly J, Rosenzweig C (2007) Crop response to elevated CO_2 and world food supply. A comment on "Food for Thought..." by Long et al. Science 312:1918-1921, 2006. European Journal of Agronomy. 26(3):215–223. https://doi.org/10.1016/j.eja.2006.10.002

Tubiello FN, Donatelli M, Rosenzweig C, Stockle CO (2000) Effects of climate change and elevated CO_2 on cropping systems: model predictions at two Italian locations. European Journal of Agronomy. 13(2–3):179–189. https://doi.org/10.1016/S1161-0301(00)00073-3

Turral H, Burke J, Faurés J-M (2011) Climate change, water and food security. FAO Water Reports 36. p. 174. Retrieved from http://www.fao.org/3/i2096e/i2096e.pdf

Ueyama M, Ichii K, Kobayashi H, Kumagai T, Beringer J, Merbold L, Euskirchen ES, Hirano T, Marchesini LB, Baldocchi D, Saitoh TM, Mizoguchi Y, Ono K, Kim J, Varlagin A, Kang M, Shimizu T, Kosugi Y, Bret-Harte MS, Machimura T, Matsuura Y, Ohta T, Takagi K, Takanash S, Yasuda Y (2020) Inferring CO_2 fertilization effect based on global monitoring land-atmosphere exchange with a theoretical model. Environmental Research Letters. 15(8):084009. https://doi.org/10.1088/1748-9326/ab79e5

UN (2019) World Population Prospects 2019. Retrieved from https://population.un.org/wpp/Download/Standard/Population/

UNCCS (2019) Climate action and support trends. Retrieved from https://unfccc.int/sites/default/files/resource/Climate_Action_Support_Trends_2019.pdf

UNDESA (United Nations-Department of Economic and Social Affairs) (2017) World population prospects: The 2017 revision, key findings and advance tables. Working Paper No. ESA/P/WP/248. Retrieved from https://population.un.org/wpp/Publications/Files/WPP2017_KeyFindings.pdf

Uniyal B, Dietrich J, Vu NQ, Jha MK, Arumí JL (2019) Simulation of regional irrigation requirement with SWAT in different agro-climatic zones driven by observed climate and two reanalysis datasets. Science of the Total Environment. 649:846–865. https://doi.org/10.1016/j.scitotenv.2018.08.248

van der Kooi CJ, Reich M, Löw M, De Kok LJ, Tausz M (2016) Growth and yield stimulation under elevated CO_2 and drought: A meta-analysis on crops. Environmental and Experimental Botany. 122:150–157. https://doi.org/10.1016/J.ENVEXPBOT.2015.10.004

Van Meijgaard E, Van Ulft LH, Van De Berg WJ, Bosveld FC, Van Den Hurk BJJM, Lenderink G, Siebesma AP (2008) The KNMI regional atmospheric climate model RACMO version 2.1. Retrieved from: http://publicaties.minienm.nl/documenten/the-knmi-regional-atmospheric-climate-model-racmo-version-2-1

van Vuuren DP, Edmonds J, Kainuma M, Riahi K, Thomson A, Hibbard K, Hurtt GC, Kram T,

Krey V, Lamarque J-F, Masui T, Meinshausen M, Nakicenovic N, Smith SJ, Rose SK (2011) The representative concentration pathways: An overview. Climatic Change. 109(1):5–31. https://doi.org/10.1007/s10584-011-0148-z

van Vuuren DP, Ochola WO, Riha S, Giampietro M, Ginzo H, Henrichs T, Hussain S, Kok K, Makhura M, Mirza M, Palanisami KP, Ranganathan CR, Ray S, Ringler C, Rola A, Westhoek H, Zurek M (2009) Outlook on agricultural change and its drivers. In McIntyre BD, Herren HR, Wakhungu J, Watson RT (Eds.). Agriculture at a Crossroads. 255–305. Retrieved from https://www.weltagrarbericht.de/reports/Global_Report/Global_4_255.html

Vanella D, Intrigliolo DS, Consoli S, Longo-Minnolo G, Lizzio G, Dumitrache RC, Mateescu E, Deelstra J, Ramírez-Cuesta JM (2020) Comparing the use of past and forecast weather data for estimating reference evapotranspiration. Agricultural and Forest Meteorology. 295:108196. https://doi.org/10.1016/j.agrformet.2020.108196

Vendrame N, Tezza L, Pitacco A (2019) Scaling-up of evapotranspiration measurements: The promising role of scintillometry. IOP Conference Series: Earth and Environmental Science. 275(1):012018. https://doi.org/10.1088/1755-1315/275/1/012018

Ventura F, Spano D, Duce P, Snyder RL (1999) An evaluation of common evapotranspiration equations. Irrigation Science. 18(4):163–170. https://doi.org/10.1007/s002710050058

Vezzoli R, Mercogliano P, Castellari S (2016) Scenari di cambiamenti climatici nel periodo 2021-2050: quale disponibilità idrica nel bacino del fiume Po? Ingegneria Dell'Ambiente. 3(1). Retrieved from https://www.ingegneriadellambiente.net/ojs/index.php/ida/article/view/47

Villani G, Tomei F, Tomozeiu R, Marletto V (2011). Climatic scenarios and their impacts on irrigated agriculture in emilia-romagna, italy. Italian Journal of Agrometeorology, (1), 5–16. http://www.agrometeorologia.it/documenti/Rivista2011_1/aiam_1_2011_villani.pdf

Villoria N (2019) Consequences of agricultural total factor productivity growth for the sustainability of global farming: Accounting for direct and indirect land use effects. Environmental Research Letters. 14(12):125002. https://doi.org/10.1088/1748-9326/ab4f57

Wada Y, Flörke M, Hanasaki N, Eisner S, Fischer G, Tramberend S, Satoh Y, van Vliet MTH,

Yillia P, Ringler C, Burek P, Wiberg D (2016) Modeling global water use for the 21st century: the Water Futures and Solutions (WFaS) initiative and its approaches. Geoscientific Model Development. 9(1):175–222. https://doi.org/10.5194/gmd-9-175-2016

Wada Y, Van Beek LPH, Bierkens MFP (2012) Nonsustainable groundwater sustaining irrigation: A global assessment. Water Resources Research. 48(1). https://doi.org/10.1029/2011WR010562

Wand SJE, Midgley GF, Jones MH, Curtis PS (1999). Responses of wild C_4 and C_3 grass (Poaceae) species to elevated atmospheric CO_2 concentration: a meta-analytic test of current theories and perceptions. Global Change Biology. 5(6):723–741. https://doi.org/10.1046/j.1365-2486.1999.00265.x

Wang D, Luo H, Grunder O, Lin Y (2017) Multi-step ahead wind speed forecasting using an improved wavelet neural network combining variational mode decomposition and phase space reconstruction. Renewable Energy. 113:1345–1358. https://doi.org/10.1016/j.renene.2017.06.095

Wang JL, Wen XF (2010) Modeling the response of stomatal conductance to variable CO_2 concentration and its physiological mechanism. Acta Ecologica Sinica. 30(17):4815–4820. Retrieved from https://www.researchgate.net/publication/289236531_Modeling_the_response_of_stomatal_conductance_to_variable_CO_2_concentration_and_its_physiological_mechanism

Wang J, Zhang W, Li Y, Wang J, Dang Z (2014). Forecasting wind speed using empirical mode decomposition and Elman neural network. Applied Soft Computing Journal. 23:452–459. https://doi.org/10.1016/j.asoc.2014.06.027

Wang L, Chen W (2014) A CMIP5 multimodel projection of future temperature, precipitation, and climatological drought in China. International Journal of Climatology. 34(6):2059–2078. https://doi.org/10.1002/joc.3822

Wang S, Yang Y, Trishchenko AP, Barr AG, Black TA, Mccaughey H (2009) Modeling the response of canopy stomatal conductance to humidity. Journal of Hydrometeorology. 10(2):521–532. https://doi.org/10.1175/2008JHM1050.1

Wang W, Xie P, Yoo SH, Xue Y, Kumar A, Wu X (2011) An assessment of the surface climate in the NCEP climate forecast system reanalysis. Climate Dynamics. 37(7–8):1601–1620. https://doi.org/10.1007/s00382-010-0935-7

Wang Y, Bakker F, de Groot R, Wortche H, Leemans R (2015) Effects of urban trees on local outdoor microclimate: synthesizing field measurements by numerical modelling. Urban Ecosystem. 18:1305–1331. https://doi.org/10.1007/s11252-015-0447-7

Whitehead D (1998) Regulation of stomatal conductance and transpiration in forest canopies. Tree Physiology. 18(8–9):633–644. https://doi.org/10.1093/treephys/18.8-9.633

Wilks DS, (2005) Statistical Methods in the Atmospheric Sciences. Vol 91. 2nd ed. Academic Press, New York.

Wu Y, Liu S, Abdul-Aziz OI (2012) Hydrological effects of the increased CO_2 and climate change in the Upper Mississippi River Basin using a modified SWAT. Climatic Change. 110(3–4):977–1003. https://doi.org/10.1007/s10584-011-0087-8

Wullschleger SD, Gunderson CA, Hanson PJ, Wilson KB, Norby RJ (2002) Sensitivity of stomatal and canopy conductance to elevated CO_2 concentration - interacting variables and perspectives of scale. New Phytologist. 153(3):485–496. https://doi.org/10.1046/j.0028-646X.2001.00333.x

WWAP (World Water Assessment Programme) (2012) The United Nations World Water Development Report 4: Managing Water under Uncertainty and Risk. Retrieved from https://unesdoc.unesco.org/ark:/48223/pf0000215644

Xu C, Gong L, Jiang T, Chen D, Singh VP (2006) Analysis of spatial distribution and temporal trend of reference evapotranspiration and pan evaporation in Changjiang (Yangtze River) catchment. Journal of Hydrology. 327(1–2):81–93. https://doi.org/10.1016/j.jhydrol.2005.11.029

Xystrakis F, Matzarakis A (2011) Evaluation of 13 Empirical Reference Potential Evapotranspiration Equations on the Island of Crete in Southern Greece. Journal of Irrigation and Drainage Engineering. 137(4):211–222. https://doi.org/10.1061/(asce)ir.1943-4774.0000283

Yan H, Zhang C, Peng G, Darko RO, Cai B (2018) Modelling canopy resistance for estimating latent heat flux at a tea field in South China. Experimental Agriculture. 54(4):563–576. https://doi.org/10.1017/S0014479717000242

Yang Q, Tian H, Li X, Tao B, Ren W, Chen G, Lu C, Yang J, Pan S, Banger K, Zhang B (2015) Spatiotemporal patterns of evapotranspiration along the North American east coast as influenced by multiple environmental changes. Ecohydrology. 8(4):714–725. https://doi.org/10.1002/eco.1538

Yang Y, Cui Y, Luo Y, Lyu X, Traore S, Khan S, Wang W (2016) Short-term forecasting of daily reference evapotranspiration using the Penman-Monteith model and public weather forecasts. Agricultural and Forest Meteorology. 177:329-339. https://doi.org/10.1016/j.agwat.2016.08.020

Yang Y, Luo Y, Wu C, Zheng H, Zhang L, Cui Y, Sun N, Wang L (2019) Evaluation of six equations for daily reference evapotranspiration estimating using public weather forecast message for different climate regions across China. Agricultural Water Management. 222:386–399. https://doi.org/10.1016/j.agwat.2019.06.014

Yang, Y, Roderick ML, Zhang S, McVicar TR, Donohue RJ (2019) Hydrologic implications of vegetation response to elevated CO_2 in climate projections. Nature Climate Change. 9(1):44–48. https://doi.org/10.1038/s41558-018-0361-0

Yang Yuting Zhang S, McVicar TR, Beck HE, Zhang Y, Liu B (2018) Disconnection Between Trends of Atmospheric Drying and Continental Runoff. Water Resources Research. 54(7):4700–4713. https://doi.org/10.1029/2018WR022593

Yao Y, Zhao S, Zhang Y, Jia K, Liu M (2014) Spatial and Decadal Variations in Potential Evapotranspiration of China Based on Reanalysis Datasets during 1982–2010. Atmosphere. 5(4):737–754. https://doi.org/10.3390/atmos5040737

Yin J, Zhan C, Ye W (2016) An Experimental Study on Evapotranspiration Data Assimilation Based on the Hydrological Model. Water Resources Management. 30(14):5263–5279. https://doi.org/10.1007/s11269-016-1485-5

Yoder R, Odhiambo L, Wright W (2005) Evaluation Of Methods For Estimating DailyReference

Crop Evapotranspiration At ASite In The Humid Southeast United States. Biological Systems Engineering: Papers and Publications. Retrieved from http://digitalcommons.unl.edu/biosysengfacpub/450

Yu G, Wang Q (2010). Ecophysiology of plant photosynthesis, transpiration, and water use. Science Press, 351–352

Yu K, Hui P, Zhou W, Tang J (2020). Evaluation of multi-RCM high-resolution hindcast over the CORDEX East Asia Phase II region: Mean, annual cycle and interannual variations. International Journal of Climatology, 40(4), 2134–2152. https://doi.org/10.1002/joc.6323.

Yue XL, Gao QX (2018) Contributions of natural systems and human activity to greenhouse gas emissions. Advances in Climate Change Research. 9(4):243–252. https://doi.org/10.1016/j.accre.2018.12.003

Zandler H, Senftl T, Vanselow KA (2020) Reanalysis datasets outperform other gridded climate products in vegetation change analysis in peripheral conservation areas of Central Asia. Scientific Reports, 10(1), 22446. https://doi.org/10.1038/s41598-020-79480-y

Zhang B, Kang S, Li F, Zhang L (2008) Comparison of three evapotranspiration models to Bowen ratio-energy balance method for a vineyard in an arid desert region of northwest China. Agricultural and Forest Meteorology. 148(10):1629–1640. https://doi.org/10.1016/j.agrformet.2008.05.016

Zhang B, Xu D, Liu Y, Li F, Cai J, Du L (2016) Multi-scale evapotranspiration of summer maize and the controlling meteorological factors in north China. Agricultural and Forest Meteorology. 216:1–12. https://doi.org/10.1016/J.AGRFORMET.2015.09.015

Zhang K, Kimball JS, Running SW (2016) A review of remote sensing based actual evapotranspiration estimation. Wiley Interdisciplinary Reviews: Water. 3(6):834–853. https://doi.org/10.1002/wat2.1168

Zhang Z, Gong Y, Wang Z (2018) Accessible remote sensing data based reference evapotranspiration estimation modelling. Agricultural Water Management. 210:59–69. https://doi.org/10.1016/j.agwat.2018.07.039

Zhou H, Kang S, Tong L, Ding R, Li S. Du T (2019) Improved application of the Penman–

Monteith model using an enhanced Jarvis model that considers the effects of nitrogen fertilization on canopy resistance. Environmental and Experimental Botany. 159:1–12. https://doi.org/10.1016/J.ENVEXPBOT.2018.12.007